The alternative complex III from Rhodothermus marinus - a prototype of a new family of quinol: electron acceptor oxidoreductase

Ana Patrícia Neto Refojo

Dissertation presented to obtain a PhD degree in Biochemistry at the Instituto de Tecnologia Química e Biológica, Universidade Nova de Lisboa

Supervisors: Prof. Miguel Teixeira and Dr. Manuela Pereira

Opponents: Dr. Wolfgang Nitschke and Dr. Arnaldo Videira

Instituto de Tecnologia Quimica e Biológica
Universidade Nova de Lisboa

FCT Fundação para a Ciência e a Tecnologia
MINISTÉRIO DA CIÊNCIA, TECNOLOGIA E ENSINO SUPERIOR

From left to right: Dr. Teresa Catarino, Dr. Maria João Romão, Dr. João Arrabaça, Dr. Inês Pereira, Dr. Wolfgang Nitschke, Ana Patrícia Refojo, Dr. Arnaldo Videira, Dr. Carlos Romão, Dr. Manuela Pereira and Prof. Miguel Teixeira.

Metalloproteins and Bioenergetic Unit
Biological Energy Transduction Laboratory
Instituto de Tecnologia Química e Biológica
Av. da República
Estação Agronómica Nacional
2780-157 Oeiras
Portugal
Tel. +351- 214 469 323

Foreword

This thesis comprises the work performed in the Metalloproteins and Bioenergetics Unit from Instituto de Tecnologia Química e Biológica, Universidade Nova de Lisboa, under the supervision of Prof. Miguel Teixeira and Dr. Manuela Pereira.

This thesis is divided into eight chapters: the first two are introductory chapters, being the first focused on electron transfer respiratory chain and its diversity and flexibility, in general, while in the second the respiratory chain of the bacterium *Rhodothermus marinus* is described. Chapters three to six are based on original published, as well as some unpublished results and may be read independently. On chapter 6, in addition to new presented results, overall aspects of the alternative complex III are also discussed. Concluding remarks of the work are presented on chapter seven. The information of the amino acids sequences used to construct the dendograms discussed on chapter six is presented as supplementary information on chapter eight while the alignment of those amino acid sequences are available on the supplied CD-ROM.

Acknowledgments

The work here presented would not be possible without the help and support of several people to whom I would like to thank…

Prof. Miguel Teixeira, my supervisor, for sharing with me his knowledge and wisdom, for his interest and dedication towards my work.

Dr. Manuela Pereira, my supervisor, for her endless support and for the dedication and enthusiasm about my work. For all the help, advises and orientation and for all the scientific discussions.

To all my colleagues and friend from the Metalloproteins and Bioenergetics Laboratory: Célia Romão, João Vicente, Filipa Sousa, Ana Paula Batista, Ana Filipa Pinto, Vera Gonçalves, Sandra Santos, Lara Paulo, Ana Teresa Bernardo, Liliana Pinto and Gabriel Martins. To the previous members of the group: Andreia Verissimo, Andreia Fernandes, João Rodrigues, Tiago Bandeiras and Susana Lobo. I specially thank the older ones who teached and helped me during my first months at ITQB. Outside the group: Sofia Venceslau, Cláudia Almeida, Marta Justino and Catarina Paquete and all the people from the 3rd floor.

Ana Paula Batista, Ana Raquel Correia, Ligia Nobre and Sofia Leite with whom I shared all the adventures of the university and later at the ITQB. Bárbara Henriques and Vera Gonçalves that joined us at ITQB. Thank you for all the help and support. Hugo Botelho for the "chás de camomila" that were so useful and of course for all the informatics help.

Dr Gudmundur O. Hreggvidsson and Dr Sigridur Hjorleifsdottir for providing the nucleotide sequences of some of the subunits of *Rhodothermus marinus* ACIII.

To Dr. Mikhail Yanuyshin for the critical reading and discussions.

To Dr. Eurico Melo for the helpful discussions about fluorescence spectroscopy measurements.

Eng. Manuela Regalla from the Amino Acid Analysis Service for N-terminus sequence determinations.

To Dr. Ana V. Coelho, Elisabete Pires and Peter from the Mass Spectrometry Lab at ITQB for the MS experiments.

To Dr. Inês Cardoso Pereira and Dr. Smilja Todorovic for the critical readings.

João Carita from the ITQB fermentation Unit for the cell growth and for all the help and support.

Although, the work performed in the Institute of Microbiology in Darmstadt was not included in this thesis, I would like to acknowledge Dr Arnulf Kletzin for receiving me in his laboratory and Christian Bauer for the help in the cloning and expression of the Rieske protein subunit of the cytochrome *ba* complex of the archaeon *Acidianus ambivalens*.

I thank to all my friends, especially Ana Paula Batista for being my everyday friend.

Another special thanks to *Ricardo* for being always there for me, for being my shining "star" especially in the bad days. Thank you.

To my parents for all the love, help, support and patient. To my sisters and brothers-in-law; and especially my nephews for fulfilling my life with happiness.

Fundação para a Ciência e Tecnologia is acknowledged for my PhD grant (SFRH XXI/BD/24745/2005) and for the financed project PTDC/QUI/66559/2006.

Thesis publications

The work presented in this dissertation is based on the publications:

Manuela M. Pereira, **Patrícia N. Refojo**, Gudmundur O. Hreggvidsson, Sigridur Hjorleifsdottir, Miguel Teixeira (2007) *The alternative complex III from Rhodothermus marinus – a prototype of a new family of quinol: electron acceptor oxidoreductase* FEBS Lett **481**, 4831-4835

Patrícia N. Refojo, Miguel Teixeira, Manuela M. Pereira (2010) *The alternative complex III from Rhodothermus marinus and its structural and functional association with caa_3 oxygen reductase* Biochim Biophys Acta **1797**, 1477-1482

Patrícia N. Refojo, Filipa L. Sousa, Miguel Teixeira, Manuela M. Pereira (2010) *The alternative complex III: A different architecture using known building modules* Biochim Biophys Acta *In Press*

Patrícia N. Refojo, Miguel Teixeira, Manuela M. Pereira (2010) *The lipid bound monoheme cytochrome c subunit of alternative complex III is the electron donor of caa_3 oxygen reductase in Rhodothermus marinus* In preparation

Publication not included in this thesis

Tiago M. Bandeiras, **Patricia N. Refojo,** Smilja Todorovic, Daniel H. Murgida, Peter Hildebrandt, Christian Bauer, Manuela M. Pereira, Arnulf Kletzin and Miguel Teixeira (2009) *The cytochrome ba complex from the thermoacidophilic crenarchaeote Acidianus ambivalens is an analog of bc_1 complexes*. Biochim Biophys Acta **1787**, 37-45.

x

Summary

The aim of the work presented in this thesis was the characterization of a complex with quinol: electron carrier oxidodoreductase activity present in the membranes of the thermohalophilic bacterium *Rhodothermus (R.) marinus.*

The complexes involved in the *R. marinus* respiratory chain have been extensively studied in the past few years. Specifically, the purification and characterization of a complex I (NADH: quinone oxidoreductase), a complex II (succinate:quinone oxidoreductase) and of three different oxygen reductases from the heme-copper oxygen reductases superfamily have been performed. Since those oxygen reductases are unable to receive electrons from quinol molecules, the presence of a complex linking complexes I and II to the oxygen reductases was needed. In fact, a complex with quinol: HiPIP oxidoreductase activity was purified and partially characterized. The absence of the Rieske protein indicated that the complex isolated from *R. marinus* has a different composition when compared with the typical cytochrome bc_1 complex.

In this thesis it is described that, indeed, the complex with quinol: electron carrier oxidoreductase activity in *R. marinus* respiratory chain is the first example of the newly identified family of oxidoreductases, named alternative complex III (ACIII), to be purified and characterized.

The ACIII of *R. marinus* is composed by seven subunits (A-G), whose coding genes are organized in a seven genes cluster (*ActABCDEFG*). Subunit A (27kDa) and subunit E (22 kDa) have, in their amino acid sequences, five and one *c*-type heme binding motifs (CXXCH),

respectively. Subunit A is also predicted to have one transmembrane helix (TMH). Subunit B (97 kDa) has three binding motifs for [4Fe-4S] $^{2+/1+}$ centers and one for a [3Fe-4S] $^{1+/0}$ center. Subunits C and F have 42 and 35 kDa, respectively, and are predicted to be integral membrane proteins with 10 TMHs. Subunits D and G are also membrane bound with two and one TMH, respectively, and no binding motifs for redox cofactors were detected.

The amino acid sequences of subunits B and C showed similarities with subunits of members of the complex iron sulfur molybdoenzyme (CISM) family. This family is characterized by the presence of three subunits: a catalytic subunit with a molybdenum cofactor in the active center, a four cluster protein (FCP) and a membrane anchor protein (MAP). The subunit B can be considered as a fusion between the catalytic subunit and the FCP since the first 800 amino acid residues of the N-terminus show similarity with the catalytic subunit of CISM family and the other 300 amino acid residues at the C-terminus show similarity with the FCP. However, it should be stressed that the subunit B of ACIII does not contain molybdenum. Subunit C shows similarity to MAP subunits, yet with a larger number of TMH. Due to the similarity between three of the seven subunits with subunits of the CISM, the relation of the ACIII with the latter family was investigated by analyzing all the available genomes by September of 2009. First, searches were performed to determine the presence of the genes coding for subunits of ACIII in other organisms. It was observed that, in fact, the ACIII is a widespread enzyme being present in genomes in which the genes coding for the typical complex III were absent, but there are also cases where the two enzymes were present. Moreover, in many cases the presence of genes coding for subunits of oxygen reductases following

those coding for ACIII was observed. From the comparison between subunits of ACIII and those from the CISM family and related complexes it was concluded that although the alternative complexes III show a completely different architecture they are composed by structural modules already observed in other enzymes.

The interaction of *R. marinus* ACIII with quinones was investigated using HQNO, a quinol analogue. Its fluorescence properties allowed the determination of, at least, one quinone binding site.

The investigation of a possible structural and functional association between the alternative complex III and the caa_3 oxygen reductase was also addressed. Several electrophoretic techniques conjugated with different staining procedures led to the identification of a complex with, approximately, 500 kDa formed by the two enzymes. By peptide mass fingerprint, subunits of the two enzymes were identified in that complex. Moreover, the association between ACIII and caa_3 oxygen reductase revealed to be also functional given that when put together the enzymes showed quinol: oxygen oxidoreductase activity which was HQNO and KCN inhibited (typical inhibitors of quinone interacting enzymes and of the oxygen reductases, respectively).

Furthermore, in this structural and functional association, the electron donor to caa_3 within ACIII was determined to be the monoheme cytochrome *c* (mhc) subunit. Oxygen consumption, which was KCN inhibited, was observed upon addition of the reduced monoheme cytochrome *c* (over expressed in *Escherichia coli*) to the caa_3 oxygen reductase. The reduction potential for mhc was determined to be +160 mV at pH 7.5. The spectroscopic characterization showed typical features of a low-spin heme with axial coordination methionine-histidine. The subunit is also predicted to have covalently

bound lipids since in the N-terminus of its amino acid sequence a characteristic consensus of a lipobox is detected. The pentaheme cytochrome *c* subunit was also cloned and expressed in *E. coli* and the UV-visible spectrum showed also characteristic features of low-spin hemes.

This work is a step forward not only in the investigation and recognition of the diversity and robustness of the electron transfer respiratory chains but also in the evaluation of how nature uses the same structural modules conjugated in several different ways.

Sumário

O trabalho apresentado nesta tese teve como objectivo a caracterização de um complexo com actividade quinol: transportador de electrões oxidorreductase presente nas membranas da bactéria termohalofilica *Rhodothermus (R.) marinus.*

Os complexos envolvidos na cadeia respiratória de *R. marinus* têm sido amplamente estudados nos últimos anos. Antes do início deste trabalho, o complexo I (NADH: quinona oxidorreductase), o complexo II (succinato: quinona oxidorreductase) e três diferentes reductases de oxigénio (pertencentes à superfamília das reductases de oxigénio hemo-cobre) foram purificados e caracterizados. Devido ao facto das reductases de oxigénio não conseguirem receber electrões directamente de quinóis, a presença de um complexo que permita a transferência de electrões entre o complexo I e II e as reductases de oxigénio era necessária. De facto, um complexo com actividade quinol: HiPIP oxidorredutase foi purificado e parcialmente caracterizado. A ausência da proteína Rieske indicou que o complexo isolado de *R. marinus* teria uma composição diferente daquela observada para o complexo citocromo bc_1.

Esta tese descreve que na cadeia respiratória de *R. marinus*, o complexo com actividade quinol: transportador de electrões oxidorreductase pertence a uma recém identificada familia de complexos. Estes últimos designaram-se complexos III alternativos sendo o complexo de *R. marinus* o primeiro membro a ser purificado e caracterizado.

O ACIII de *R. marinus* é composto por sete subunidades (A-G), cujos genes codificantes estão organizados numa associação (*ActABCDEFG*). A subunidade A (27kDa) e a subunidade E (22 kDa) têm, nas suas

sequências de resíduos de aminoácidos, cinco e um motivos de ligação a hemos do tipo *c* (CXXCH), respectivamente. Para a subunidade A prevê-se, também, a presença de uma hélice transmembranar (TMH). A sequência de resíduos de aminoácidos da subunidade B (97 kDa) apresenta três motivos de ligação para centros do tipo $[4Fe\text{-}4S]^{2+/1+}$ e um para um centro do tipo $[3Fe\text{-}4S]^{1+/0}$. As subunidades C e F têm 42 e 35 kDa, respectivamente e dez hélices transmembranares foram previstas para estas subunidades. Duas e uma hélices transmembranares foram, respectivamente, previstas para as subunidades D e G. Nestas últimas subunidades, não foram detectados motivos de ligação para cofactores redox.

A sequência de aminoácidos das subunidades B e C revelou que estas apresentam similaridade com subunidades de membros da família de complexos enzimáticos com ferro, enxofre e molibdénio (complex iron sulfur molybdoenzymes -CISM). Esta família é caracterizada pela presença de três subunidades: uma subunidade catalítica com um cofactor com molibdénio no centro activo, uma subunidade com quatro centros de ferro e enxofre (FCP) e uma subunidade de ligação à membrana (MAP). A subunidade B pode ser vista como uma fusão entre as subunidades catalítica e FCP, dado que os primeiros 800 resíduos de aminoácidos do N-terminal revelam similaridade com a subunidade catalítica enquanto que os restantes 300 resíduos de aminoácidos do C-terminal mostram similaridade com a FCP. No entanto, deve salientar-se que a subunidade B do ACIII não contém molibdénio. A subunidade C revela similaridade com subunidades MAP, ainda que tenha um número maior de TMH. Devido à similaridade entre três das sete subunidades do ACIII e subunidades da familia CISM, a relação do ACIII com esta família foi investigada através da análise de todos os

genomas completamente sequênciados disponíveis até Setembro de 2009. Em primeiro lugar, foram realizadas pesquisas para determinar a presença dos genes que codificam para subunidades do ACIII em outros organismos. Observou-se que, de facto, o ACIII não é exclusivo de *R. marinus*, estando presente em genomas que não possuem os genes que codificam subunidades do complexo III típico, mas também foram encontrados genomas onde os genes codificantes para ambos os enzimas foram detectados. Além disso, observou-se, em alguns casos, que a associação de genes que codifica o ACIII é seguida por genes que codificam subunidades de reductases de oxigénio. Através da comparação entre as subunidades do ACIII e das subunidades de membros da familia CISM e outras relacionadas com esta, concluiu-se que os complexos III alternativos apresentam uma arquitectura completamente diferente. No entanto, utilizam módulos estruturais já observados em outros enzimas.

A interação do ACIII de *R. marinus* com quinois foi estudada recorrendo às propriedades fluorescentes do HQNO, um análogo do quinol. Assim, determinou-se a presença de, pelo menos, um motivo de ligação a quinóis.

A associação estrutural e funcional estabelecida entre o complexo III alternativo e a reductase de oxigénio caa_3 foi também investigada. Várias técnicas electroforéticas conjugadas com diferentes procedimentos de coloração levaram à identificação de um complexo com, aproximadamente, 500 kDa formado pelo dois enzimas. Através de técnicas de espectrometria de massa, subunidades dos dois enzimas foram identificadas naquele complexo. Além disso, a associação entre o ACIII e a reductase de oxigénio caa_3 é, também, funcional dado que quando colocados juntos estes apresentam actividade quinol: oxigénio

oxidorreductase, inibida por HQNO e KCN (inibidores típicos de enzimas que interactuam, respectivamente, com quinonas e de reductases de oxigénio).

Determinou-se que na associação estrutural e funcional estabelecida entre os dois complexos, o citocromo *c* monohémico (mhc) do ACIII é responsável por transferir os electrões para a reductase de oxigénio caa_3. Isto porque se observou um consumo de oxigénio, inibido pelo KCN, por parte da reductase de oxigénio caa_3 aquando da adição do citocromo *c* monohémico reduzido (expresso em *Escherichia coli*). O mhc foi caracterizado bioquimica e espectroscopicamente determinando-se um potencial de redução de +160 mV a pH 7.5. O seu espectro de absorção no visivel revelou as características típicas de um hemo de baixo-spin com uma coordenação metionina-histidina. A presença de lípidos covalentemente ligados à subunidade monohémica está prevista, dado que no N-terminal da sua sequência de aminoácidos observa-se uma *lipobox*. A subunidade citocromo *c* pentahémica foi, também, clonada e expressa em *E. coli* e o seu espectro de UV-visivel mostra caracteristicas típicas de hemos de baixo-spin.

Este trabalho contribuiu para a investigação e reconhecimento da diversidade e robustez existente nas cadeias respiratórias, observando-se um novo exemplo de como a natureza utiliza os mesmos módulos estruturais e os conjuga de diferentes maneiras.

Abbreviations

ACIII	alternative complex III
BN	blue native
CISM	complex iron-sulfur molybdoenzyme
DDM	n- dodecyl-β -D-maltoside
DMSO	dimethyl sulfoxide
EDTA	Ethylenediamine tetraacetic acid
FCP	four cluster protein
HiPIP	High Potential Iron-Sulfur protein
HQNO	2-heptyl-4-hydroxyquinoline-N-oxide
MAP	membrane anchor protein
MFIcc	molybdopterin, FeS, integral membrane subunit (two cytochrome *c* subunits)
mhc	monoheme cytochrome *c*
OD	optical density
PAGE	polyacrylamide gel electrophoresis
phcT	pentaheme cytochrome *c* truncated
PMSF	phenylmethylsulfonyl fluoride
R.	*Rhodothermus*
SDS	sodium dodecyl sulfate
TMAO	trimethylamine N-oxide
TMH	transmembrane helix

Table of contents

Chapter 1 Electron transfer respiratory chains

Chapter 2 *Rhodothermus marinus* electron transfer respiratory chain

Chapter 3 — Characterization of the alternative complex III from *Rhodothermus marinus*

Chapter 4

Structural and functional association of the Alternative complex III with *caa*$_3$ oxygen reductase

Chapter 5

Characterization of the *c*-type cytochromes subunits of ACIII from *Rhodothermus marinus*

Chapter 8 Supplementary information

Chapter 1

Electron transfer respiratory chains

1.1- *Electron transfer respiratory chain* [1-7]

Life is only possible with the existence of systems for storage and transmission of information and of mechanism(s) for energy control.

The information is stored in the linear sequence of DNA, in the form of the genetic code, and its replication allows the transmission of this information through generations. The DNA is transcript into RNA which is translated into proteins essential for the cell function.

The mechanisms for control of energy are not so easy to describe and even the definition of energy is not simple. Energy is described as the "capacity to do work" and although a correct measurement of energy is not possible, a difference in energy between a system and its surroundings is. Energy can thus be measured in terms of the heat released during a reaction. In order for living systems to do work they have to change energy from one form to another without using heat as an intermediate, since this means wasting of energy. This issue is achieved by coupling reactions consuming energy and those releasing energy. ATP is considered the energetic currency of cells being its hydrolysis coupled to energy consuming reactions.

Electrons obtained from the catabolism of organic substrates are transferred by electron carriers (such as NADH) to an electron transfer chain. Here the electrons are transported through membrane bound complexes, with increasing redox potentials, to a final electron acceptor (O_2 in the aerobic organisms). However, the redox potential is not the only property determining the transfer of electrons along this sequence of electron transfer complexes. The interaction between the redox components must be specific, since in the absence of specificity the electron transfer would occur directly from the first electron donor

to the final oxidant and all the energy would be released in only one reaction. In fact, in electron transport chains the electron flow between individual components is performed in small steps and with a controlled release of energy from separated redox reactions. Moreover, the possible consumption of the substrates/products of each enzymatic complex by other enzymes outside the main electron transfer chain is another advantage of this electron transfer being preceded in small steps. In order to avoid loss of energy by short circuit reactions (incorrect transfers or back flow of electrons) it is also important that the electron transfer besides being specific is reasonably fast, in the desired direction.

Some of the complexes of the respiratory electron transfer chains couple the transfer of electrons to the translocation of protons across the membrane. This will lead to the formation of a transmembrane electrochemical potential (or proton motive force, *pmf*) composed by two distinct components: one originated by the concentration difference of an ion (in the specific case of a proton, ΔpH), and another due to an electrical potential difference ($\Delta\psi$) between the two sides of the membrane.

The dissipation of the transmembrane electrochemical potential releases energy which is used and transduced into chemical energy by ATP synthase to produce ATP from ADP and phosphate. This enzyme is also able to hydrolyze ATP in order to pump protons against a transmembrane electrochemical difference contributing to its reestablishment [1].

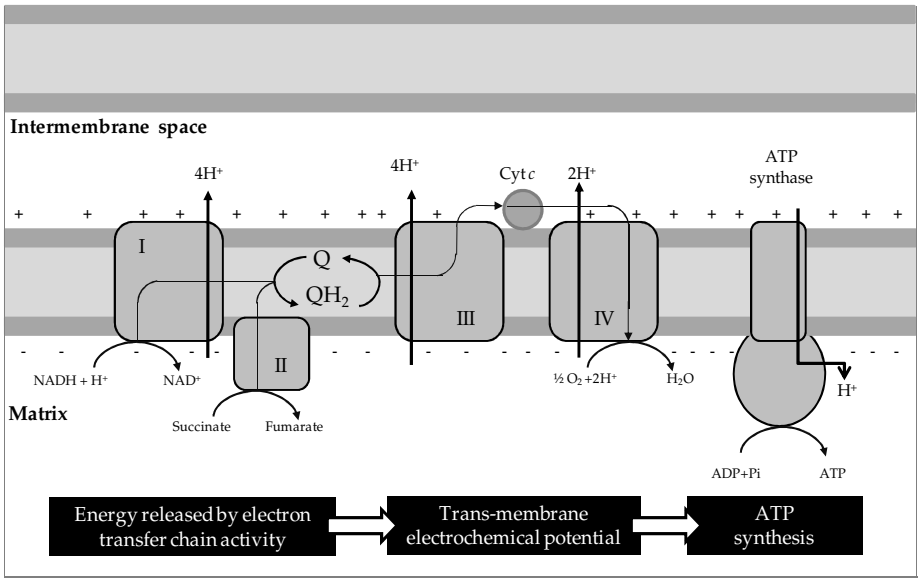

Figure 1.1

Generation of a transmembrane electrochemical potential by the mitochondrial electron transfer chain (complexes I-IV) coupled to the production of ATP by ATP synthase.

1.2 - Diversity and flexibility of the electron transfer respiratory chains

In general, electron transfer chains are composed by membrane bound enzymatic complexes with three different activities: electron donor:quinone oxidoreductase, quinol:electron carrier oxidoreductase and electron carrier: final electron acceptor oxidoreductase (figure 1.2). In prokaryotes the latter two complexes can be replaced by a quinol: final electron acceptor oxidoreductase complex. A quinone pool (Q/QH_2) and, in some cases, an electron carrier mediate the transfer of electrons between the enzymatic complexes. The mammalian respiratory chain (figures 1.1 and 1.3) is the most studied electron transfer chain being composed by four different complexes (named

complex I to IV) [4, 8]. The complex I and II have NADH: and succinate: quinone oxidoreductase activity, respectively. The dioxygen is the last electron acceptor being reduced to water by the complex IV (cytochrome aa_3 oxygen reductase) while the complex III (cytochrome bc_1 complex) transfers electrons from complexes I and II to complex IV, with quinones and cytochrome *c* as electron carriers. [1] Flavins (FMN or FAD), hemes (*a*, *b*, and *c*), iron-sulfur centers and copper ions are the redox centers present in the mitochondrial complexes.

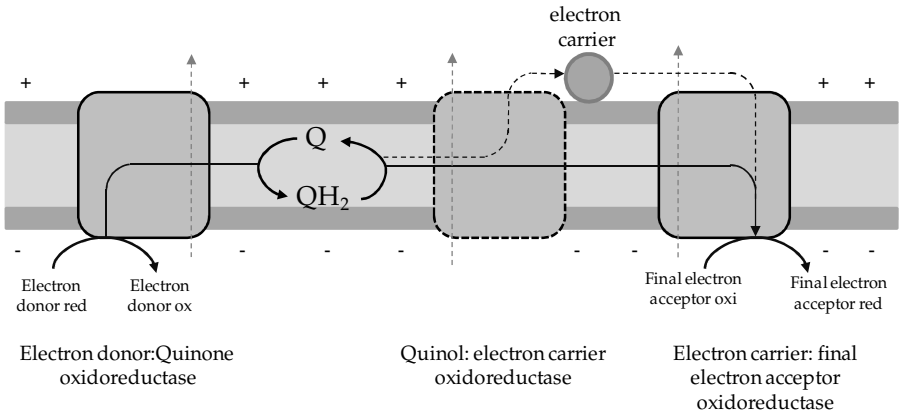

Figure 1.2

General schematic representation of electron transfer respiratory chains. The quinol: electron carrier oxidoreductase path can be suppressed by the transfer of electrons directly from the quinone/quinol pool to a quinol: final electron acceptor oxidoreductase complex. Adapted from [9].

Although mammalian mitochondria present a simple respiratory chain, some diversity is observed with the presence of several electron donor:quinone oxidoreductases. Besides the complex I and complex II, an electron transfer flavoprotein-ubiquinone oxidoreductase and an α-glycero-phosphate dehydrogenase are also responsible for the supply of electrons into the quinone pool [1]. It is worth mentioning that plant mitochondria have an alternative path, in which a so-called alternative

oxidase (quinol: dioxygen oxidoreductase) may act as the last electron accepting complex; also, plant mitochondria have a type II (or alternative) NADH: quinone oxidoreductase. Both these alternatives complexes do not couple electron transfer to charge translocation/separation, and thus energy is lost in the form of heat [10-12].

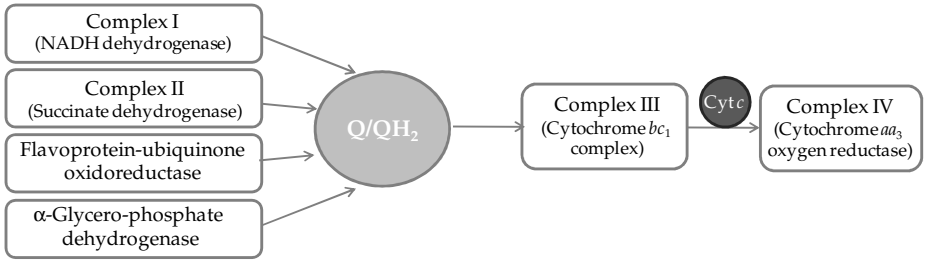

Figure 1.3

Schematic representation of the flexibility presented by the mammalian electron transfer respiratory chain. The ubiquinone/ubiquinol pool is the link between the quinone reductases (complex I, complex II, flavoprotein-ubiquinone oxidoreductase and α-glycero-phosphate dehydrogenase) and cytochrome bc_1 complex. The final electron acceptor, dioxygen, is reduced by complex IV which has received the electrons from cytochrome *c*.

The respiratory chains of prokaryotic organisms are more robust than mitochondrial ones since they have several alternative pathways. The ability of these organisms to use different electron donors and final acceptors depending on the growth conditions contributes for the diversity and flexibility observed on their respiratory chains. Therefore, the same organism can present different electron transfer complex composition depending on its growth conditions. The type of quinone and electron carrier expressed may also depend on those conditions. Analogous complexes to the mitochondrial ones are observed in prokaryotes; however, they are simpler having fewer polypeptide chains.

The respiratory chain of *Escherichia coli* is the most studied and a good example of the diversity and flexibility of prokaryotic respiratory chains [4, 13, 14]. *E. coli* is one of the cases where a complex with quinol: final acceptor oxidoreductase replaces the quinol: electron carrier oxidoreductase complex (cytochrome bc_1 complex), which is absent. Hence, in this bacterium the quinone/quinol pool is the link

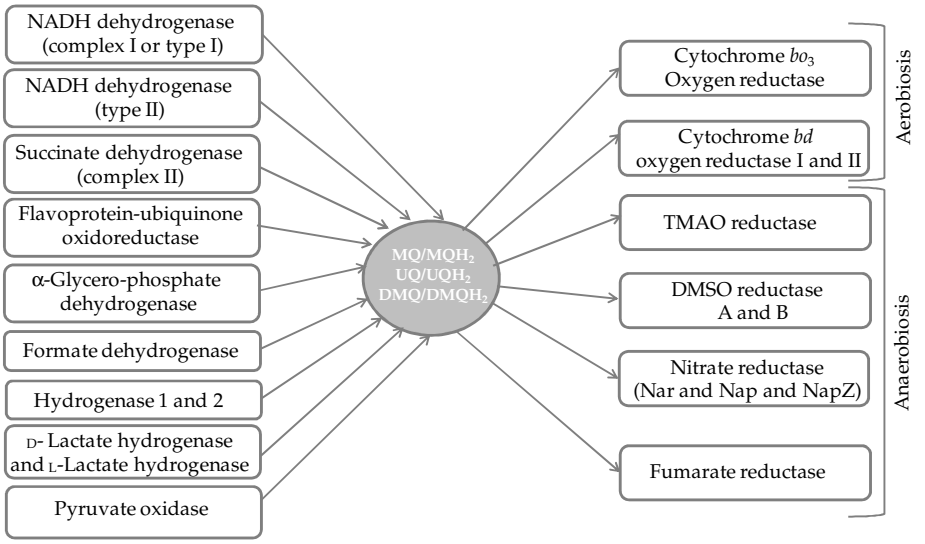

Figure 1.4

Schematic representation of the *Escherichia coli* electron transfer respiratory chain as an example of the high diversity and robustness of respiratory chains. In aerobic conditions NADH dehydrogenase II together with quinol oxidases are expressed and ubiquinone (UQ/UQH_2) mediates the electron transfer. In anaerobiosis the nitrate is the preferred final electron acceptor. MQ, menaquinone; DMQ, dimethylmenoquinone.

between 15 primary dehydrogenases and 10 terminal reductases [14]. *E. coli* is able to grow in diverse oxygen concentrations including total anaerobiosis using nitrate, nitrite, dimethylsulphoxide (DMSO), trimethylamine N-oxide (TMAO) and fumarate as electron acceptors. NADH, succinate, glycerol-3-phosphate, H_2, formate, piruvate, and lactate are the possible electron donors [13, 14]. The expression of the different enzymes is induced by the growth conditions and it was

observed that dioxygen represses the anaerobic respiratory pathways. In anaerobic conditions nitrate is the preferred electron acceptor. The expression of the three types of quinones also depends on the growth conditions being ubiquinone the most abundant quinone in aerobic conditions [15], while in anaerobic growth conditions naphthoquinones are preferred: menaquinone (MK) with fumarate or DMSO as electron acceptors and dimethylmenaquinone (DMK) with nitrate [16].

Additional electron donors can be used such as proline and malate as in the case of *Corynebacterium glutamicum* [17, 18], or sulfide as in the case of *Paracoccus denitrificans* [19]. A surprising aspect of the respiratory chain of the latter bacterium is its capacity to grow on methanol or methylamine as the carbon source, since methanol dehydrogenase and methylamine dehydrogenase transfer the electrons directly to the aa_3 oxygen reductase. In the case of methanol dehydrogenase the electron transfer occurs through cytochrome c_{551}, while in the case of methylamine dehydrogenase aminocyanin, a copper protein, mediates the transfer to the cytochrome c_{551} [4, 20].

The presence of different enzymes performing the same reaction is an additional evidence of the flexibility of the prokaryotic respiratory chains. An example is the existence of three enzymes with NADH: quinone oxidoreductase activity; besides a complex I

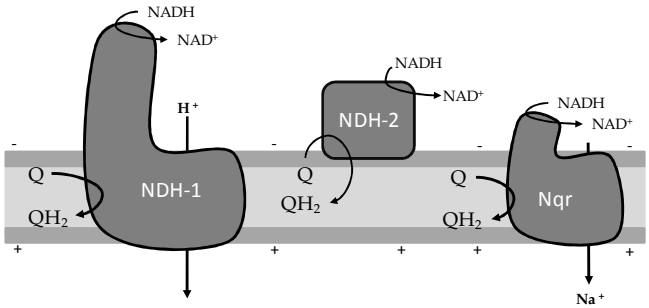

Figure 1.5
Schematic representation of the different types of NADH dehydrogenase.

analogue (NADH dehydrogenase type I, NDH1) [21], the presence of a so called alternative NADH dehydrogenase (type II, NDH-2), and NADH dehydrogenase type III (or Na^+- translocating NDH or Nqr) is also observed [22]. In addition to the cytochrome aa_3 oxygen reductase, more types of dioxygen reductases exist, and three different groups can be considered: heme-copper oxygen reductases [23, 24], cytochrome *bd* oxidases [25, 26] and alternative oxidases. The latter is believed to be exclusive of mitochondria; however, it was also found in α-proteobacteria [15, 27, 28].

Despite the large diversity, flexibility and robustness observed in the electron transfer respiratory chains, the cytochrome bc_1 complex was, until now, the only family of enzymes known to perform the quinol: electron carrier oxidoreductase activity (see 1.3.1).

In the work presented in this thesis a complex with quinol:electron carrier oxidoreductase activity which does not belong to the cytochrome bc_1 complex family was, for the first time, identified and characterized. Since this complex, named alternative complex III, is functionally related to the cytochrome bc_1 complex family but structurally related to the complex iron-sulfur molybdoenzymes (CISM) family, in the next section a brief introduction of the two families will be presented.

1.3 – Alternative complex III related complexes

1.3.1- Functionally related complexes - Cytochrome bc_1 complex family

Cytochrome bc_1 complexes, complexes III of mitochondria respiratory chain, are integral membrane proteins with quinol: cytochrome *c* oxidoreductase activity. The related cytochrome b_6f complexes are present in cyanobacteria and involved in the photosynthetic pathway in chloroplasts (for a recent review see [30]). A cytochrome *b*, a cytochrome c_1 and a Rieske iron sulfur subunit are the three catalytic subunits of this enzyme family (figure 1.6). The cytochrome *b* subunit has two *b*-type hemes, named b_H and b_L (H and L stand for high and low redox potential, respectively), and two quinone/quinol (Q/QH_2) binding sites located towards opposites sides of the membrane.

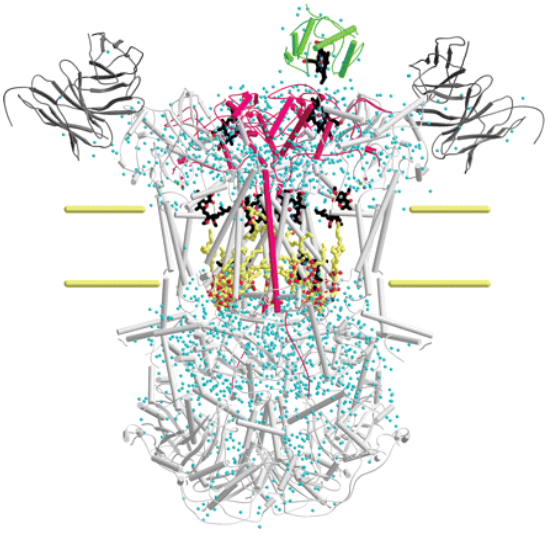

Figure 1.6

Structure of the *Saccharomyces cerevisiae* cytochrome bc_1 complex with bound cytochrome c in the reduced state at 1.9 Å resolution. One molecule of cytochrome *c* (*green*) binds to one of the cytochromes c_1 (*pink*) of the cytochrome bc_1 dimer (*light gray*). The protein was crystallized with antibody fragments (*dark gray*). Water molecules are shown in *cyan*. Lipid and detergent molecules are colored in *yellow* with oxygen atoms in *red*. Carbon and oxygen atoms of heme groups and stigmatellin are in *black* and *red*, respectively. *Yellow horizontal lines* indicate the relative position of the membrane. Image from [29].

The prokaryotic enzymes are composed only by these three subunits or in some cases have one extra subunit, whereas

the mitochondrial enzymes can have up to eleven subunits. Recently, Kramer, Nitschke and Cooley proposed to term these complexes as Rieske/cyt *b* (RB) complexes since they observed that only the Rieske protein and the cytochrome *b* subunits are conserved, while the cytochrome c_1 is not. This subunit was even considered to be a phylogenetic marker since each phylum has, apparently, its characteristic heme subunit. For example, the "standard" cytochrome c_1 is only present in α-, β- and γ-proteobacteria, whilst the ε-proteobacteria branch contains a diheme cytochrome *c* belonging to the cytochrome c_4 family. δ-proteobacteria have a tetraheme cytochrome c_3 and the major difference is observed for cyanobacteria where a cytochrome *f* is present (cytochrome b_6f) [31].

Although related to cytochrome bc_1 complexes, cytochrome b_6f complexes have additional prosthetic groups such as one chlorophyll *a*, one β-carotene and a heme c_n (also called c_i). The latter heme has a unique property which is the absence of an amino acid side chain as an axial ligand; instead heme c_n is positioned close to heme b_n and a water molecule or a OH^- group bridge the iron of c_n and the propionate of b_n [30, 32].

1.3.1.1- Q-cycle mechanism

The cytochrome bc_1 complexes couple the electron transfer to the translocation of protons through a Q-cycle mechanism (figure 1.7), first proposed by Peter Mitchell in the seventies [33, 34] who named it proton-motive Q cycle. Later modified versions were proposed taking into account the data obtained by x-ray and spectroscopic kinetic analysis. This cycle postulates the presence of two quinone binding sites in opposite sides of the membrane: a quinone oxidation site Q_o

(also called Q_P) located towards the outer or positive side of the membrane and a reduction site Q_i (also called Q_N) located close to the inner or negative side of the membrane. One of the most important features of this model is the oxidation of the quinol being proceed in two steps: in the first step one quinol molecule is oxidized in the Q_o site and one of the electrons is transferred to the cytochrome *c* through the FeS center and cytochrome c_1 ("high potential chain"), while the other electron is transferred through the cytochrome *b* (b_L and b_H) ("low potential chain") to the Q_i site where a quinone molecule is one electron reduced. In the second step a second quinol molecule is oxidized at the Q_o site and the electrons are transferred in a similar way. The quinone molecule at the Q_i site is totally reduced and a second cytochrome *c* molecule is reduced. In this process two protons are uptaken from the negative side of the membrane and four are delivered at the positive side contributing to the formation of the transmembrane electrochemical potential. Another important property of bc_1 complexes is the mobility of the peripheral arm of the Rieske protein. The available structures of the complex, determined several years after the Q-cycle was proposed, showed that the peripheral arm of the Rieske center is mobile [35]

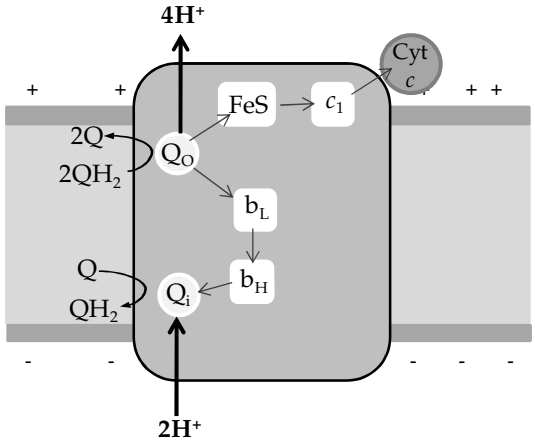

Figure 1.7

Q-cycle mechanism of cytochrome bc_1 complexes by which the electron transfer is coupled to proton translocation.

being able to move approximately 20Å. In the oxidized state the Rieske protein is close to the surface of the polypeptide near the Qo site. In the reduced state the interaction becomes weaker and the Rieske protein moves to a new position closer to the cytochrome c_1. After transferring the electrons to the cytochrome c_1 the Rieske protein returns to the oxidized state and the affinity for cytochrome c_1 becomes lower and thus the position near the Qo site is adopted again [4].

Even though the basic fundaments of the mechanism proposed by Peter Mitchell are still valid and accepted nowadays, several proposals have been made in order to overcome some unexplained details. One of those is that the modified Q-cycle mechanism was proposed considering the bc_1 complex as a one monomer only; however, structural information showed that, in fact, the bc_1 complexes are homodimers [29, 35, 37-44], and also the monomer of the complex is inactive [35, 45-49]. Therefore, it was questioned whether the Q-cycle was viable in the dimer or not. Mechanisms in which the peripheral arm of the Rieske protein of one monomer interacts with the catalytic interface of the other monomer (figure 1.8) and the *b*-type hemes of the two monomers are in close contact and a direct interaction between the active centers of each monomer were proposed [45, 50, 51]. Another issue is related to the formation of reactive oxygen species (ROS, which can lead to the damage of cellular components) due to the high reactivity of the semiquinone intermediates, formed during the Q-cycle, with oxygen. Several studies were performed with the intent of detecting the semiquinone radical, but these turned out to be unsuccessful [52-55]. The investigation of how those side reactions are

avoided was also the aim of several studies and different types of mechanism were proposed. The gated and the double gated

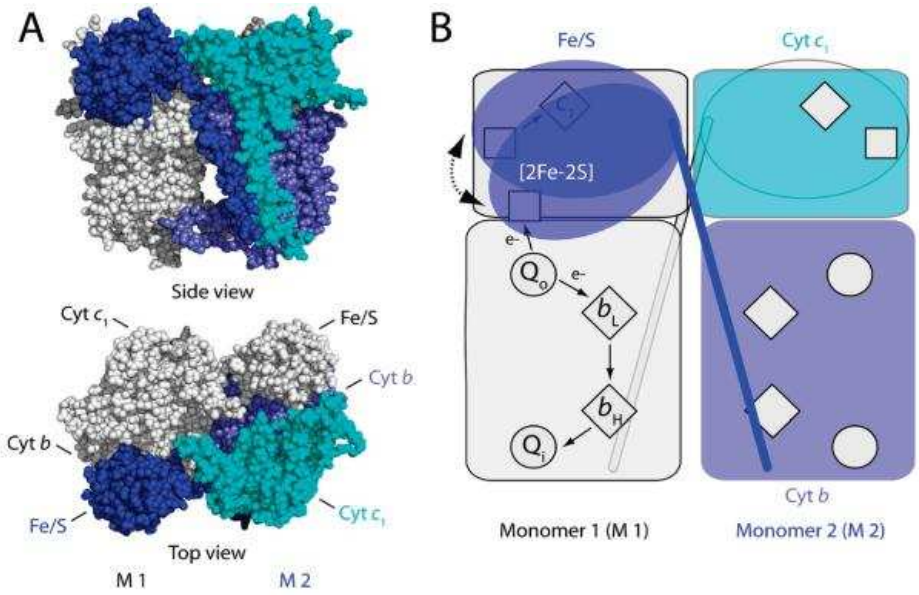

Figure 1.8

Structure of the dimeric cytochrome bc_1 from *Rhodobacter capsulatus* and its components. A) Both a side view (top) and a top view (bottom) of the dimeric cyt bc_1 are shown using space-filling representations. Three subunits of one monomer (M2, right) representing the cytochrome b, the cytochrome c_1, and the Fe/S protein are in slate, cyan, and blue, whereas those of the other monomer (M1, left) are in white and gray. (B) Modified Q-cycle mechanism of cytochrome bc_1. The three catalytic subunits (cyt b, cyt c_1, and Fe/S), the cofactors (hemes b_L, b_H, and c_1, shown as diamonds, and the [2Fe-2S] cluster as a square), and the active sites (Q_o and Q_i, shown as circles) of the cytochrome bc_1 are represented schematically. Electron transfer (e^-) steps catalyzed by the enzyme via the bifurcation reaction at the Q_o site are shown with black arrows on the monomer 1(M1) only. The dashed arrows refer to the mobility of the extrinsic domain of the Fe/S protein. From [36].

mechanisms are based on the allowance or not of an electron transfer to occur depending on the reduction state of the redox partner. For example, in a double gated mechanism the oxidation of the quinol is only allowed when the Rieske protein and the heme b_L are both oxidized. In a concerted mechanism the two electrons from the quinol are transferred to the Rieske protein and to heme b_L at the same time

and therefore the formation of the semiquinone is completely avoided. Another type of proposal takes into account the stabilization of the semiquinone radical making the reaction with oxygen an endoenergetic reaction. However, these mechanisms are difficult to validate since the intermediates of Qo site were never detected [56-59].

1.3.1.2- Inhibitors

Several compounds were described as inhibitors of bc_1 complexes, being associated to the Q_o site. Antimycin was the only one observed to be associated to the Q_i site. The Q_o site inhibitors were classified in class I and II according to the distance of their binding position to the heme b_L; class I (such as stigmatellin and HHDBT) bind to a domain distal from heme b_L and interact with the FeS center, class II (such as mixothiazol and MOA-stilbene) bind to a domain proximal to the heme b_L. The local where NQNO (or HQNO) binds is still controversial, since although it has been described to bind to the Q_i site [60], in the structure of the bovine mitochondrial bc_1 complex this inhibitor was identified in the two quinone sites (Q_o and Q_i sites) [61].

1.3.2 - Structurally related complexes – Complex iron-sulfur molybdoenzyme (CISM) family

Complex iron-sulfur molybdoenzyme (CISM) is an important family of molybdenum containing enzymes that play a crucial role in supporting respiratory diversity. This family includes enzymes such as DMSO reductase, polysulfide reductase, formate dehydrogenase and nitrate reductase.

The overall composition of the members of this family comprises three subunits: a catalytic subunit, a four cluster protein (FCP) subunit and a membrane anchor protein (MAP) [63]. These subunits are also designated as α, β and γ subunits, respectively [64]. Besides the overall composition, all the CISM family members interact with quinones (or quinols). A remarkable feature of this family is the diversity observed in the orientation of the catalytic and FCP subunits in respect to the membrane. This orientation is dependent of the presence of a twin arginine translocase (*tat*) leader sequence [65, 66] in the N-terminus of the catalytic subunit [63]. In its presence, the catalytic and the FCP subunits are transported across the cytoplasmic membrane into the periplasmic space. In figure 1.9 are represented the structures of two

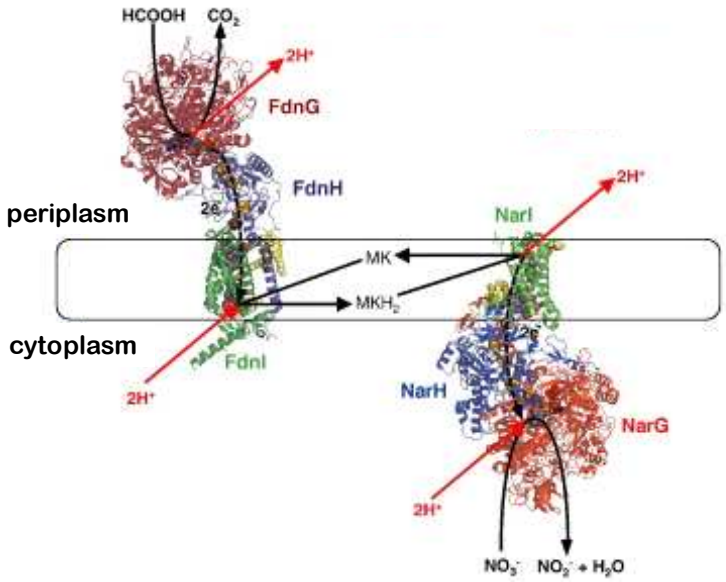

Figure 1.9

Structures of the CISM family members: nitrate reductase (NarGHI) and formate reductase (FdnGHI) from *Escherichia coli* oriented towards opposite sides of the membrane and therefore creating a redox loop. Adapted from [62].

CISM family members, nitrate reductase (NarGHI) and formate reductase (FdnGHI) that have the catalytic and FCP subunits oriented towards opposite sides of the membrane. In this case, the two enzymes interact by means of the quinol pool creating a redox loop [62, 67] where two protons are translocated across the membrane contributing to the electrochemical membrane potential. Even for the same enzyme, this diversity in the enzyme orientation may exist; for example, it was observed that the nitrate reductase (NarGHI) depending on the organisms, can adopt one or the other orientation [64].

The catalytic subunit has the Mo-*bis*PGD (molybdo-*bis*(pyranopterin guanine dinucleotide) (figure 1.10) and can also have a $[4Fe\text{-}4S]^{2+/1+}$ cluster (named FS0) located in the N-terminus of the subunit and close to the Mo-*bis*PGD cofactor. The FCP subunit contains four $[4Fe\text{-}4S]^{2+/1+}$ centers named FS1 to FS4 in sequence according to the increasing distance to the catalytic subunit. These Fe-S centers are coordinated by four Cys residues ($C_AxxC_Bx_{2\text{-}11}C_CC_DP$). A $[3Fe\text{-}4S]^{1+/0}$ center replaces the $[4Fe\text{-}4S]^{2+/1+}$ FS4 in NarH of nitrate reductase A [69].

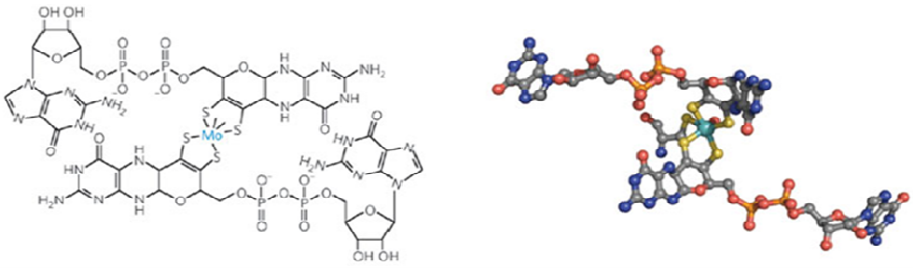

Figure 1.10

Chemical and three dimensional structure of the molybdo-bis(pyranopterin guanine dinucleotide) (Mo-bisPGD). The three dimensional structure is represented in ball and stick presentation (cyan-Mo, grey-C, red-O, yellow- S, brown- Fe, blue-N). Adapted from [68].

The MAP subunit is responsible for the anchoring of the catalytic and FCP subunits to the membrane and also provides a redox quinol/quinone–binding site. This subunit is the one that presents less similarity within the members of this family. The differences reside in the size of the sequence, the number of transmembrane helices, in the presence or absence of two *b*-types hemes and in the amino acid sequence.

The FS0 of the catalytic subunit and FS1-FS4 of the FCP subunit are described to mediate the electron transfer between the Mo-*bis*PGD and the quinone/quinol binding site in the MAP subunit [63].

1.3.2.1- CISM family related complexes

The subunits of the CISM family can be also found as components of other enzymes. The *Rhodovulum sulfidovilum* dimethyl sulfide dehydrogenase (DdhABC) [70, 71] is one example in which the catalytic dimer, formed by the catalytic and FCP subunits, exists without the MAP subunit. Interestingly, DdhC has also two *b*-type hemes but it is not membrane bound. The catalytic subunit can also be found isolated as in the case of TMAO reductase (TorA) [72-74], conjugated with other subunit as a Rieske center containing subunit as in the case of arsenite oxidase (AoxAB)[75], or with a diheme cytochrome *c* as observed for the periplasmatic nitrate reductase (NapAB) [76-78]. In cytochrome *c* Nitrite reductase (NrfABCD) enzyme, the MAP subunit (NrfD) forms a complex with the FCP subunit (NrfC) and with two pentaheme cytochrome c subunits (NrfA and NrfB) [79].

1.4- References

1. Saraste, M., *Oxidative phosphorylation at the fin de siecle.* Science, 1999. **283**(5407): p. 1488-93.
2. Nelson, D.L. and M.M. Cox, *Lehninger Principles of Biochemistry*. 4 ed. 2000: W.H. Freeman.
3. Cramer, W.A. and G.M. Soriano, *Thermodynamics of energy transduction in biological membranes*. 2002: Cramer and Soriano.
4. Nicholls, S.J.F.a.D.G., *Bioenergetics 3*. 2002: Academic Press.
5. Morange, M., *What history tells us. XI. The complex history of the chemiosmotic theory.* J Biosci, 2007. **32**(7): p. 1245-50.
6. Rich, P.R., *A perspective on Peter Mitchell and the chemiosmotic theory.* J Bioenerg Biomembr, 2008. **40**(5): p. 407-10.
7. Wrigglesworth, J., *Energy and Life*. 1997, London: Taylor and Francis.
8. Nelson, M.C.a.D.L., *Lehninger Principles of Biochemistry*. 2005: WH Freeman
9. Pereira, M.M., et al., *Respiratory chains from aerobic thermophilic prokaryotes.* J Bioenerg Biomembr, 2004. **36**(1): p. 93-105.
10. Rasmusson, A.G., D.A. Geisler, and I.M. Moller, *The multiplicity of dehydrogenases in the electron transport chain of plant mitochondria.* Mitochondrion, 2008. **8**(1): p. 47-60.
11. Rasmusson, A.G., H. Handa, and I.M. Moller, *Plant mitochondria, more unique than ever.* Mitochondrion, 2008. **8**(1): p. 1-4.
12. Richardson, D. and G. Sawers, *Structural biology. PMF through the redox loop.* Science, 2002. **295**(5561): p. 1842-3.
13. Richardson, D.J., *Bacterial respiration: a flexible process for a changing environment.* Microbiology, 2000. **146 (Pt 3)**: p. 551-71.
14. Unden, G. and J. Bongaerts, *Alternative respiratory pathways of Escherichia coli: energetics and transcriptional regulation in response to electron acceptors.* Biochim Biophys Acta, 1997. **1320**(3): p. 217-34.

15. Suzuki, T., et al., *Alternative oxidase (AOX) genes of African trypanosomes: phylogeny and evolution of AOX and plastid terminal oxidase families.* J Eukaryot Microbiol, 2005. **52**(4): p. 374-81.
16. Unden, G., *Differential roles for menaquinone and demethylmenaquinone in anaerobic electron transport of E. coli and their fnr-independent expression.* Arch Microbiol, 1988. **150**(5): p. 499-503.
17. Bott, M. and A. Niebisch, *The respiratory chain of Corynebacterium glutamicum.* J Biotechnol, 2003. **104**(1-3): p. 129-53.
18. Kalinowski, J., et al., *The complete Corynebacterium glutamicum ATCC 13032 genome sequence and its impact on the production of L-aspartate-derived amino acids and vitamins.* J Biotechnol, 2003. **104**(1-3): p. 5-25.
19. Schütz, M., et al., *Sulfide-quinone reductase activity in membranes of the chemotrophic bacterium Paracoccus denitrificans GB17.* Arch Microbiol, 1998. **170**: p. 353–360.
20. Baker, S.C., et al., *Molecular genetics of the genus Paracoccus: metabolically versatile bacteria with bioenergetic flexibility.* Microbiol Mol Biol Rev, 1998. **62**(4): p. 1046-78.
21. Brandt, U., *Energy converting NADH:quinone oxidoreductase (complex I).* Annu Rev Biochem, 2006. **75**: p. 69-92.
22. Kerscher, S., et al., *The Three Families of Respiratory NADH Dehydrogenases*, in *Bio*. 2007, Springer. p. 185-222.
23. Pereira, M.M., et al., *Looking for the minimum common denominator in haem-copper oxygen reductases: towards a unified catalytic mechanism.* Biochim Biophys Acta, 2008. **1777**(7-8): p. 929-34.
24. Pereira, M.M. and M. Teixeira, *Proton pathways, ligand binding and dynamics of the catalytic site in haem-copper oxygen reductases: a comparison between the three families.* Biochim Biophys Acta, 2004. **1655**(1-3): p. 340-6.
25. Bloch, D.A., et al., *Heme/heme redox interaction and resolution of individual optical absorption spectra of the hemes in cytochrome bd from Escherichia coli.* Biochim Biophys Acta, 2009. **1787**(10): p. 1246-53.

26. Junemann, S., *Cytochrome bd terminal oxidase.* Biochim Biophys Acta, 1997. **1321**(2): p. 107-27.
27. Atteia, A., et al., *Identification of prokaryotic homologues indicates an endosymbiotic origin for the alternative oxidases of mitochondria (AOX) and chloroplasts (PTOX).* Gene, 2004. **330**: p. 143-8.
28. Stenmark, P. and P. Nordlund, *A prokaryotic alternative oxidase present in the bacterium Novosphingobium aromaticivorans.* FEBS Lett, 2003. **552**(2-3): p. 189-92.
29. Lange, C. and C. Hunte, *Crystal structure of the yeast cytochrome bc_1 complex with its bound substrate cytochrome c.* Proc Natl Acad Sci U S A, 2002. **99**(5): p. 2800-5.
30. Baniulis, D., et al., *Structure-function of the cytochrome b_6f complex.* Photochem Photobiol, 2008. **84**(6): p. 1349-58.
31. Kramer, D.M., W. Nitschke, and J.W. Cooley, *The cytochrome bc_1 and related bc complexes: The Rieske/Cytochrome b Complex as the Functional Core of a Central Electron/Proton Transfer Complex*, in *The Purple Phototrophic Bacteria*, C.N. Hunter, et al., Editors. 2009, Springer Science and Business MediaB.V. p. 451-473.
32. Stroebel, D., et al., *An atypical haem in the cytochrome b(6)f complex.* Nature, 2003. **426**(6965): p. 413-8.
33. Mitchell, P., *Protonmotive redox mechanism of the cytochrome b-c_1 complex in the respiratory chain: protonmotive ubiquinone cycle.* FEBS Lett, 1975. **56**(1): p. 1-6.
34. Mitchell, P., *Possible molecular mechanisms of the protonmotive function of cytochrome systems.* J Theor Biol, 1976. **62**(2): p. 327-67.
35. Zhang, Z., et al., *Electron transfer by domain movement in cytochrome bc_1.* Nature, 1998. **392**(6677): p. 677-84.
36. Cooley, J.W., D.W. Lee, and F. Daldal, *Across membrane communication between the Q(o) and Q(i) active sites of cytochrome bc(1).* Biochemistry, 2009. **48**(9): p. 1888-99.

37. Berry, E.A., et al., *A new crystal form of bovine heart ubiquinol: cytochrome c oxidoreductase: determination of space group and unit-cell parameters.* Acta Crystallogr D Biol Crystallogr, 1995. **51**(Pt 2): p. 235-9.

38. Xia, D., et al., *Crystal structure of the cytochrome bc_1 complex from bovine heart mitochondria.* Science, 1997. **277**(5322): p. 60-6.

39. Iwata, S., et al., *Complete structure of the 11-subunit bovine mitochondrial cytochrome bc_1 complex.* Science, 1998. **281**(5373): p. 64-71.

40. Berry, E.A., et al., *Structure of the avian mitochondrial cytochrome bc_1 complex.* J Bioenerg Biomembr, 1999. **31**(3): p. 177-90.

41. Iwata, M., J. Bjorkman, and S. Iwata, *Conformational change of the Rieske [2Fe-2S] protein in cytochrome bc_1 complex.* J Bioenerg Biomembr, 1999. **31**(3): p. 169-75.

42. Berry, E.A., et al., *Crystallographic location of two Zn(2+)-binding sites in the avian cytochrome bc(1) complex.* Biochim Biophys Acta, 2000. **1459**(2-3): p. 440-8.

43. Hunte, C., et al., *Structure at 2.3 A resolution of the cytochrome bc(1) complex from the yeast Saccharomyces cerevisiae co-crystallized with an antibody Fv fragment.* Structure, 2000. **8**(6): p. 669-84.

44. Solmaz, S.R. and C. Hunte, *Structure of complex III with bound cytochrome c in reduced state and definition of a minimal core interface for electron transfer.* J Biol Chem, 2008. **283**(25): p. 17542-9.

45. Covian, R. and B.L. Trumpower, *Rapid electron transfer between monomers when the cytochrome bc_1 complex dimer is reduced through center N.* J Biol Chem, 2005. **280**(24): p. 22732-40.

46. Gong, X., et al., *Evidence for electron equilibrium between the two hemes b_L in the dimeric cytochrome bc_1 complex.* J Biol Chem, 2005. **280**(10): p. 9251-7.

47. Huang, D., et al., *Characterization of the chloroplast cytochrome b_6f complex as a structural and functional dimer.* Biochemistry, 1994. **33**(14): p. 4401-9.

48. Yu, C.A., et al., *Three-dimensional structure and functions of bovine heart mitochondrial cytochrome bc_1 complex.* Biofactors, 1998. **8**(3-4): p. 187-9.
49. Yu, C.A., et al., *Structural basis of functions of the mitochondrial cytochrome bc_1 complex.* Biochim Biophys Acta, 1998. **1365**(1-2): p. 151-8.
50. Covian, R. and B.L. Trumpower, *Regulatory interactions in the dimeric cytochrome bc(1) complex: the advantages of being a twin.* Biochim Biophys Acta, 2008. **1777**(9): p. 1079-91.
51. Crofts, A.R., et al., *The Q-cycle reviewed: How well does a monomeric mechanism of the bc(1) complex account for the function of a dimeric complex?* Biochim Biophys Acta, 2008. **1777**(7-8): p. 1001-19.
52. Cape, J.L., M.K. Bowman, and D.M. Kramer, *A semiquinone intermediate generated at the Qo site of the cytochrome bc_1 complex: importance for the Q-cycle and superoxide production.* Proc Natl Acad Sci U S A, 2007. **104**(19): p. 7887-92.
53. de Vries, S., et al., *A new species of bound ubisemiquinone anion in QH_2: cytochrome c oxidoreductase.* J Biol Chem, 1981. **256**(23): p. 11996-8.
54. Junemann, S., P. Heathcote, and P.R. Rich, *On the mechanism of quinol oxidation in the bc_1 complex.* J Biol Chem, 1998. **273**(34): p. 21603-7.
55. Zhang, H., et al., *Exposing the complex III Qo semiquinone radical.* Biochim Biophys Acta, 2007. **1767**(7): p. 883-7.
56. Cape, J.L., M.K. Bowman, and D.M. Kramer, *Understanding the cytochrome bc complexes by what they don't do. The Q-cycle at 30.* Trends Plant Sci, 2006. **11**(1): p. 46-55.
57. Chobot, S.E., et al., *Breaking the Q-cycle: finding new ways to study Qo through thermodynamic manipulations.* J Bioenerg Biomembr, 2008. **40**(5): p. 501-7.
58. Crofts, A.R., et al., *Proton pumping in the bc_1 complex: a new gating mechanism that prevents short circuits.* Biochim Biophys Acta, 2006. **1757**(8): p. 1019-34.
59. Osyczka, A., C.C. Moser, and P.L. Dutton, *Fixing the Q cycle.* Trends Biochem Sci, 2005. **30**(4): p. 176-82.

60. Van Ark, G. and J.A. Berden, *Binding of HQNO to beef-heart sub-mitochondrial particles.* Biochim Biophys Acta, 1977. **459**(1): p. 119-27.

61. Gao, X., et al., *Structural basis for the quinone reduction in the bc_1 complex: a comparative analysis of crystal structures of mitochondrial cytochrome bc_1 with bound substrate and inhibitors at the Qi site.* Biochemistry, 2003. **42**(30): p. 9067-80.

62. Simon, J., R.J. van Spanning, and D.J. Richardson, *The organisation of proton motive and non-proton motive redox loops in prokaryotic respiratory systems.* Biochim Biophys Acta, 2008. **1777**(12): p. 1480-90.

63. Rothery, R.A., G.J. Workun, and J.H. Weiner, *The prokaryotic complex iron-sulfur molybdoenzyme family.* Biochim Biophys Acta, 2008. **1778**(9): p. 1897-929.

64. Martinez-Espinosa, R.M., et al., *Look on the positive side! The orientation, identification and bioenergetics of 'Archaeal' membrane-bound nitrate reductases.* FEMS Microbiol Lett, 2007. **276**(2): p. 129-39.

65. Lee, P.A., D. Tullman-Ercek, and G. Georgiou, *The bacterial twin-arginine translocation pathway.* Annu Rev Microbiol, 2006. **60**: p. 373-95.

66. Natale, P., T. Bruser, and A.J. Driessen, *Sec- and Tat-mediated protein secretion across the bacterial cytoplasmic membrane--distinct translocases and mechanisms.* Biochim Biophys Acta, 2008. **1778**(9): p. 1735-56.

67. Jormakka, M., B. Byrne, and S. Iwata, *Protonmotive force generation by a redox loop mechanism.* FEBS Lett, 2003. **545**(1): p. 25-30.

68. Schwarz, G., R.R. Mendel, and M.W. Ribbe, *Molybdenum cofactors, enzymes and pathways.* Nature, 2009. **460**(7257): p. 839-47.

69. Guigliarelli, B., et al., *Complete coordination of the four Fe-S centers of the beta subunit from Escherichia coli nitrate reductase. Physiological, biochemical, and EPR characterization of site-directed mutants lacking the highest or lowest potential [4Fe-4S] clusters.* Biochemistry, 1996. **35**(15): p. 4828-36.

70. Hanlon, S.P., et al., *Dimethylsulfide:acceptor oxidoreductase from Rhodobacter sulfidophilus. The purified enzyme contains b-type haem and a pterin molybdenum cofactor.* Eur J Biochem, 1996. **239**(2): p. 391-6.

71. McDevitt, C.A., et al., *Molecular analysis of dimethyl sulphide dehydrogenase from Rhodovulum sulfidophilum: its place in the dimethyl sulphoxide reductase family of microbial molybdopterin-containing enzymes.* Mol Microbiol, 2002. **44**(6): p. 1575-87.

72. Ansaldi, M., et al., *Aerobic TMAO respiration in Escherichia coli.* Mol Microbiol, 2007. **66**(2): p. 484-94.

73. Mejean, V., et al., *TMAO anaerobic respiration in Escherichia coli: involvement of the tor operon.* Mol Microbiol, 1994. **11**(6): p. 1169-79.

74. Zhang, L., et al., *Structure of the molybdenum site of Escherichia coli trimethylamine N-oxide reductase.* Inorg Chem, 2008. **47**(3): p. 1074-8.

75. Ellis, P.J., et al., *Crystal structure of the 100 kDa arsenite oxidase from Alcaligenes faecalis in two crystal forms at 1.64 A and 2.03 A.* Structure, 2001. **9**(2): p. 125-32.

76. Coelho, C., et al., *Heterodimeric nitrate reductase (NapAB) from Cupriavidus necator H16: purification, crystallization and preliminary X-ray analysis.* Acta Crystallogr Sect F Struct Biol Cryst Commun, 2007. **63**(Pt 6): p. 516-9.

77. Potter, L.C., et al., *Competition between Escherichia coli strains expressing either a periplasmic or a membrane-bound nitrate reductase: does Nap confer a selective advantage during nitrate-limited growth?* Biochem J, 1999. **344 Pt 1**: p. 77-84.

78. Stewart, V., Y. Lu, and A.J. Darwin, *Periplasmic nitrate reductase (NapABC enzyme) supports anaerobic respiration by Escherichia coli K-12.* J Bacteriol, 2002. **184**(5): p. 1314-23.

79. Clarke, T.A., et al., *Purification and spectropotentiometric characterization of Escherichia coli NrfB, a decaheme homodimer that transfers electrons to the decaheme periplasmic nitrite reductase complex.* J Biol Chem, 2004. **279**(40): p. 41333-9.

Chapter 2

Rhodothermus marinus
electron transfer respiratory chain

2.1- Rhodothermus marinus

Rhodothermus (R.) marinus (figure 2.1) was isolated for the first time from shallow marine hot springs in Iceland by Alfredsson and coworkers [1] and later was also found in shallow marine hot springs in Praia da Ribeira Quente, Azores, Portugal [2]. It is a strict aerobic, heterotrophic, thermohalophilic Gram-negative bacterium which grows optimally at 65 ºC, pH 7 and at 1-2 % of NaCl [1, 2].

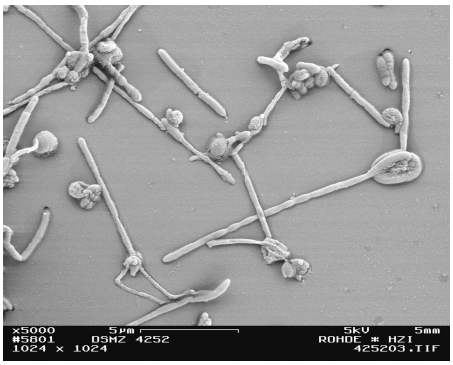

Figure 2.1
Rhodothermus marinus DMS4252 cells (from www.jgi.doe.gov)

Comparison of the 16S rRNA gene sequence placed *Rhodothermus* close to the root of the *Flexibacter-Cytophaga-Bacteroides* (FCB) group with affinities to green sulphur bacteria, fibrobacteria and spirochaetes [1]. The recently defined *Bacteroidetes* phylum substituted the former FBC group and *R. marinus* was included as member of the *Crenotrichacea* family within the *Sphingobacteria* class (figure 2.2) [3]. Within *Bacteroidetes*, *Rhodothermus* and *Thermonema* are the only described thermophilic species while *Salinibacter ruber* (close relative to *R. marinus*) is an extreme halophile and *Toxothrix trichogenes* is a psychrophile.

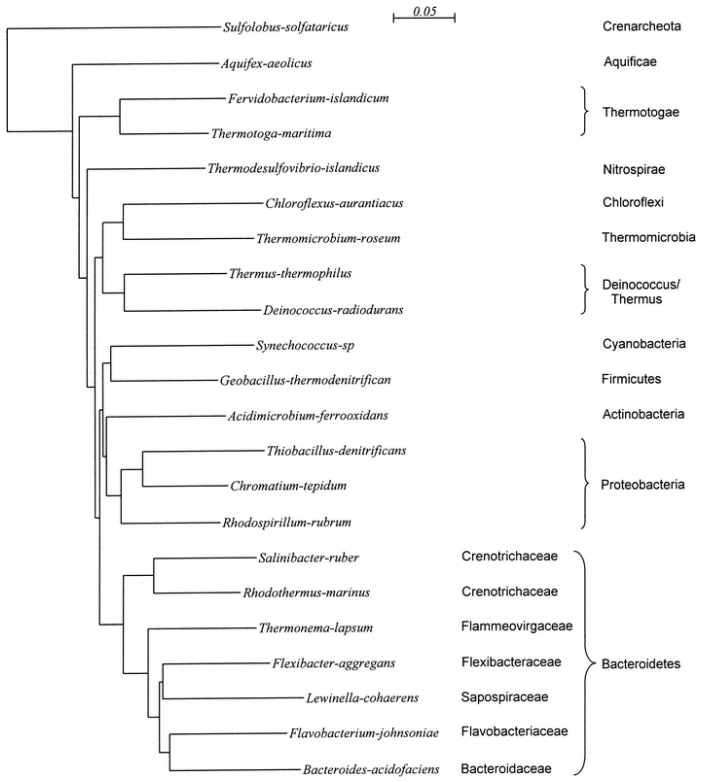

Figure 2.2

Phylogenetic position of *Rhodothermus marinus*. From [3].

2.2- *Rhodothermus marinus respiratory chain*

Rhodothermus marinus has been extensively studied and most of the known enzymes of this bacterium were identified during screenings for thermostables enzymes with potential biotechnological application. The electron transfer respiratory chain of *R. marinus* has also been extensively studied, namely the identification, purification and characterization of its components. For that, a non-pigmented strain of *R. marinus*, PRQ-62B strain, is used.

The electrons enter the respiratory chain of *R. marinus* at the level of a typical complex I with NADH:quinone oxidoreductase activity. This

complex was isolated with a non-covalently bound FMN and six to eight iron sulfur centers of the $[2Fe\text{-}2S]^{2+/1+}$ and $[4Fe\text{-}4S]^{2+/1+}$ types were observed by EPR spectroscopy [4, 5]. This complex was, recently, described to have two translocation sites, one of which, translocates sodium ions in the opposite direction of protons [6]. A succinate: quinone oxidoreductase complex (complex II) is another entry point for the electrons. It is composed by three subunits (70, 32 and 18 kDa) and has a covalently bound FAD, 2 *b*-type hemes and three iron sulfur centers ($[2Fe\text{-}2S]^{2+/1+}$,$[4Fe\text{-}4S]^{2+/1+}$, and $[3Fe\text{-}4S]^{1+/0}$) [7, 8]. According to the proposed classification for the succinate: quinone oxidoreductases and quinol:fumarate oxidoreductases, complex II from *R. marinus* is a type B enzyme [9].

Three different oxygen reductases, a caa_3 [10, 11], a ba_3 [12] and a cbb_3 [13] belonging to the A2, B and C families of heme-copper oxygen reductases, respectively, have been also characterized. The caa_3 oxygen reductase is composed by four subunits with apparent molecular masses of 42, 35, 19 and 15 kDa. It has a *c*- and two *a*-type hemes with redox potentials of 260, 255 and 180 mV, respectively [10]. The cbb_3 oxygen reductase was purified as a five subunits complex with apparent molecular masses of 64, 57, 36, 26 and 13 kDa. Two low-spin *c*-type heme (26 kDa subunit) and one low- and one high-spin *b*-type hemes were observed in this enzyme with redox potentials ranging from -50 to +195 mV [13]. The ba_3 oxygen reductase was isolated with two subunits with apparent molecular masses of 42 and 38 kDa. The heme content of the enzyme comprises a low-spin *b*-type heme and a high-spin *a*-type heme [12]. A periplasmatic cytochrome *c* [14] and a membrane-bound HiPIP (high-potential iron-sulfur protein) [15-17]

were described as the electron transfer proteins. The quinone pool is composed in its majority by menaquinone-7 [18].

The three oxygen reductases present in this bacterium are oxidases of periplasmatic electron carriers, being unable to receive electrons directly from reduced quinones. Therefore, the presence of a bc_1 complex or an analogue with quinol: periplasmatic electron carrier oxidoreductase activity is required to link complex I and II to complex IV. To investigate the presence of a cytochrome bc_1 complex, genomic and biochemical searches for a Rieske centre were performed, without success. Furthermore, the typical inhibitors of bc_1 complexes such as antimycin A, mixothiazol and DBMIB, showed to have no effect in *R. marinus* electron transfer respiratory chain [15, 19]. In fact, a complex with menadiol:HiPIP oxidoreductase activity [16] was purified from *R. marinus* membranes [19]. It was proposed to be a multihemic cytochrome complex containing at least five low-spin heme centers (figure 2.3A). Spectroscopic data strongly suggested that two of the hemes are in van

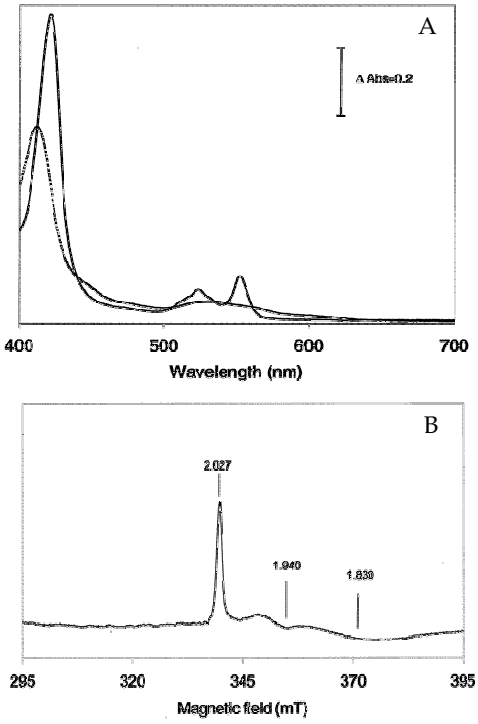

Figure 2.3

The redox cofactors of *R. marinus* complex III Upper- Visible spectra of oxidized (---) and reduced (—) *R. marinus* complex III with the characteristic fingerprints of cytochromes. Down- EPR spectrum of the [3Fe-4S] center [19].

der Waals contact, yielding a split Soret band. EPR spectra of the oxidized complex showed resonances of five low-spin ferric heme centers and of a [3Fe-4S]$^{1+/0}$ centre (figure 2.3B), which has a high reduction potential of +140 mV. The hemes have reduction potentials in the range of -45 to +235 mv [20].

The further and deep characterization of this different complex III present in the *Rhodothermus marinus* respiratory chain (figure 2.4) was the aim of the work presented in this dissertation.

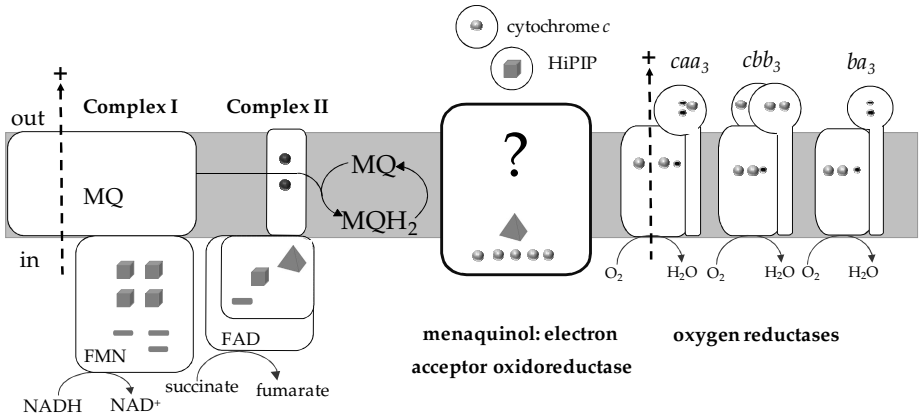

Figure 2.4

Rhodothermus marinus electron transfer respiratory chain. The gray and black spheres represent *c*- and *b*-type hemes, respectively, while the smaller spheres represent copper ions. Cubes, pyramids and rectangles represent [4Fe-4S]$^{2+/1+}$, [3Fe-4S]$^{1+/0}$ and [2Fe-2S]$^{2+/1+}$ centers, respectively.

2.3- References

1. Alfredsson, G.A., et al., *Rhodothermus marinus, gen. nov., sp. nov., a thermophilic, halophilic bacterium from submarin hot springs in Iceland.* J. Gen Microbiol., 1988. **134**: p. 299-306.

2. Nunes, O.C., M.M. Donato, and M.S. da Costa, *Isolation and characterization of Rhodothermus strains from S. Miguel, Azores.* Syst. Appl. Microbiol., 1992. **15**: p. 92-97.
3. Bjornsdottir, S.H., et al., *Rhodothermus marinus: physiology and molecular biology.* Extremophiles, 2006. **10**(1): p. 1-16.
4. Fernandes, A.S., M.M. Pereira, and M. Teixeira, *Purification and characterization of the complex I from the respiratory chain of Rhodothermus marinus.* J Bioenerg Biomembr, 2002. **34**(6): p. 413-21.
5. Fernandes, A.S., et al., *Electron paramagnetic resonance studies of the iron-sulfur centers from complex I of Rhodothermus marinus.* Biochemistry, 2006. **45**(3): p. 1002-8.
6. Batista, A.P., et al., *Energy conservation by Rhodothermus marinus respiratory complex I.* Biochim Biophys Acta. **1797**(4): p. 509-15.
7. Fernandes, A.S., et al., *Quinone reduction by Rhodothermus marinus succinate:menaquinone oxidoreductase is not stimulated by the membrane potential.* Biochem Biophys Res Commun, 2005. **330**(2): p. 565-70.
8. Fernandes, A.S., M.M. Pereira, and M. Teixeira, *The succinate dehydrogenase from the thermohalophilic bacterium Rhodothermus marinus: redox-Bohr effect on heme b_L.* J Bioenerg Biomembr, 2001. **33**(4): p. 343-52.
9. Lemos, R.S., et al., *Quinol:fumarate oxidoreductases and succinate:quinone oxidoreductases: phylogenetic relationships, metal centres and membrane attachment.* Biochim Biophys Acta, 2002. **1553**(1-2): p. 158-70.
10. Pereira, M.M., et al., *The caa_3 terminal oxidase of the thermohalophilic bacterium Rhodothermus marinus: a HiPIP:oxygen oxidoreductase lacking the key glutamate of the D-channel.* Biochim Biophys Acta, 1999. **1413**(1): p. 1-13.
11. Pereira, M.M., et al., *A tyrosine residue deprotonates during oxygen reduction by the caa_3 reductase from Rhodothermus marinus.* FEBS Lett, 2006. **580**(5): p. 1350-4.

12. Verissimo, A.F., et al., *A ba_3 oxygen reductase from the thermohalophilic bacterium Rhodothermus marinus.* FEMS Microbiol Lett, 2007. **269**(1): p. 41-7.
13. Pereira, M.M., et al., *Heme centers of Rhodothermus marinus respiratory chain. Characterization of its cbb_3 oxidase.* J Bioenerg Biomembr, 2000. **32**(2): p. 143-52.
14. Stelter, M., et al., *A novel type of monoheme cytochrome c: biochemical and structural characterization at 1.23 A resolution of Rhodothermus marinus cytochrome c.* Biochemistry, 2008. **47**(46): p. 11953-63.
15. Pereira, M.M., et al., *A membrane-bound HIPIP type center in the thermohalophile Rhodothermus marinus.* FEBS Lett, 1994. **352**(3): p. 327-30.
16. Pereira, M.M., J.N. Carita, and M. Teixeira, *Membrane-bound electron transfer chain of the thermohalophilic bacterium Rhodothermus marinus: characterization of the iron-sulfur centers from the dehydrogenases and investigation of the high-potential iron-sulfur protein function by in vitro reconstitution of the respiratory chain.* Biochemistry, 1999. **38**(4): p. 1276-83.
17. Stelter, M., et al., *Structure at 1.0 A resolution of a high-potential iron-sulfur protein involved in the aerobic respiratory chain of Rhodothermus marinus.* J Biol Inorg Chem, 2009.
18. Tindall, B.J., *Lipid-composition of Rhodothermus marinus.* FEMS Microbiol Lett, 1991. **80**: p. 65-68.
19. Pereira, M.M., J.N. Carita, and M. Teixeira, *Membrane-bound electron transfer chain of the thermohalophilic bacterium Rhodothermus marinus: a novel multihemic cytochrome bc, a new complex III.* Biochemistry, 1999. **38**(4): p. 1268-75.
20. Pereira, M.M., J.N. Carita, and M. Teixeira, *Membrane-bound electron transfer chain of the thermohalophilic bacterium Rhodothermus marinus: a novel multihemic cytochrome bc, a new complex III.* Biochemistry, 1999. **38**: p. 1268-1275.

Chapter 3

Characterization of the alternative complex III from Rhodothermus marinus

The results presented in this chapter were published in:

Manuela M. Pereira, **Patrícia N. Refojo**, Gudmundur O. Hreggvidsson, Sigridur Hjorleifsdottir, Miguel Teixeira (2007) *The alternative complex III from Rhodothermus marinus – a prototype of a new family of quinol: electron acceptor oxidoreductase* FEBS Letters **481**, 4831-4835

Patrícia N. Refojo, Filipa L. Sousa, Miguel Teixeira, Manuela M. Pereira (2010) *The alternative complex III: A different architecture using known building modules* Biochim Biophys Acta *IN PRESS*

Acknowledgements:

Dr João Carita is acknowledged for cell growth and Eng. Manuela Regalla for N-terminal sequencing. Dr. Mikhail Yanuyshin, from The Institute of Basic Biological Problems, Pushino, Russia, is acknowledged for the critical reading and discussions.

Dr. Gudmundur O. Hreggvidsson and Dr. Sigridur Hjorleifsdottir performed the partial DNA sequencing of *Rhodothermus marinus*.

3.1 – Summary

Rhodothermus marinus is a thermohalophic bacterium, whose respiratory chain has been extensively studied. The biochemical, spectroscopic and genetic search for a bc_1 complex was always fruitless; however a functional equivalent complex, i.e. having quinol:cytochrome *c* oxidoreductase activity was purified from the membranes and biochemically and spectroscopically characterized [1]. Now, with the sequencing of *R. marinus* genome it was possible to assign the N-terminal sequences obtained from several proteins of this complex to its coding genes. It was observed that the *R. marinus* complex III has the same genomic organisation of the so called MFIcc complexes, which have been proposed to be oxidoreductases participating in the respiratory, as well as in the photosynthetic electron transfer chains [2]. Furthermore, it was observed the presence of this complex in several genomes in which the genes coding for the bc_1 complex are absent and in which a quinol:cytochrome *c* oxidoreductase has to be present. *R. marinus* alternative complex III is coded by a seven gene cluster. Three of these genes codify for peripheral proteins; two cytochromes *c*, a pentahemic and a monohemic one, and a large protein containing a $[3Fe\text{-}4S]^{1+/0}$ and three $[4Fe\text{-}4S]^{2+/1+}$ centres. The other four genes code for transmembrane proteins: two are predicted to have ten transmembrane helices with putative quinone binding motifs and are homologous to each other and to membrane subunits present in several members of the complex iron-sulfur molybdoenzyme family; the two other genes code for one and two transmembrane helices proteins. This is the first time that an assignment of a biochemically characterized alternative complex III to its coding gene cluster is performed.

3.2 – Introduction

The presence of a typical bc_1 complex in the membranes of *Rhodothermus marinus* has been excluded given that the Rieske center EPR signal was never detected, and the typical inhibitors of this family of enzymes were showed to be inefficient. In fact, the presence of a completely different complex III in *R. marinus* has been described [1, 3]. The green non-sulfur bacterium *Chloroflexus aurantiacus* is another organism in which a complex with quinol: mobile electron carrier oxidoreductase activity should exist. Furthermore, when the membrane cytochrome-containing complexes from this bacterium were analyzed, no complex matching the features of a bc_1 complex was found [4].

With the increasing number of prokaryotic genome sequences, it is now possible to identify *in silico* so far unknown respiratory complexes, namely when accompanied with a thorough biochemical characterization at the protein level, which results from the still largely unexplored enormous biodiversity of the microbial world. Based on sequence analysis of the genomes so far sequenced, Yanyushin and coworkers anticipated the presence of a protein complex, proposing it to be an alternative complex III, involved in the respiratory and in the photosynthetic electron transfer chains [2]. Furthermore, it was observed the presence of this complex in several genomes in which the genes coding for the bc_1 complex are absent and in which it is expected to exist a quinol: electron acceptor oxidoreductase, since genes coding for oxygen reductases, oxidizing periplasmatic electron donors are present. The gene cluster identified by those authors is constituted by six genes. Two of those are homologous to genes coding for the three

subunits of molybdopterin containing oxidoreductases of the DMSO reductase family and other two code for *c* type cytochromes [2].

In this report the genes coding for the subunits of the *R. marinus* complex III [1] were identified and it is shown that this complex is a MFIcc complex like the one proposed by Yanyushin and coworkers [2]. It is thus established undoubtedly the existence of a different complex III, named alternative complex III (ACIII), by its identification at the biochemical and genomic levels.

3.3 – Material and methods

3.3.1 - Bacterial growth and protein purification

Rhodothermus marinus strain PRQ62b growth and protein purification were performed as described in [5].

3.3.2 – Electrophoresis techniques

Tricine-SDS-PAGE was carried out as described by Schägger and von Jagow [6] with 10%T, 3%C, and heme staining followed Goodhew *et al* [7].

3.3.3 – Protein, heme and metal determination

Protein concentrations were determined using the bicinchoninic acid (BCA) method [8] and an apparent molecular mass of 266 kDa, determined by Tricine-SDS-PAGE (considering a 1:1 stoichiometry for all subunits) was considered to define metal and heme contents. Heme content was determined by pyridine hemochrome [9], and HPLC analysis after heme extraction as described in [5]. Iron and molybdenum were analyzed by atomic absorption on a graphite

chamber, at the Laboratório de Análises, Instituto Superior Técnico, Lisbon and Faculdade de Ciencias e Tecnologia, Universidade Nova de Lisboa.

3.3.4 – N-terminal amino acid sequence determination

The enzyme subunits were transferred from the SDS-PAG to a polyvinylidene difluoride (PVDF) membrane. Each transferred sample was submitted to N-terminal protein sequence analysis by automated Edman degradation [10] using an Applied Biosystems Procise 491 HT protein sequencer.

3.3.5 – Amino acid sequence identification

The sequence of the genes coding for the subunits of the ACIII from *Rhodothermus marinus* were partially identified in silico from a local Prokaria genome database of *R. marinus* ITI378 by using the N-terminal sequences determined for the several proteins. The gene library was obtained by Gudmundur O. Hreggvidsson and Sigridur Hjorleifsdottir (Iceland) and it was prepared as follows. DNA was fragmented by nebulization and cloned into pTrueBlue (Stratagene). Plasmids were isolated by high-throughput minipreparation, and sequencing was performed. Contigs were assembled with the Phred–Phrap package [11], and putative open reading frames (ORFs) were identified with the GetORF program from the EMBOSS package [12], followed by BLASTP searches [13] against protein sequence databases. Gaps were closed by PCR amplification using sequences from flanking contigs. Neither the full sequence of gene *F* nor gene *G* were obtained at this stage. In order to obtain the complete gene sequence of the gene

F and taking into account that in some organisms the genes coding for subunits of ACIII are followed by those coding for subunits of the caa_3 oxygen reductase [2], appropriate primers were designed and PCRs were performed at ITQB. The forward primer (5′-ATG GCC GAA G TG AAA GCG AA -3′) was designed to hybridize with the available gene sequence of *AtcF*, while the reverse primer (5′- CCT TTA CCC CAC CAC CGC AT-3′) was designed to hybridize with the first gene of the cluster coding for the caa_3 oxygen reductase. The sequence of the PCR product obtained was translated using an expasy tool (http://www.expasy.org/tools/dna.html).

3.3.6 – Mass spectrometry experiments

The protein band with an apparent molecular mass of 18 kDa from the Tricine- SDS-PAG of the alternative complex III was excised and submitted to proteolytic digestion with Trypsin and analyzed by mass spectrometry. The mass spectra of the peptides were acquired by MALDI-TOF in the positive reflection mode in the Mass Spectrometry Laboratory, Analytical Services Unit of ITQB/IBET. The identification of the peptides was performed by direct comparison of the molecular masses predicted for the peptides with those experimentally obtained. The molecular masses of the peptides were predicted using PeptideMass at http://expasy.org/cgi-bin/peptide-mass.pl [14].

3.3.7 – Prediction of transmembrane topology

Transmembrane topology was predicted using ConpredII at http://bioinfo.si.hirosaki-u.ac.jp/~ConPred2/ [15].

3.3.8 – Nucleotide sequence accession number

The gene sequence coding for alternative complex III gene cluster of *R. marinus* has been deposited in GenBank under accession no. 924811.

3.4– Results

3.4.1 – Subunits and prosthetic groups composition

The purified *R. marinus* ACIII shows seven bands in a Tricine-SDS-PAGE, corresponding to subunits with apparent molecular masses of 97, 42, 35, 27, 25, 22 and 18 kDa (figure 3.1-A). The bands corresponding to subunits with apparent molecular masses of 27 and 22 kDa have also colored with heme staining, indicating the presence of *c*- type hemes (figure 3.1-B).

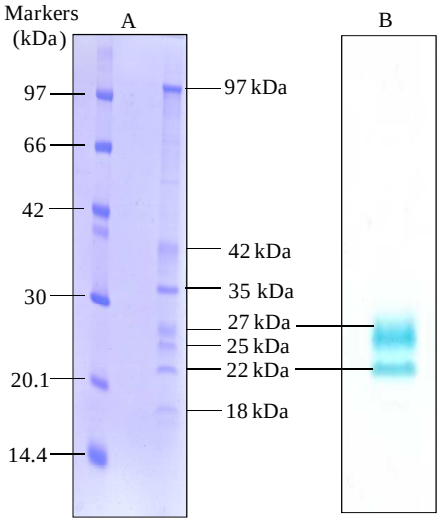

Figure 3.1
Tricine- SDS-PAGE of the alternative complex III from *R. marinus* stained by Commasie (A) and for hemes (B).

The cytochromes of the ACIII from *R. marinus* have been previously characterized by HPLC analysis and UV-visible and EPR

spectroscopies and a total of 5 hemes were showed to be present in the complex [5]. Besides the presence of *c*-type hemes, the presence of a *b*-type heme was reported based on the maximum absorption band at 557 nm for one of the hemes and on HPLC analysis. The heme content was here reanalyzed. The peak at 557 nm is still present, but no hemes were detected by HPLC analysis, meaning that only *c*-type hemes are present in the complex. The complex did not contain molybdenum and the iron content was now determined by atomic absorption and a value of 20±0.5 Fe per protein molecule was obtained.

3.4.2 – Amino acid sequence comparison

The N-terminal sequences for four of the bands have been determined: for the 97 kDa band, RYPVEKILPYV, for the 42 kDa band, AHATKDL, for the 35 kDa band, AEVKANGFPGWLLDP, and for the 25 kDa band, EARDGS. Attempts to sequence the N-terminal of the other bands were always fruitless. Search in *R. marinus* strain ITI378 gene database showed that the first sequence corresponds to the N-terminal sequence of a putative molybdopterin containing reductase which is fused to an iron-sulfur protein. The two sequences obtained for the 42 and 35 kDa bands correspond to two N-terminal sequences of different transmembrane proteins present in several complexes of the DMSO reductase family (eg DmsC; PsrC, NrfD). The last sequence is the N-terminal of a hypothetical protein present in several genomes.

3.4.3 – Gene cluster organization and gene sequence analysis

The genes coding for the above mentioned proteins seem to form a cluster with two other genes coding for two type *c* cytochromes with predicted molecular masses of 27 and 23.5 kDa, which is in agreement with the results of the heme staining of the SDS- PAGE.

The genomic organization of the alternative complex III seems to be the same observed by Yanyushin and coworkers [2], which was proposed to codify for a new class of bacterial membrane bound oxidoreductases involved in the respiratory and in the photosynthetic electron transfer chains. Searching in all genomes so far available the authors observed that these complexes are distributed in almost all bacterial phyla, with special relevance for those in which genes coding for a bc_1 complex are not present, but a quinol: electron acceptor activity has to be present.

Gene *ActA* codes for a protein containing five heme C binding motifs, CXXCH, being the fifth motive one amino acid residue apart from the C-terminal. Seven other histidine and three methionine residues are present in the sequence being candidates for the sixth ligand of the heme irons. A possible signal peptide in the N-terminal region may be present, but the putative cleavage site is inside the predicted transmembrane helix and thus it is possible that this cytochrome is attached to the membrane by that helix. Gene *ActB* is the fusion of two genes, encoding a putative molybdpterin containing protein (N-terminal) and an iron-sulfur protein (C-terminal), whose genes cluster together in several genomes coding for complexes of the DMSO reductase family. Three binding sites for $[4Fe\text{-}4S]^{2+/1+}$ clusters and one for a $[3Fe\text{-}4S]^{1+/0}$ cluster are observed in the deduced sequence; in the previous characterization of *R. marinus* complex the

[3Fe-4S]$^{1+/0}$ cluster was identified by EPR spectroscopy. This gene, like the ones coding for the molybdpterin containing oxidoreductase of the DMSO reductase family has a twin arginine translocase (Tat) signal peptide [16, 17]. Gene *ActC* codes for a homologue of nrfD, which as mentioned above is a transmembrane protein of some members of the DMSO reductase family responsible for the interaction with quinones. Topology prediction reveals the possibility of ten transmembrane helices. Two possible quinone binding sites, as proposed by Fisher and Rich [18], are present in the transmembranes helices. Gene *ActD* codes for a hypothetical protein predicted to have two transmembrane helices. The protein coded by gene *ActE* contains one CXXCH motif, and several histidines and methionines residues that can be the heme sixth ligand. However, this is most probably a methionine residue in the conserved motive MPA present in other cytochromes (e.g.[19]). No transmembrane helices were predicted to be present. Finally gene *ActF* codes for a protein homologous to the one coded by gene *ActC*. However, when comparing the gene sequence of gene *ActF* deposited in the local Prokaria genome database with those from other MFIcc complexes, the *R. marinus* gene seemed to be incomplete. In order to obtain the complete sequence of *ActF*, suitable primers were designed taking into consideration that in several organisms the gene cluster conding for MFIcc is followed by that coding for subunits of caa_3 oxygen reductase [2] and PCRs were performed. A PCR product with ca 1800 bp was obtained and sequenced. The sequencing revealed the total sequence of the *ActF* gene and also an ORF which did not correspond to any subunit of the already known subunits of the alternative complex III and of the caa_3 oxygen reductase complexes. The protein encoded by this gene, named G, was predicted to have

14.5 kDa and one transmembrane helix. No binding motifs for redox cofactors were observed. The subunit G was assigned to the protein band observed in the SDS-PAG of the alternative complex III with an apparent molecular mass of 18 kDa (figure 3.1). This assignment was confirmed by peptide mass fingerprint analysis.

Table 3.1: **Peptide mass fingerprint of in-gel tryptic digest of the band with an apparent molecular mass of 18 kDa in the SDS-PAG of figure 3.1.**

Comparision of the molecular masses values experimentaly obtained for the protein band with an apparent molecular mass of 18 kDa in the Tricine-SDS-PAGE of ACIII (fig 3.1) with those predicted for subunit G of the ACIII (accession number YP_003289521). Zero and one possible miss cleavage were considered for the comparison.

Start-End	m/z (Observed)	m/z (predicted)	Miss cleavage	Sequence
7-30	2577.1926	2577.2943	1	KQPAVAEAELPAVQPD EANF EAPR
8-30	2449.1035	2449.1993	0	QPAVAEAELPAVQPDE ANFE APR
70-81	1471.6918	1471.7288	1	YPLREETEAHAR
82-89	1895.8868	1895.9497	0	QLLEGYGVVDAEQGVY R
104-128	2692.2048	2692.2922	0	AMEEIVEAYGGDSVWT LPQP SAVSR
104-128	2708.2380	2708.2872	0	AMEEIVEAYGGDSVWT LPQP SAVSR (oxidation M)

The gene cluster of *R. marinus* alternative complex III is thus composed by seven genes organized as in figure 3.2. This cluster has one more gene than the gene cluster of MFIcc proposed by Yanyushin and coworkers.

Figure 3.2

Gene cluster organization of the alternative complex III from *R. marinus*. The gene cluster is composed of seven genes (*ActA - G*). *ActA* codes for a protein containing five heme *c* binding motifs. *ActB* is the fusion of two genes, a putative molybdopterin containing protein (N-terminal) and an iron-sulfur protein (C-terminal), containing three binding sites for $[4Fe\text{-}4S]^{2+/1+}$ clusters and one for a $[3Fe\text{-}4S]^{1+/0}$ cluster. *ActC* and *ActF* code for transmembrane proteins with 10 TM helices each and are both homologs of the membrane proteins of some members of the DMSO reductase family responsible for the interaction with quinones. *ActD* and *ActG* code for hypothetical proteins predicted to have two and one transmembrane helices, respectively. *ActE* codes for a monohemic cytochrome *c*.

3.4.4 – Protein complex composition

Based on the genomic organization, on previous biochemical and functional studies and on the available information for members of the CISM family, the *R. marinus* alternative complex III may look like schematized in figure 3.3. The order of prosthetic groups is not known; here it is only intended to show that subunits containing the prosthetic groups should be peripheral

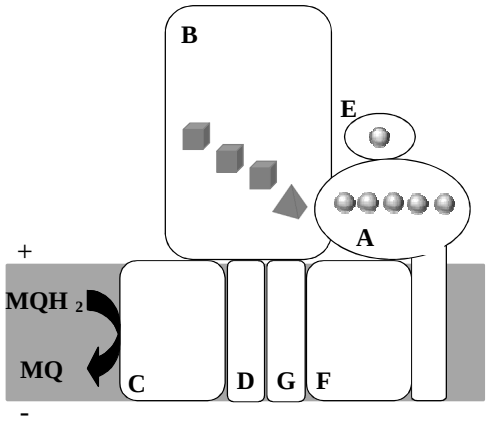

Figure 3.3

Schematic representation of the alternative complex III from *R. marinus*. Based on the genomic organization, on our previous biochemical and functional studies and on what is known for members of the DMSO reductase family. The gray spheres represents the *c*-type hemes and cubes and pyramides represents $[4Fe\text{-}4S]^{2+/1+}$ and $[3Fe\text{-}4S]^{1+/0}$ centers, respectively.

and facing the periplasm, based on the observation of the signal peptides present in the genes coding for these proteins. The presence of *c* type cytochromes and of a [3Fe-4S]$^{1+/0}$ centre has already been established in the previous characterization of *R. marinus* alternative complex III. The presence of three [4Fe-4S]$^{2+/1+}$ centers, besides the similarity with the members of DMSO reductase family, from which several structures are known, is highly supported by the iron content of the sample, considering the presence of five hemes, three [4Fe-4S]$^{2+/1+}$ centers and one [3Fe-4S]$^{1+/0}$ center.

At a first glance it may appear unexpected that having a protein similar to a molybdopterin reductase this complex does not contain molybdenum. This situation is not unique. The structure of the C-terminal part of Nqo3/NuoG, the largest subunit of respiratory chain complex I, is also similar to the family of molybdopterin reductases [20]. In fact it presents the same four structural domains, where domains II and III create a cavity, which in the other members of the family is occupied by the molybdopterin guanine dinucleotide (MGD) prosthetic group. In the case of Nqo3 the cavity is occupied by domain IV. The function of the C-terminal of Nqo3 is not known, being a flexible area and suggested to have a regulatory role [20].

Similarly to what is observed for the nitrate reductases that are members of the DSMO reductase family, coded by the NarGHI operons, for the succinate:quinone oxidoreductase [21, 22] and for the DMSO reductase of *E. coli* engineered with a [3Fe-4S]$^{1+/0}$ cluster [23], this centre should be the one that interacts with the quinone/quinol. In this case, the subunit of *R. marinus* alternative complex III containing the iron-sulfur centers should be the one receiving the electrons from the membrane subunits and transferring these to the *c* type

cytochromes. Also taking into account the structure of the formate dehydrogenase from *Escherichia coli*, the iron-sulfur centers should form a wire for electron transfer [24].

The two transmembrane subunits with the higher molecular mass are homologous to each other and homologous to several membrane proteins of the DMSO reductase family. Interaction studies of 2-n-heptyl-4-hydroxyquinoline-N-oxide (HQNO) with DMSO reductase from *E. coli* showed a binding stoichiometry of 1:1, thus indicating the presence of one quinone binding site [25]. As mentioned above, inspection of the amino acid sequences of these subunits reveals the presence of at least two possible quinone binding sites, as proposed by Fisher and Rich [18], and so the presence of more than one quinone binding site can not be excluded. The reason that the alternative complex III from *R. marinus* contains two of such membrane subunits is not known, but again taking the example of complex I this is not unique since in this type of complex it is observed the presence of homologous subunits within the complex, such as Nqo 12, Nqo13 and Nqo14 [26, 27].

The small transmembrane subunits seem to be unique for these alternative complexes and its function is unknown and quinone binding sites seem not to be present.

3.5 – Conclusion

The alternative complex III of *R. marinus* is a newly identified quinol: electron acceptor oxidoreductase complex composed by seven subunits: two *c*-type heme containing subunits (a mono and a pentaheme); four membrane bound subunits, and a peripheral subunit

with three [4Fe-4S]$^{2+/1+}$ and one [3Fe-4S]$^{1+/0}$ centers. Comparing the composition of the alternative complex III here described with the one of the bc_1 it can be observed that, generically, they are not completely different. Both have transmembrane subunits, which interact with quinone/quinols and transfer electrons to an iron-sulfur containing protein, which in its turn promotes the electron transfer to cytochromes.

The existence of two complexes performing the same reaction, i.e. two different complexes III, in this case, is not unique in respiratory chains. For all the other respiratory complexes there are alternatives. In the case of complex I, Type II (NDH-II) and Na^+-pumping NADH:quinone oxidoreductases are alternatives. Different types of oxygen reductases of the heme-copper family and of the *bd* family are observed as well as succinate:quinone oxidoreductases with different types of membrane attachments. In this report we have established undoubtedly the existence of an alternative complex III by its identification at the biochemical and genomic levels.

3.6 - References

1. Pereira, M.M., J.N. Carita, and M. Teixeira, *Membrane-bound electron transfer chain of the thermohalophilic bacterium Rhodothermus marinus: a novel multihemic cytochrome bc, a new complex III.* Biochemistry, 1999. **38**(4): p. 1268-75.
2. Yanyushin, M.F., et al., *New class of bacterial membrane oxidoreductases.* Biochemistry, 2005. **44**(30): p. 10037-45.

3. Pereira, M.M., J.N. Carita, and M. Teixeira, *Membrane-bound electron transfer chain of the thermohalophilic bacterium Rhodothermus marinus: characterization of the iron-sulfur centers from the dehydrogenases and investigation of the high-potential iron-sulfur protein function by in vitro reconstitution of the respiratory chain.* Biochemistry, 1999. **38**: p. 1276-1283.
4. Yanyushin, M.F., *Fractionation of cytochromes of phototrophically grown Chloroflexus aurantiacus. Is there a cytochrome bc complex among them?* FEBS Lett, 2002. **512**(1-3): p. 125-8.
5. Pereira, M.M., J.N. Carita, and M. Teixeira, *Membrane-bound electron transfer chain of the thermohalophilic bacterium Rhodothermus marinus: a novel multihemic cytochrome bc, a new complex III.* Biochemistry, 1999. **38**: p. 1268-1275.
6. Schägger, H. and G. Von Jagow, *Tricine-Sodium Dodecyl Sulfate-Polyacrylamide Gel Electrophoresis for the Separation of Proteins in the Range of 1 to 100 kDA.* Anal. Biochem., 1987. **166**: p. 368-379.
7. Goodhew, C.F., K.R. Brown, and G.W. Pettigrew, *Haem Staining in Gels, a Useful Tool in the Study of Bacterial c-type Cytochromes.* Biochim. Biophys. Acta, 1986. **852**: p. 288-294.
8. Smith, P.K., et al., *Measurement of protein using bicinchoninic acid.* Anal Biochem, 1985. **150**(1): p. 76-85.
9. Berry, E.A. and B.L. Trumpower, *Simultaneous determination of hemes a, b, and c from pyridine hemochrome spectra.* Anal Biochem, 1987. **161**(1): p. 1-15.
10. Edman, P. and G. Begg, *A protein sequenator.* Eur J Biochem, 1967. **1**(1): p. 80-91.
11. Ewing, B. and P. Green, *Base-calling of automated sequencer traces using phred. II. Error probabilities.* Genome Res, 1998. **8**(3): p. 186-94.
12. Rice, P., I. Longden, and A. Bleasby, *EMBOSS: the European Molecular Biology Open Software Suite.* Trends Genet, 2000. **16**(6): p. 276-7.

13. Altschul, S.F., et al., *Gapped BLAST and PSI-BLAST: a new generation of protein database search programs.* Nucleic Acids Res, 1997. **25**(17): p. 3389-402.
14. Wilkins, M.R., et al., *Detailed peptide characterization using PEPTIDEMASS--a World-Wide-Web-accessible tool.* Electrophoresis, 1997. **18**(3-4): p. 403-8.
15. Arai, M., et al., *ConPred II: a consensus prediction method for obtaining transmembrane topology models with high reliability.* Nucleic Acids Res, 2004. **32**(Web Server issue): p. W390-3.
16. Berks, B.C., T. Palmer, and F. Sargent, *Protein targeting by the bacterial twin-arginine translocation (Tat) pathway.* Curr Opin Microbiol, 2005. **8**(2): p. 174-81.
17. Palmer, T., F. Sargent, and B.C. Berks, *Export of complex cofactor-containing proteins by the bacterial Tat pathway.* Trends Microbiol, 2005. **13**(4): p. 175-80.
18. Fisher, N. and P.R. Rich, *A motif for quinone binding sites in respiratory and photosynthetic systems.* J Mol Biol, 2000. **296**(4): p. 1153-62.
19. Srinivasan, V., et al., *Structure at 1.3 A resolution of Rhodothermus marinus caa(3) cytochrome c domain.* J Mol Biol, 2005. **345**(5): p. 1047-57.
20. Sazanov, L.A. and P. Hinchliffe, *Structure of the hydrophilic domain of respiratory complex I from Thermus thermophilus.* Science, 2006. **311**(5766): p. 1430-6.
21. Iverson, T.M., et al., *Structure of the Escherichia coli fumarate reductase respiratory complex.* Science, 1999. **284**(5422): p. 1961-6.
22. Lancaster, C.R.D., et al., *Structure of fumarate reductase from Wolinella succinogenes at 2.2 A resolution.* Nature, 1999. **402**: p. 377-385.
23. Rothery, R.A. and J.H. Weiner, *Interaction of an engineered [3Fe-4S] cluster with a menaquinol binding site of Escherichia coli DMSO reductase.* Biochemistry, 1996. **35**(10): p. 3247-57.
24. Jormakka, M., et al., *Molecular basis of proton motive force generation: structure of formate dehydrogenase-N.* Science, 2002. **295**(5561): p. 1863-8.

25. Zhao, Z. and J.H. Weiner, *Interaction of 2-n-heptyl-4-hydroxyquinoline-N-oxide with dimethyl sulfoxide reductase of Escherichia coli.* J Biol Chem, 1998. **273**(33): p. 20758-63.

26. Mathiesen, C. and C. Hagerhall, *The 'antiporter module' of respiratory chain complex I includes the MrpC/NuoK subunit -- a revision of the modular evolution scheme.* FEBS Lett, 2003. **549**(1-3): p. 7-13.

27. Friedrich, T. and B. Bottcher, *The gross structure of the respiratory complex I: a Lego System.* Biochim Biophys Acta, 2004. **1608**(1): p. 1-9.

Chapter 4

The structural and functional association of Alternative complex III and caa_3 oxygen reductase

The results presented in this chapter were published in:

Patrícia N. Refojo, Miguel Teixeira and Manuela M. Pereira (2010) *The alternative complex III from Rhodothermus marinus and its structural and functional association with caa_3 oxygen reductase* Biochim Biophys Acta **1797**, 1477-1482

Acknowledgments:

Dr. João Carita is acknowledged for cell growth.

Dr. Ana Coelho and Ana P. Batista are acknowledged for the Peptide Mass Fingerprint identifications.

Dr. Eurico Melo is acknowledged for all the help with the Fluorescence measurements.

4.1 – Summary

An alternative complex III (ACIII) is a respiratory complex with quinol: electron acceptor oxidoreductase activity. It is the only example of an enzyme performing complex III function that does not belong to the bc_1 complex family. ACIII from *Rhodothermus (R.) marinus* was the first enzyme of this type to be isolated and characterized, and in this work we deepen its characterization. We addressed its interaction with the quinol substrate and with the caa_3 oxygen reductase, whose coding gene cluster follows that of the ACIII. There is at least, one quinone binding site present in *R. marinus* ACIII as observed by fluorescence quenching titration of HQNO, a quinone analogue inhibitor. Furthermore, electrophoretic and spectroscopic evidence, taken together with mass spectrometry revealed a structural association between ACIII and caa_3 oxygen reductase. The association was also shown to be functional, since quinol: oxygen oxidoreductase activity was observed when the two isolated complexes were put together. This work is thus a step forward in the recognition of the structural and functional diversities of prokaryotic respiratory chains.

4.2- Introduction

Until now the bc_1 complexes were considered to be the only complexes involved in the aerobic respiratory chains to have quinol: cytochrome *c* oxidoreductase activity. The alternative complex III from *Rhodothermus marinus* was the first purified and characterized example of an enzyme with the equivalent function but showing a completely different constitution [1, 2].

In the study performed by Yanyushin and coworkers [3] it was observed that in several genomes the gene cluster coding for ACIII (called MFIcc in the cited reference) is followed by the gene cluster coding for oxygen reductases. The clustering between the genes coding for subunits of complex III and complex IV have been also observed for *Mycobacterium smegmatis* [4] and *Corynebacterium glutamicum* [5]. In the two cases the gene cluster coding for subunits of the aa_3 oxygen reductase is preceded by that coding for subunits of the cytochrome *bc* complex and a functional association between the two complexes was observed [4-7]. The cytochrome c_1 subunits of the *bc* complexes of *Mycobacterium smegmatis* [4, 6] and *Corynebacterium glutamicum* [8] have an extra domain with a *c*-type heme binding motif (CxxCH), proposed to replace the soluble cytochrome *c* [4-7] (showed to be absent [7, 9]).

Functional associations of complex III and IV were also observed in other bacteria where the gene clusters of these complexes are not consecutive namely in *Thermophilic bacterium PS3* [10], *Paracoccus denitrificans* [11] and *Thermus thermophilus* [12].

In this work we address the structural and functional association of the ACIII of *R. marinus* with the caa_3 oxygen reductase and also the interaction with menadiol (analogue of the *R. marinus* physiologic quinol).

4.3 - Materials and Methods

4.3.1 – Bacterial growth and protein purification

Growth of *Rhodothermus marinus* strain PRQ62b was performed as described before [1]. Solubilised membranes (prepared according to

[1]) in 20 mM Tris-HCl, 1 mM PMSF, 0.05% n-Dodecyl β–D-maltoside (DDM) pH8 were applied into a Q-Sepharose High Performance column. The sample was eluted applying a gradient from 0 to 0.5 M of NaCl in the same buffer. A fraction eluted with approximately 0.35 M of NaCl, called D5, and containing both the ACIII and the *caa*$_3$ oxygen reductase was obtained. This fraction was used for further studies, including a Blue Native (BN)-PAGE and a Tricine-SDS-PAGE. The same fraction was also submitted to further chromatographic procedures in order to isolate the ACIII and the *caa*$_3$ oxygen reductase as described before [1, 13].

4.3.2 – DNA techniques

R. marinus genomic DNA was extracted from a liquid grown culture using GenElute Bacterial Genomic DNA kit (Sigma). In order to confirm that the gene clusters coding for the ACIII and for the *caa*$_3$ oxygen reductase were consecutive, appropriate primers were designed. The forward primer (5'-ATG GCC GAA G TG AAA GCG AA -3') was designed to hybridize with the last gene of the cluster coding for ACIII while the reverse primer (5'- CCT TTA CCC CAC CAC CGC AT-3') was designed to hybridize with the first gene of the cluster coding for the *caa*$_3$ oxygen reductase. The sequence of the PCR product obtained was translated using an expasy tool (http://www.expasy.org/tools/dna.html).

4.3.3 – Fluorescence spectroscopy

The binding of HQNO (2-heptyl-4-hydroxyquinoline-N-oxide) to the ACIII was measured on a Cary Varian Eclipse fluorescence spectrophotometer. The excitation wavelength was set at 341 nm and

the emission spectra were recorded between 370 and 600 nm. These measurements were performed considering the quenching of the HQNO fluorescence by the addition of ACIII. The complex was added to a 6 µM HQNO solution in small aliquots to a maximum concentration value of 4.4 µM. The fluorescence of the ACIII at the mentioned wavelengths was also measured and subtracted. The number of binding sites (n) and the binding constant (K) were determined from the following equation, $log\ (F_0\text{-}F)/\ F = log\ K + n log\ [Q]$ (equation 1) [14], where the values F and F_0 are the fluorescence intensities of HQNO in the presence and absence of the ACIII (quencher), respectively.

4.3.4 – Electrophoresis techniques

The BN-PAGE was performed as in [15] and the Tricine-SDS-PAGE was carried out as in [16] with 10% T, 3% C. Heme staining was done as in [17] to identify the protein bands of the complex having covalently bound hemes. The bands of BN-PAGE were also stained for cytochrome *c* oxidase activity according to [18].

4.3.5 – Mass spectrometry assays

The protein bands present in the Tricine-SDS-PAGE having as sample the D5 lane of the BN-PAGE were excised from the gel and submitted to proteolytic digestion with Trypsin or Chymotrypsin. The mass spectra of the peptides were acquired by MALDI-TOF in the positive reflection mode in the Mass Spectrometry Laboratory, Analytical Services Unit of ITQB/IBET. The identification of the peptides was performed either by searching in the data bases with

Mascot software (http://www.matrixscience.com, [19]) or by direct comparison of the molecular masses predicted for the peptides with those experimentally obtained. The molecular masses of the peptides were predicted using PeptideMass at http://expasy.org/cgi-bin/peptide-mass.pl [20].

4.3.6– UV-Visible absorption spectroscopy

UV-visible absorption spectroscopy was performed using a Shimadzu UV-1603 spectrophotometer. The ACIII (0.28 μM) spectra were measured under anaerobic conditions using a mixture of glucose (3 μM), glucose oxidase (4U/mL) and catalase (132U/mL). HQNO (used three times more concentrated than ACIII) was used as inhibitor.

4.3.7– Activity assays

The menaquinol: oxygen oxidoreductase activity was determined by the oxygen consumption measured polarographically with a Clark-type oxygen electrode, YS Model 5300, from Yellow Springs. The assays were carried out at 30 ºC in 20 mM potassium phosphate pH6.5 buffer. Menadiol, obtained by reducing menadione with sodium dithionite [21], was used as the electron donor for the menaquinol: oxygen oxidoreductase activity measurements. The ACIII and the caa_3 oxygen reductase were used in a 1:1 ratio. KCN (≈0.7 mM) and HQNO (the same ratio as before) were used as inhibitors of caa_3 oxygen reductase and ACIII, respectively. The activity values were calculated per milligram of caa_3 oxygen reductase. HiPIP, when used, was six times more concentrated than ACIII and caa_3 oxygen reductase.

4.4 – Results

4.4.1 – The genomic organization

In the genome of several organisms the gene cluster coding for the ACIII precedes the gene cluster coding for oxygen reductases [3, 22]. In most genomes in which this type of organization is observed the oxygen reductases genes code for a caa_3, nevertheless examples of genes coding for other oxygen reductases, such as cbb_3 oxygen reductases are also observed [22].

In order to investigate whether *R. marinus* genome contains such a gene organization, suitable primers were designed to amplify the region between the two clusters. A PCR product with ca 1800 bp was obtained and sequenced. The N-terminal and C-terminal part of this sequence corresponded to those of the *ActF* and *SCOI* (codes for a protein involved in the incorporation of copper) gene sequences, showing that indeed in *R. marinus* the gene clusters coding for the ACIII and for the caa_3 oxygen reductase were consecutive (figure 4.1).

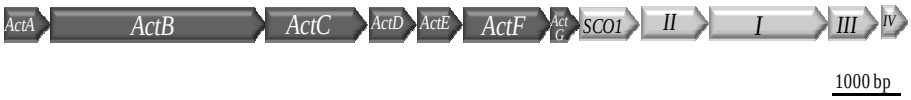

Figure 4.1

Rhodothermus marinus genomic organization of the genes coding for the alternative complex III (black boxes) and those coding for the caa_3 oxygen reductase (grey boxes).

4.4.2 – Interaction of alternative complex III with menadiol

The interaction of ACIII with menadiol, a menaquinol analogue, was investigated by UV-Visible absorption spectroscopy. It was observed that the oxidized ACIII was approximately 60 % reduced by menadiol (figure 4.2-A).

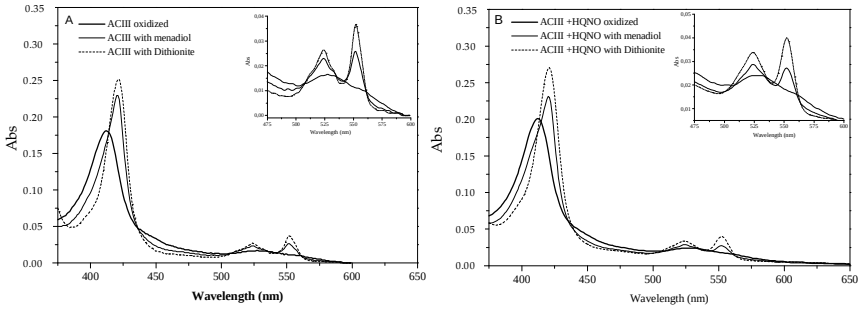

Figure 4.2

UV-Visible Absorption Spectra of the alternative complex III in the oxidized state (—) and reduced by menadiol (—) or by sodium dithionite (---). In the absence (A) and presence (B) of HQNO.

The fully reduced state of the complex was achieved by the addition of sodium dithionite. In order to check the specificity of menadiol reduction, HQNO, a menadiol structural analogue and an inhibitor of several quinone interacting enzymes, was used. In its presence the reduction by menadiol was 25 % inhibited (figure 4.2-B).

Several studies showed that the fluorescence intensity of HQNO is quenched upon its binding to a protein (e.g. DMSO reductase [23] and nitrate reductase [24]). HQNO has a maximum of fluorescence at 479 nm when excited at 341 nm. A decrease in its fluorescence intensity with the increasing concentration of the ACIII was observed (figure 4.3). The

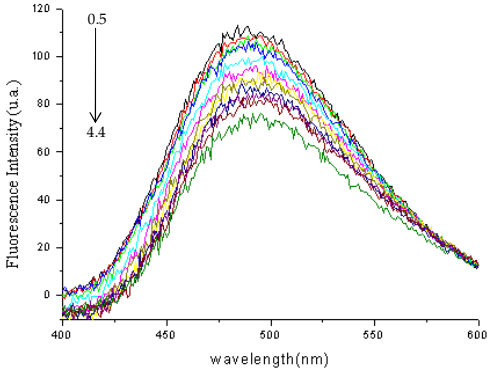

Figure 4.3

ACIII (concentrations ranging between 0.5 and 4.4 µM) quenching effect on HQNO fluorescence. Emission spectra with excitation at 341 nm.

fluorescence quenched titration data were analyzed considering the quenching of HQNO fluorescence intensity by ACIII as a static process [25]. A binding constant of 159 nM and the presence of 1 binding site (n=1.1) were calculated from the fitting of equation 1 (figure 4.4).

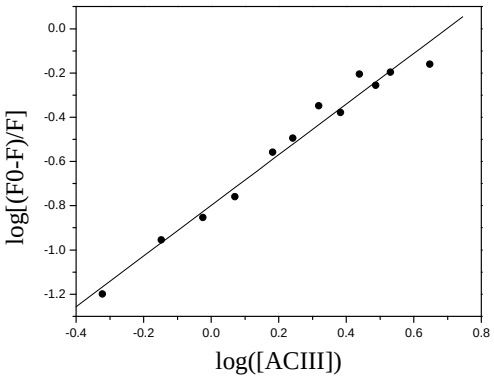

Figure 4.4

Double-log plot of the quenching effect on HQNO fluorescence by the alternative complex III monitored at 479 nm. The data were fitted using equation 1.

Our results indicate that the ACIII of *R. marinus* has one binding site for HQNO, which nevertheless does not exclude the presence of more quinone binding sites, as observed for the bc_1 complex.

4.4.3 – Interaction between alternative complex III and caa_3 oxygen reductase

4.4.3.1- Structural association

The structural association of the ACIII and the caa_3 oxygen reductase was investigated by native gel electrophoresis (figure 4.5). For this process, i-the fraction D5, obtained after the first chromatographic step; ii- the isolated ACIII and iii- the caa_3 oxygen reductase were applied in independent lanes in a BN-PAG. The result of this electrophoresis showed that ACIII migrated with an apparent molecular mass of 361 kDa, while the caa_3 oxygen reductase showed an apparent molecular mass of 210 kDa. Bands corresponding to these

masses could not be observed in the lane of the D5 fraction. Instead, a band with an apparent molecular mass of 550 kDa was detected, which suggested that D5 fraction contained an association of ACIII and *caa*$_3$ oxygen reductase. Replicates of the gel were submitted to other staining procedures. Heme staining (figure 4.5B) revealed that the 550 kDa band was the only band which stained for covalently bound hemes in the lane of D5 (figure 4.5B, lane 2). This result was consistent with the presence of an association of ACIII and *caa*$_3$ oxygen reductase. Lanes 3 and 4, containing ACIII and *caa*$_3$ oxygen reductase, respectively, as expected, stained both under this procedure. The *in gel* cytochrome *c* oxidase activity assays (figure 4.5C) showed a positive result for the *caa*$_3$ oxygen reductase and in the case of D5 fraction the activity marker was spread in the first half of the lane but it was absent

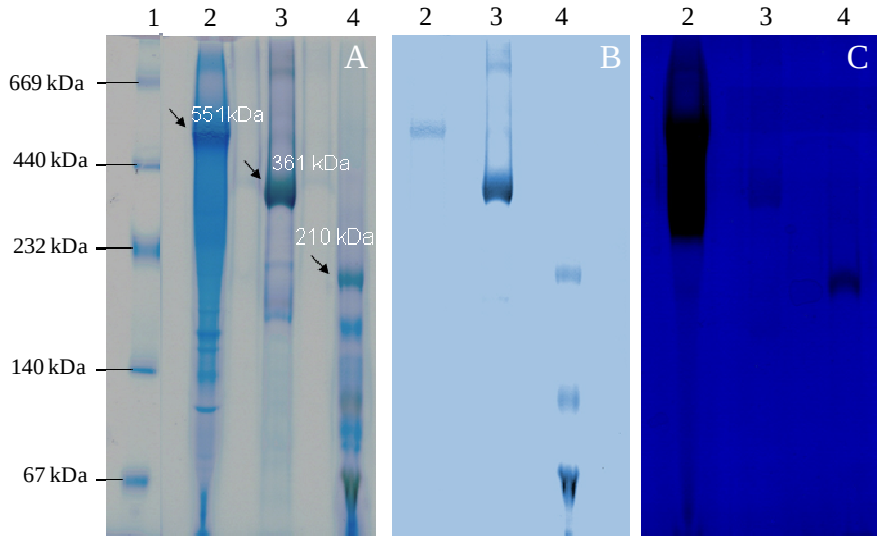

Figure 4.5

Blue Native-PAGE of D5 fraction (lane 2), alternative complex III (lane 3) and *caa*$_3$ oxygen reductase (lane 4). Molecular mass protein markers are present in lane 1. The native gel was stained with Coomassie (A), with Heme-staining procedures (B) and cytochrome *c* oxidase in gel activity (C).

in the 200 kDa region. The results from the two staining procedures corroborated the association of the ACIII and *caa*$_3$ oxygen reductase.

The upper part (669-232 kDa) of the D5 lane of the BN gel lane was submitted to a Tricine-SDS-PAGE (2D) (figure 4.6). Several bands were observed in this denaturant second dimension. Nevertheless, in the lane corresponding to the band with the apparent molecular mass of 550 kDa only subunits with apparent molecular masses compatible with subunits of the complexes III and IV were observed. It was not possible to assign the bands to each subunit just by analysing the migration profiles of the subunits because two of the subunits of ACIII [26] and two of the *caa*$_3$ oxygen reductase [13] show the same apparent molecular masses upon electrophoresis. The protein bands were further identified by MS analysis: bands 1, 3 and 4 were assigned to

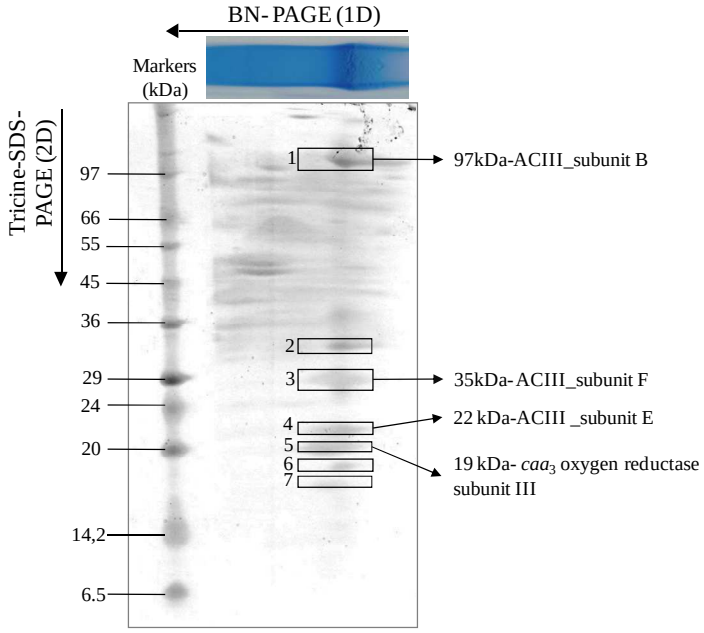

Figure 4.6

Tricine SDS-PAGE of the lane of the D5 fraction obtained after its subjection to BN-PAGE. Left Lane – molecular mass protein markers.

subunits B, F and E (monohemic cytochrome *c*), respectively, of the ACIII; band 5 was identified as subunit III of caa_3 oxygen reductase (see tables 4.1-4.4). These results unequivocally showed that both, ACIII and caa_3 oxygen reductase were present in the complex observed at 550 kDa in the BN gel.

Table 4.1: Peptide mass fingerprint of in-gel tryptic digest of the band 1.

Comparision of the molecular masses values experimentaly obtained for the protein band 1 in the Tricine-SDS-PAGE of the lane D5 (fig 4.6) with those predicted for subunit B of the ACIII (accession number ABV55245). Zero and one possible miss cleavage were considered for the comparison.

Start-End	m/z (Observed)	m/z (predicted)	Miss cleavage	Sequence
81-86	760.4097	760.4716	0	ILPYVR
87-106	2305.9522	2306.1889	0	QPEEIIPGIPLYYATAMPFR
135-153	2065.8349	2066.0189	0	GATGVFEQASLLNLYDPDR
160-174	1694.6764	1694.8285	1	KGEPASWGDFVQFAR
247-261	1617.8482	1617.6747	0	VIVSLDADFLGPTDR
334-345	1358.6003	1358.7215	0	FAGHPYVVEIAR
527-535	1092.4279	1092.5221	0	GAFEQAWQR
914-922	1296.5487	1296.6636	1	RFNWFNWVK
915-939	3031.5610	3032.0200	1	FNWFNWVKTLPIQVQMAQNP DVTVR

Table 4.2: Peptide mass fingerprint of in-gel tryptic digest of the band 3.

Comparision of the molecular masses values experimentaly obtained for the protein band 3 in the Tricine-SDS-PAGE of the lane D5 (fig 4.6) with those predicted for subunit F of the ACIII (accession number ABV55249). Zero and one possible miss cleavage were considered for the comparison.

Start- End	m/z (Observed)	m/z (predicted)	Miss	Sequence
6-21	1809.5911	1809.9758	0	ANGFPGWLLDPLRPTR
28-35	1047.3486	1047.5581	1	YRLPEDVR
92-99	928.3425	928.5363	0	AQWVVAVR
183-186	1565.4198	1565.7554	0	QDVDPDPSIPAQQR
256-264	995.4024	995.6108	1	RGPLQGIVR
400-412	1527.4330	1527.7372	0	HSLVPQNDPYMAR
400-412	1543.4287	1543.7322	0	HSLVPQNDPYMAR (oxidation M)

Table 4.3: Peptide mass fingerprint of in-gel tryptic digest of the band 4.

Comparision of the molecular masses values experimentaly obtained for the protein band 4 in the Tricine-SDS-PAGE of the lane D5 (fig 4.6) with those predicted for subunit E of the ACIII (accession number ABV55248). Zero and one possible miss cleavage were considered for the comparison.

Start- End	m/z (Observed)	m/z (predicted)	Miss cleavage	Sequence
46-58	1583.7494	1582.7421	0	KFEAQELNPFFADRR
46-59	1739.8518	1738.8445	1	KFEAQELNPFFADRRA
59-71	1433.8068	1432.7995	1	RRAMRPPVPGTVPRG
59-71	1449.7962	1448.7889	1	RRAMRPPVPGTVPRG oxidation (M)
60-71	1277.7105	1276.7032	0	RAMRPPVPGTVPRG
60-71	1293.7033	1292.6960	0	RAMRPPVPGTVPRG oxidation (M)
72-84	1514.7863	1513.7790	1	RGLLKEDTPFYFGKT
94-105	1264.7692	1263.7619	0	RIPVAVTPELVARG
164-177	1568.7833	1568.7760	0	RNMPAYGHQIPVADRW
178-185	977.5670	976.5597	0	RWAIVAYVRA

Table 4.4: Peptide mass fingerprint of in-gel chymotryptic digest of the band 5.

Comparision of the molecular masses values experimentaly obtained for the protein band 5 in the Tricine-SDS-PAGE of the lane D5 (fig 4.6) with those predicted for subunit III of the caa_3 oxygen reductase (accession number CAC08533). Zero and one possible miss cleavage were considered for the comparison.

Start- End	m/z (Observed)	m/z (predicted)	Miss cleavage	Sequence
34-41	891.292	891.921	0	DAAKLGMW
44-51	947.852	947.5812	0	LVTEILLF
116-124	904.5502	903.816	0	LTIALAGVF
184-193	1088.341	1088.6574	0	VALKAQRGVF
199-207	991.921	992.5292	0	TPVEISALY

4.4.3.1- Functional association

The functional association of the ACIII and the caa_3 oxygen reductase was addressed by investigating the direct oxidation of the former by the oxygen reductase. Figure 4.8 shows the UV-Visible spectra of the

ACIII in the oxidized state and reduced by sodium dithionite. In the presence of oxygen, sub-stoichiometric amounts of *caa*$_3$ oxygen reductase could reoxidise the ACIII.

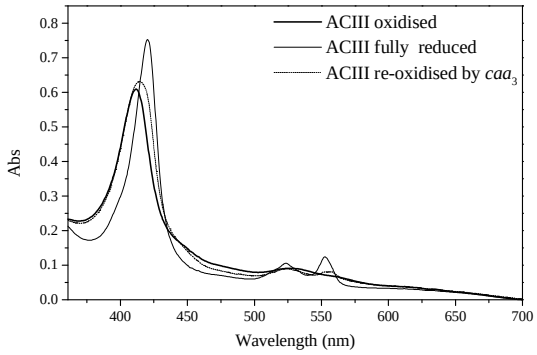

Figure 4.7

UV-Visible absorption spectra of the alternative complex III in the oxidized and reduced state, and re-oxidized by the *caa*$_3$ oxygen reductase.

Moreover, if the ACIII receives electrons from quinol and gives electrons to the *caa*$_3$ oxygen reductase, a complex formed by the two enzymes should have quinol: oxygen oxidoreductase activity. This activity was determined by measuring oxygen consumption by a 1:1 mixture of the two complexes upon addition of menadiol and a value of 77.3 µM O_2 .min^{-1}.mg^{-1} was obtained. Addition of KCN (the typical oxygen reductases inhibitor) completely abolished O_2 consumption, while the addition of HQNO inhibited this activity by 45 % (34.8 µM O_2 .min^{-1}.mg^{-1}).

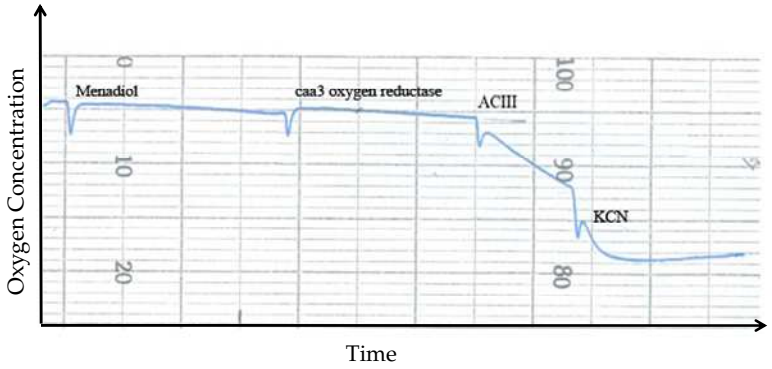

Figure 4.8

Example of the menadiol: oxygen oxidoreductase activity measurements of the structural and functional association of the ACIII and the *caa*$_3$ oxygen reductase. Inhibitory effect of KCN in oxygen consumption.

HiPIP was described as being one of the electron acceptors of the ACIII [1]. Therefore, in order to investigate its effect on the menadiol: oxygen oxidoreductase activity, the same experiment was performed in its presence. An increase of 20% in the activity (97 μM O_2 .min^{-1}.mg^{-1}) was observed. This result can be interpreted as HiPIP being able to mediate the electron transfer but not being essential.

4.5 – Discussion

In the electron transfer respiratory chain of the bacterium *R. marinus* the ACIII is the only enzyme which accepts electrons directly from reduced quinones. As previously shown, it is capable of performing the same function as the cytochrome *bc*$_1$ complex, although it does not belong to its family.

Here we addressed the interaction of ACIII with quinol and *caa*$_3$ oxygen reductase. We observed that the complex is reduced by menadiol, the analogue of *R. marinus* physiologic quinone, and that this reduction is inhibited by HQNO. The presence of at least one quinol binding site in the ACIII was determined by fluorescence

quenching titration of HQNO. In the case of cytochrome *bc*$_1$ complexes the HQNO binds only to one (Qi) of the two quinone binding sites [27]; therefore, the presence of two or more quinol binding sites in the ACIII could not be excluded.

In several organisms, including *R. marinus*, ACIII coding genes are followed by those coding for *caa*$_3$ oxygen reductase. This observation led to the hypothesis of a direct interaction between the two complexes. The findings here presented showed that the ACIII and *caa*$_3$ oxygen reductase are structurally and functionally associated into a 550 kDa complex (figure 4.9).

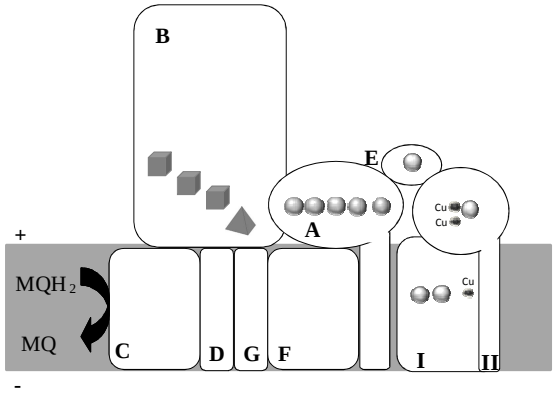

Figure 4.9

Schematic representation of the structural and functional association between the alternative complex III (subunits A-G) and the *caa*$_3$ oxygen reductase (catalytic subunits I and II). The gray spheres represent *c*-type hemes, the smaller gray and black spheres represent copper ions while cubes and pyramids represent $[4Fe\text{-}4S]^{2+/1+}$ and $[3Fe\text{-}4S]^{1+/0}$ clusters, respectively.

The functional association of the ACIII and the *caa*$_3$ oxygen reductase was further demonstrated by the observation of menadiol: oxygen

oxidoreductase activity, upon mixing the two purified complexes, which was KCN and HQNO inhibited. In cytochrome bc_1 complexes, and according to the Q-cycle mechanism, the cytochrome c_1 is the last electron acceptor within the complex, transferring electrons to the periplasmatic cytochrome *c* [28, 29]. The monohemic subunit of the ACIII is proposed to perform an equivalent role. In the case of direct interaction with caa_3 oxygen reductase this subunit is also proposed to replace the role of the periplasmatic electron carriers (such as cytochrome *c* and HiPIP).

4.6 - References

1. Pereira, M.M., J.N. Carita, and M. Teixeira, *Membrane-bound electron transfer chain of the thermohalophilic bacterium Rhodothermus marinus: a novel multihemic cytochrome bc, a new complex III.* Biochemistry, 1999. **38**(4): p. 1268-75.
2. Pereira, M.M., J.N. Carita, and M. Teixeira, *Membrane-bound electron transfer chain of the thermohalophilic bacterium Rhodothermus marinus: characterization of the iron-sulfur centers from the dehydrogenases and investigation of the high-potential iron-sulfur protein function by in vitro reconstitution of the respiratory chain.* Biochemistry, 1999. **38**(4): p. 1276-83.
3. Yanyushin, M.F., et al., *New class of bacterial membrane oxidoreductases.* Biochemistry, 2005. **44**(30): p. 10037-45.
4. Matsoso, L.G., et al., *Function of the cytochrome bc_1-aa_3 branch of the respiratory network in mycobacteria and network adaptation occurring in response to its disruption.* J Bacteriol, 2005. **187**(18): p. 6300-8.

5. Niebisch, A. and M. Bott, *Purification of a cytochrome bc-aa_3 supercomplex with quinol oxidase activity from Corynebacterium glutamicum. Identification of a fourth subunity of cytochrome aa_3 oxidase and mutational analysis of diheme cytochrome c_1.* J Biol Chem, 2003. **278**(6): p. 4339-46.
6. Megehee, J.A., J.P. Hosler, and M.D. Lundrigan, *Evidence for a cytochrome bcc-aa_3 interaction in the respiratory chain of Mycobacterium smegmatis.* Microbiology, 2006. **152**(Pt 3): p. 823-9.
7. Niebisch, A. and M. Bott, *Molecular analysis of the cytochrome bc_1-aa_3 branch of the Corynebacterium glutamicum respiratory chain containing an unusual diheme cytochrome c_1.* Arch Microbiol, 2001. **175**(4): p. 282-94.
8. Sone, N., et al., *A novel hydrophobic diheme c-type cytochrome. Purification from Corynebacterium glutamicum and analysis of the QcrCBA operon encoding three subunit proteins of a putative cytochrome reductase complex.* Biochim Biophys Acta, 2001. **1503**(3): p. 279-90.
9. Sakamoto, J., et al., *Cytochrome c oxidase contains an extra charged amino acid cluster in a new type of respiratory chain in the amino-acid-producing Gram-positive bacterium Corynebacterium glutamicum.* Microbiology, 2001. **147**(Pt 10): p. 2865-71.
10. Sone, N., M. Sekimachi, and E. Kutoh, *Identification and properties of a quinol oxidase super-complex composed of a bc_1 complex and cytochrome oxidase in the thermophilic bacterium PS3.* J Biol Chem, 1987. **262**(32): p. 15386-91.
11. Berry, E.A. and B.L. Trumpower, *Isolation of ubiquinol oxidase from Paracoccus denitrificans and resolution into cytochrome bc_1 and cytochrome c-aa_3 complexes.* J Biol Chem, 1985. **260**(4): p. 2458-67.
12. Janzon, J., B. Ludwig, and F. Malatesta, *Electron transfer kinetics of soluble fragments indicate a direct interaction between complex III and the caa_3 oxidase in Thermus thermophilus.* IUBMB Life, 2007. **59**(8-9): p. 563-9.

13. Pereira, M.M., et al., *The caa_3 terminal oxidase of the thermohalophilic bacterium Rhodothermus marinus: a HiPIP:oxygen oxidoreductase lacking the key glutamate of the D-channel.* Biochim Biophys Acta, 1999. **1413**(1): p. 1-13.
14. Gok, E., C. Ozturk, and N. Akbay, *Interaction of thyroxine with 7 hydroxycoumarin: a fluorescence quenching study.* J Fluoresc, 2008. **18**(5): p. 781-5.
15. Schagger, H., *Membrane Protein Purification and Crystallization 2/e: A Practical Guide*. 2003, New York: Elsevier Science.
16. Schagger, H. and G. von Jagow, *Tricine-sodium dodecyl sulfate-polyacrylamide gel electrophoresis for the separation of proteins in the range from 1 to 100 kDa.* Anal Biochem, 1987. **166**(2): p. 368-79.
17. Goodhew, C.F., K.R. Brown, and G.W. Pettigrew, *Haem staining in gels, a useful tool in the study of bacterial c-type cytochromes. .* Biochem. Biophys. Acta, 1986. **852**: p. 288-294.
18. Molnar, A.M., et al., *Evaluation by blue native polyacrylamide electrophoresis colorimetric staining of the effects of physical exercise on the activities of mitochondrial complexes in rat muscle.* Braz J Med Biol Res, 2004. **37**(7): p. 939-47.
19. Perkins, D.N., et al., *Probability-based protein identification by searching sequence databases using mass spectrometry data.* Electrophoresis, 1999. **20**(18): p. 3551-67.
20. Wilkins, M.R., et al., *Detailed peptide characterization using PEPTIDEMASS--a World-Wide-Web-accessible tool.* Electrophoresis, 1997. **18**(3-4): p. 403-8.
21. Fieser, L.F., *Convinient procedures for the preparation of antihemorragic compounds.* The Journal of Biological Chemistry, 1940: p. 391-396.
22. Refojo, P.N., et al., *The alternative complex III: a different architecture using known building modules. in press*, 2010.

23. Cheng, V.W., et al., *Investigation of the environment surrounding iron-sulfur cluster 4 of Escherichia coli dimethylsulfoxide reductase.* Biochemistry, 2005. **44**(22): p. 8068-77.
24. Bertero, M.G., et al., *Structural and biochemical characterization of a quinol binding site of Escherichia coli nitrate reductase A.* J Biol Chem, 2005. **280**(15): p. 14836-43.
25. Lakowicz, J.R., *Principles of Fluorescence Spectroscopy*. second edition ed. 1999: Kluwer Academic/ Plenum Publishers.
26. Pereira, M.M., et al., *The alternative complex III from Rhodothermus marinus - a prototype of a new family of quinol:electron acceptor oxidoreductases.* FEBS Lett, 2007. **581**(25): p. 4831-5.
27. Cooley, J.W., T. Ohnishi, and F. Daldal, *Binding dynamics at the quinone reduction (Qi) site influence the equilibrium interactions of the iron sulfur protein and hydroquinone oxidation (Qo) site of the cytochrome bc_1 complex.* Biochemistry, 2005. **44**(31): p. 10520-32.
28. Mitchell, P., *Protonmotive redox mechanism of the cytochrome b-c_1 complex in the respiratory chain: protonmotive ubiquinone cycle.* FEBS Lett, 1975. **56**(1): p. 1-6.
29. Mitchell, P., *Possible molecular mechanisms of the protonmotive function of cytochrome systems.* J Theor Biol, 1976. **62**(2): p. 327-67.

Chapter 5

Characterization of the c-type cytochromes subunits of ACIII from Rhodothermus marinus

The results presented in this chapter will be published in:

Patrícia N. Refojo, Miguel Teixeira and Manuela M. Pereira (2010) *The lipid bound monoheme cytochrome c subunit of alternative complex III is the electron donor of caa_3 oxygen reductase in Rhodothermus marinus membranes* ***In preparation***

Acknowledgements

Lara Paulo is acknowledged for the growths of *E. coli* cells expressing the pentaheme cytochrome *c*.

5.1- Summary

The alternative complex III of *Rhodothermus marinus* has two subunits with *c*-type hemes: a monoheme and a pentaheme. The objective of the work presented was to structurally and functionally characterize these subunits. Thus, their coding genes were cloned and expressed in *Escherichia coli.* The UV-Visible spectra of the monoheme cytochrome *c* subunit and of the partially purified pentaheme cytochrome *c* showed characteristic features of low-spin hemes. For the monoheme subunit, a reduction potential of +160 mV was determined at pH 7.5.

Previously, alternative complex III and caa_3 oxygen reductase were reported to be structural and functionally associated. This work allowed the identification of the monoheme cytochrome *c* as the electron donor of caa_3 oxygen reductase which presented an oxygen consumption of 459 μM $O_2.min^{-1}.mg^{-1}$ in the presence of the cytochrome. A lipobox observed at the N-terminus of the amino acid sequence of the monoheme cytochrome *c* led to the prediction of the presence of lipids covalently bound to a conserved cysteine residue, which was here investigated.

5.2 – Introduction

Cytochromes (meaning cellular pigment [1]) are heme (iron-protoporphyrin IX) containing proteins involved in electron transfer reactions. Cytochromes differ from each other according to the type of incorporated heme (heme *b*, *c*, *d*, *a*, *o*), which have distinct porphyrin substituents or even a different degree of porphyrin reduction. The modifications occur at the level of carbon 2 and/or 4 (Fisher

numbering system) with heme *d* as the exception since the modifications are at the carbons 5 and 6.

In cytochrome *c*, in contrast to the other cytochromes, the *c*-type heme is covalently bound to the protein via two thioether bonds between the heme and two cysteine residues in a characteristic heme binding motif CXXCH. The histidine residue serves as axial ligand to iron and X represents any amino acid residue (except cysteine) (figure 5.1). Although CXXCH is the most observed *c*-type heme binding motif some deviations were observed. A higher number of X amino acid residues were observed for several multihemes cytochromes c_3 [2], for cytochrome c_{552} [3] (CXXXCH), and also for the multiheme cytochrome *c* MccA from *Wolinella succinogenes* ($CX_{15}CH$) [4]. The catalytic heme of the pentaheme nitrite reductase (NrfA) has a lysine residue as the axial ligand to the iron (CXXCK) instead of the histidine [5]. The hemes can also be bound to only one cysteine residue as in the case of some cytochromes fromf *Euglena gracilis* and *Crithidia oncopelti* [6, 7].

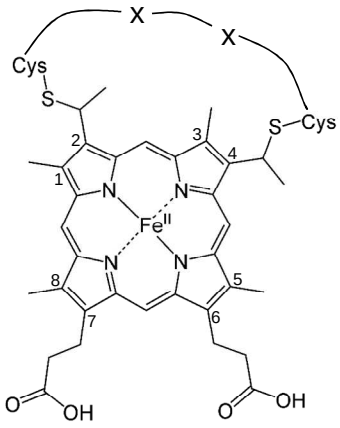

Figure 5.1
Chemical structure of *c*-type heme. The Fisher numbering system for the heme substituints is shown.

The covalent binding of *c*-type hemes to the protein requires the existence of maturation systems. So far, three different systems have been identified namely system I, II and III [1, 8, 9]. System I, also called cytochrome *c* maturation (Ccm), is found mostly in Gram-negative bacteria and in plant mitochondria and has up to nine different proteins (CcmABCDEFGHI). System II or cytochrome *c* synthesis (Ccs)

can be found in Gram-positive bacteria, cyanobacteria, chloroplasts of plants and algae, and some β-, δ-, and ε-Proteobacteria. System III is a cytochrome *c* heme lyase (CCHL) and is just found in mitochondria.

The number of *c*-type hemes in a single polypeptide chain ranges between one and 45 [10]. While monoheme cytochromes *c* function in its majority as electron transfer proteins within redox chains, multiheme cytochromes *c* are able to perform a larger number of biochemical roles, including enzymatic activity [11]. One example is the already mentioned NrfA in which the heme bound to the CXXCK motif is the active site of the enzyme. The close proximity of the hemes in the multiheme cytochromes *c* allows a fast transfer of electrons through relatively long distances [10]. This can be further improved by the interaction between two or more multiheme cytochromes *c*.

This chapter describes the cloning, expression and characterization of the cytochrome *c* subunits (monoheme cytochrome *c* –mhc and pentaheme cytochrome *c*- phc) of the alternative complex III from *Rhodotherimus marinus*.

5.3 - Materials and Methods

5.3.1. - Cloning and expression of the cytochrome c subunits of the alternative complex III

Rhodothermus marinus genomic DNA was extracted from a liquid growth culture using GenElute Bacterial Genomic DNA kit (Sigma). The gene encoding the mhc subunit (*ActE*) of ACIII was amplified by a PCR using the genomic DNA of *R. marinus* as template and the following oligonucleotides: 5'AAT GGA TCC AAT GCA GAA CAT CAC AGC A 3' and 5' GAA TTC TTA CTC TCC CT GAA GCC GAG-

3′ with restrictions sites (underlined) for BamHI and EcoRI, respectively. A truncated form of the gene coding for the pentaheme cytochrome *c* (*ActA*) was also constructed in order to express the protein without the N-terminal region which corresponds to a transmembrane helix. The same procedure was performed using the oligonucleotides: 5′- ATCCAT GGA CTT TTC GCC C -3′and 5′ AAC TCG AGT CAA TAG TGG CAG 3′ with restrictions site (underlined) for NcoI and XhoI, respectively.

In order to express also a *pelB* signal sequence for potential periplasmatic localization of the target proteins, the amplified fragments were cloned into a pET22b(+) vector (Novagen), previously digested with the appropriate restriction enzymes for each case. The cloning result was confirmed by nucleotide sequencing of the entire coding region. *E. coli* C41 (DE3) cells harboring a plasmid with auxiliary genes for heme *c* maturation (pEC86- ccmABCDEFGH) [12] were used to express the cytochromes *c*.

Monoheme cytochrome *c* expressing cells were grown at 37 ºC (180 rpm), in LB medium containing ampicilin (100 µg/mL) and chloramphenicol (34 µg/mL), until an OD_{600nm} of approximately 0.6. At this point, 0.5 mM of IPTG was added to the medium and the culture was harvested after 16 hours. The cells for the expression of the truncated form of the pentaheme cytochrome *c* were grown at 30 ºC (150 rpm), in TB medium containing the same antibiotics used for the mhc expression. The culture was harvested after, approximately, 45 hours.

5.3.2 - Protein purification

The same procedures were followed for obtaining the soluble fraction with the monoheme cytochrome *c* and that of the pentaheme cytochrome *c.* The cells were harvested by centrifugation and the pellet resuspended in 20 mM Tris-HCl, 1 mM EDTA, 1 mM PMSF pH 7.5. These were then disrupted by passing through a French Press at 19000 psi and the unbroken cells were separated by centrifugation at 22000 g for 15 min at 4 ºC. Soluble and membrane fractions were separated by centrifugation at 200000 g, for 45 min at 4 ºC. The soluble fraction, containing the mhc subunit, was applied into a Q- Sepharose Fast Flow column using 20 mM Tris-HCl, 1 mM PMSF and pH 7.5 as buffer (buffer A). The sample was eluted applying a linear gradient from 0 to 0.5 M of NaCl. The mhc subunit, eluted with approximately 0.1 M NaCl, was concentrated and loaded into a gel filtration chromatographic column S200 using buffer A with 150 mM NaCl. The soluble fraction containing the truncated form of pentaheme cytochrome *c* was applied also a into a Q- Sepharose Fast Flow column using buffer A.

5.3.3 - Protein and heme quantification

Protein concentrations were determined by the bicinchoninic acid (BCA) method [13]. Heme content was determined by the pyridine hemochrome method [14].

5.3.4 - Electrophoretic techniques

The purity of the samples was investigated by SDS-PAGE [15]. Tricine-SDS-PAGE of ACIII was carried out as in [16] with 10 % T, 3 %

C. Heme staining was done as in [17], previously described to identify the covalently bound hemes.

5.3.5- Mass spectrometry assays

The protein bands observed in the SDS-PAG of the mhc were excised and submitted to proteolytic digestion with trypsin. The mass spectra of the peptides were acquired with positive reflection MS and MS/MS modes using MALDI-TOF/TOF MS instrument (4800plus MALDI TOF/TOF analyzer) in the Mass Spectrometry Laboratory, Analytical Services Unit of ITQB/IBET. The collected MS and MS/MS spectra were analysed in combined mode using Mascot search engine and NCBI database. The identification of the peptides was also performed by direct comparison of the molecular masses predicted for the peptides with those experimentally obtained. The molecular masses of the peptides were predicted using PeptideMass at http://expasy.org/cgi-bin/peptide-mass.pl [18].

5.3.6 - Spectroscopic characterization

UV-Visible absorption spectra were recorded in a Shimadzu UV-1603 spectrophotometer at room temperature. The anaerobic potentiometric titration of the mhc (≈ 2.5 μM in 40 mM Tris-HCl pH 7.5) was monitored by visible absorption spectroscopy in a glass cuvette of 1 cm path-length and 2.5 mL working volume continuously flushed with argon. By stepwise addition of buffered sodium dithionite, spectra from 380 to 700 nm were obtained at each solution redox potential, after attaining equilibrium. The mixture of redox mediators, at a final concentration of ≈16 μM, used was: N,N-dimethyl-p-phenylenodiamine (E′o=+340 mV), p-benzoquinone (E′o=+240 mV),

1,2-naphtoquinone-4-sulphonic acid (E'o=+215 mV), 1,2-naphtoquinone (E'o=+180 mV), trimethylhydroquinone (E'o=+115 mV), phenazine methosulfate (E'o=+80 mV), 1,4-naphtoquinone (E'o=+60 mV), duroquinone (E'o=+5 mV), menadiona (E'o= 0 mV), plumbagin (E'o= -40 mV) and phenazine (E'o=-125 mV). The redox mediators were chosen in order to minimize spectral overlaps and to cover the relevant redox potential range. The experimental data was analyzed using MATLAB (Mathworks, South Natick, MA) for Windows, and were fitted with a single-electron Nernst curve.

5.3.7 – Experiments with lipase

The mhc (15 µM) and the ACIII (15 µM) were incubated with 5 µM of lipase from *Rhizopus arrhizus* in 20 mM Tris-HCl pH 7.5 at 37 ºC for 24 h. The incubated and not incubated mhc and ACIII were subjected to SDS-PAGE (Tricine-SDS-PAGE in the case of ACIII). The protein bands of mhc with apparent molecular masses of 18 and 20 kDa and that of the ACIII with an apparent molecular mass of 22 KDa were excised from the gel and analyzed by mass spectrometry.

5.3.8 - Activities Assays

The mhc: oxygen oxidoreductase activity was determined by the oxygen consumption measured polarographically with a Clark-type oxygen electrode, YS Moldel 5300, from Yellow Springs. The assays were carried out at 30 ºC using 20 mM potassium phosphate pH 6.5 as buffer. The mhc (2.2 µM) was reduced during the assay by sodium ascorbate (≈300 µM) and used as electron donor of caa_3 oxygen reductase (80 nM). Potassium cyanide (0.7 mM) was used as oxygen reductase inhibitor. As a control, the oxygen consumption by caa_3

oxygen reductase with sodium ascorbate as electron donor was measured.

5.4 - Results and Discussion

5.4.1- Purification and characterization of the cytochromes *c* subunits of ACIII

In order to structurally and functionally characterize the cytochromes *c* subunits of the alternative complex III of *R. marinus*, the genes coding for the mhc (*ActE*) and for the phc (*ActA*) were cloned and expressed in *E. coli*. For the phc, a truncated form (phcT) was constructed to express the protein without the N-terminal region which corresponds to a transmembrane helix. The expression cells also harbored the pEC86 plasmid with the auxiliary genes for the maturation of the *c*-type hemes in *E. coli* and thus allowing the expression of *c*-type cytochromes in aerobic conditions. The UV-Visible spectrum of the as isolated mhc showed a typical oxidized *c*-type heme cytochrome with a Soret band maximum at 410.5 nm and a broad band between 500 and 600 nm (figure 5.2A). A band with a maximum at 695 nm was also present indicating a histidine-methionine-Fe coordination. After reduction with sodium dithionite, typical features of low-spin ferrous hemes were observed in which the Soret band maximum shifted to 417 nm and the α and β bands became visible with maxima at 553.5 and 523 nm, respectively (figure 5.2A). The difference between the spectrum of the reduced protein and that of the as isolated protein (oxidized) showed a Soret band with maximum at 418 nm and a α band with maximum at 553.5 nm (figure 5.2B). The Visible spectra of the soluble fraction containing phcT

(figure 5.3A) and of this partially purified cytochrome (figure 5.3B) showed also typical features of an oxidized cytochrome *c* with a Soret band maximum at 409 nm and a broad band between 500 and 600 nm; when in the reduced state the Soret band shifted to a maximum of 419 nm and the α- and β-bands became visible with maxima at 552.5 and 524 nm, respectively.

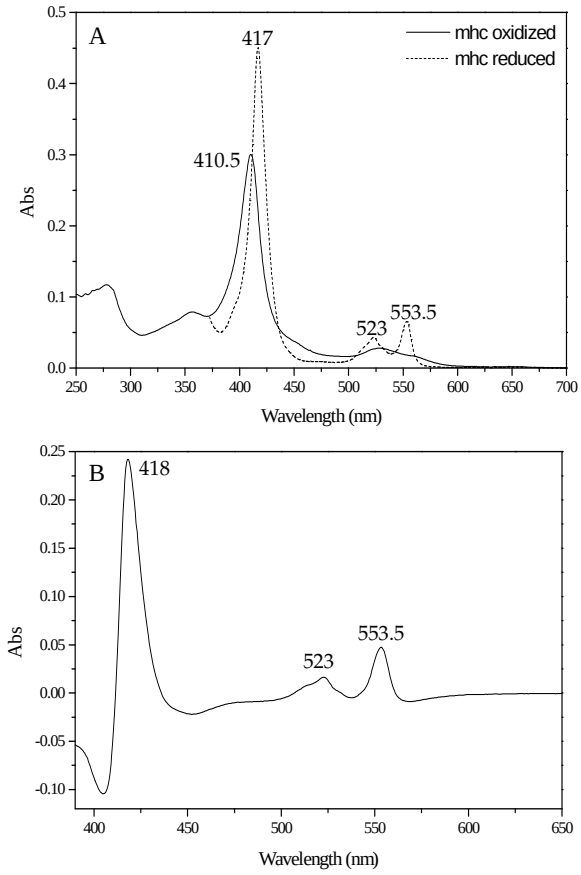

Figure 5.2

UV-Visible absorption spectra of the mhc of ACIII. A) Absolute spectra in the oxidized (—) and reduced (---) state, B) difference between the spectrum of the reduced and that of the oxidized protein. In the spectrum of the reduced protein, the absorbance between 250 and 375 nm was omitted due to the interference of sodium dithionite.

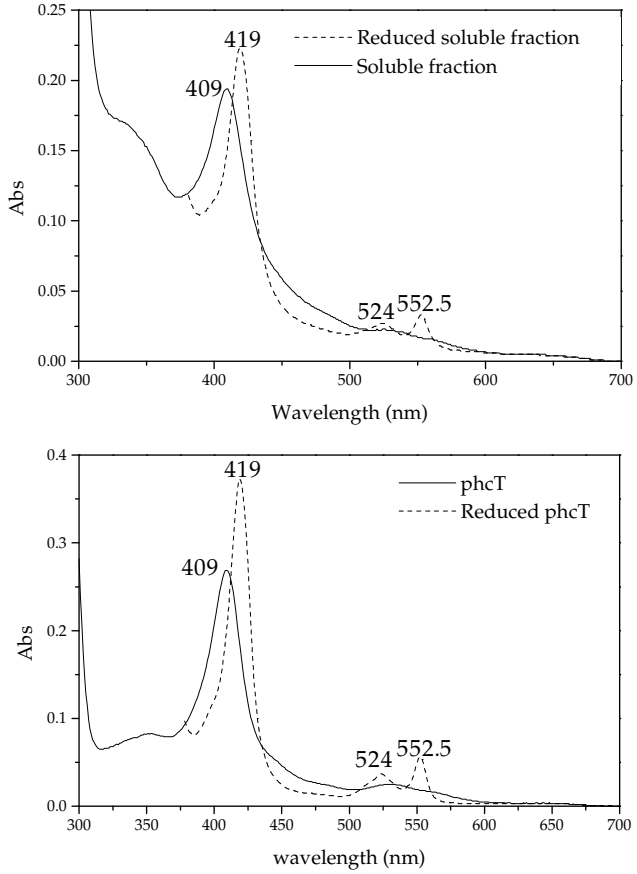

Figure 5.3

Visible absorption spectra of the soluble fraction containing the truncated pentaheme cytochrome *c* (A) and of a partially purified sample of the protein (B) in the oxidized (—) and reduced (- -) state. In the spectrum of the reduced protein, the absorbance between 250 and 375 nm was omitted due to the interference of sodium dithionite.

The *c*-type heme content of mhc subunit was determined to be 0.95 mol per mol of protein, which is in agreement with the presence of one CXXCH binding motif in the amino acid sequence and meaning that most protein has heme incorporated. The UV-Visible spectrum and the heme content indicated that mhc sample has a high level of purity;

however, the SDS-PAG showed three protein bands with apparent molecular masses of 44, 20 and 18 kDa (figure 5.4B). Heme staining (figure 5.4A) indicated clearly that the two smallest protein bands have covalently bound hemes. The 44 kDa protein band also stained under this procedure but with less intensity. In order to identify the proteins present in these bands, mass spectrometry analyses (MALDI-TOF/TOF) were performed, and, in fact, the three protein bands were identified as the mhc protein subunit (see tables 5.1-5.3). Therefore, the 44 kDa protein band is proposed to be a homodimeric form of the mhc protein while the two other protein bands are proposed to be different structural conformations, since peptides with molecular masses compatible with N- and C- termini were observed.

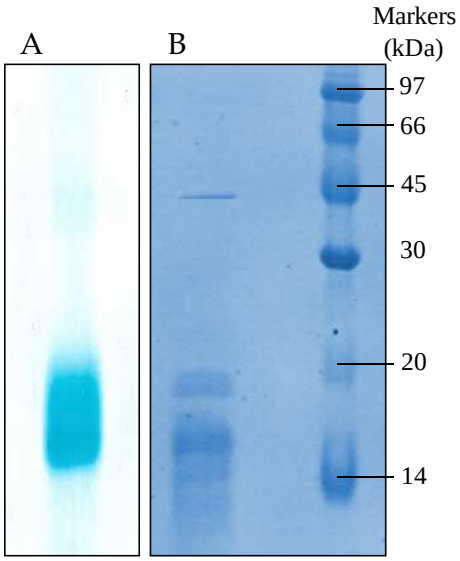

Figure 5.4

Heme (A) and coomassie (B) stained SDS-PAG of the monoheme cytochrome *c* of the ACIII from *R. marinus.*

Table 5.1: Peptide mass fingerprint of in-gel tryptic digest of the band with an apparent molecular mass of 40 kDa in the SDS-PAG of figure 5.3B.

Comparision of the molecular masses values experimentaly obtained for the protein band with an apparent molecular mass of 40 kDa in the SDS-PAGE of mhc of ACIII (fig 5.3B) with those predicted for this subunit (accession number ABV55248). Zero and one possible miss cleavage were considered for the comparison.

Start-End	m/z (observed)	m/z (predicted)	Miss cleavage	Sequence
72-84	1514.790	1514.7889	1	GLLKEDTPFYFGK
94-105	1264.772	1264.7623	0	IPVAVTPELVAR
164-177	1568.792	1568.7638	0	NMPAYGHQIPVADR
164-177	1584.773	1584.7587	0	NMPAYGHQIPVADR (oxidation M)
178-185	977.566	977.5567	0	WAIVAYVR
190-203	1509.757	1509.7292	0	SQHATAADVPEEVR

Table 5.2: Peptide mass fingerprint of in-gel tryptic digest of the band with an apparent molecular mass of 20 kDa in the SDS-PAG of figure 5.4B.

Comparision of the molecular masses values experimentaly obtained for the protein band with an apparent molecular mass of 20 kDa in the SDS-PAGE of mhc of ACIII (fig 5.4B) with those predicted for this subunit (accession number ABV55248). Zero and one possible miss cleavage were considered for the comparison.

Start-End	m/z (observed)	m/z (predicted)	Miss cleavage	Sequence
72-84	1514.802	1514.7889	0	GLLKEDTPFYFGK
76-84	1103.505	1103.5044	0	EDTPFYFGK
85-105	2227.219	2227.2080	0	TADGAYVERIPVAVTPELVAR
94-105	1264.7603	1264.7625	0	IPVAVTPELVAR§
110-130	2285.187	2285.0260	0	YNIYCAVCHGQAGDGQGIIMR (M oxidation)
148-163	1819.882	1819.8973	0	NVEDGYIFDVISHGVR
164-177	1568.766	1568.7639	0	NMPAYGHQIPVADR
164-177	1584.759	1584.7587	0	NMPAYGHQIPVADR (M oxidation)
164-185	2543.317	2543.2987	0	NMPAYGHQIPVADRWAIVAYV R
178-575	977.575	977.5567	0	WAIVAYVR
186-203	1977.94	1978.0100	0	ALQRSQHATAADVPEEVR

§ - Peptide identified by MS/MS

Table 5.3: Peptide mass fingerprint of in-gel tryptic digest of the band with an apparent molecular mass of 18 kDa in the SDS-PAG of figure 5.4B.

Comparision of the molecular masses values experimentaly obtained for the protein band with an apparent molecular mass of 18 kDa in the SDS-PAGE of mhc of ACIII (fig 5.3B) with those predicted for this subunit (accession number ABV55248). Zero and one possible miss cleavage were considered for the comparison.

Start-End	m/z (observed)	m/z (predicted)	Miss cleavage	Sequence
60-71	1293.685	1293.7096	0	AMRPPVPGTVPR
72-84	1514.7206	1514.7889	1	GLLKEDTPFYFGK
76-84	1103.4857	1103.5044	0	EDTPFYFGK
85-93	981.4451	981.4636	0	TADGAYVER
85-105	2227.2063	2227.1885	1	TADGAYVERIPVAVTPELVAR
94-105	1264.7422	1264.7625	0	IPVAVTPELVAR §
148-163	1819.863	1819.8973	0	NVEDGYIFDVISHGVR
164-177	1568.7527	1568.7639	0	NMPAYGHQIPVAVR
164-177	1584.789	1584.7587	0	NMPAYGHQIPVAVR (M oxidation)
178-185	977.5207	977.5567	0	WAIVAYVR
186-203	1977.96	1978.0100	0	ALQRSQHATAADVPEEVR

§ - Peptide identified by MS/MS

A redox titration performed at pH 7.5 was monitored by visible absorption spectroscopy revealing a mid-point reduction potential of +160 mV (figure 5.5), which is different from the reduction potential determined for the hemes within the ACIII (235, 80 and -45 mV) [19]. Nevertheless, it should be stressed that the value obtained for the isolated mhc may not reflect the redox potential of the subunit inside the ACIII, since when present in the complex mhc experiences a different environment.

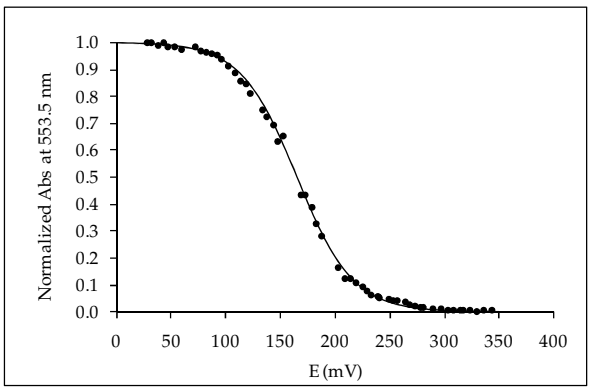

Figure 5.5

Reductive titration of the monoheme cytochrome *c* subunit of the ACIII of *R. marinus* at pH 7.5. Data collected at the α-band maximum 553.5 nm (•). The solid line was obtained fitting a single electron Nernst curve with E=160 mV.

5.4.2 – Is monoheme cytochrome *c* a lipoprotein?

Lipids covalently bound to proteins constitute a possible way to associate proteins to the membrane since it provides the protein with a hydrophobic anchor.

The monoheme cytochrome *c* is predicted to be a lipid modified protein due to the presence of a signal peptide, lipobox, in its N-terminal amino acid sequence. According to Babu and coworkers [20] a typical signal peptide for lipid incorporation is composed by three distinct regions: a n-region containing five to seven amino acid residues including two positively charged residues (lysine or arginine); a hydrophobic region constituted by seven to twenty two amino acid residues, and a c-region with the consensus [LVI][ASTVI][GAS]C. The consensus in the c-region is the, so called, lipobox and the last cysteine residue is the amino acid to which the lipid molecules are bound (figure 5.6). In the case of mhc, the n-region

has nine amino acids residues with an arginine as the positively charged residue, the hydrophobic region is composed by eleven amino acid residues and LAGC form the lipobox (figure 5.6).

The prediction of mhc as a lipid modified protein was corroborated by several informatics programs available online such as: i) A database of bacterial lipoproteins (DOLOP) (http://www.mrc-lmb.cam.ac.uk/genomes/dolop/analysis.shtml) [20] and ii) LipoP 1.0 Server (http://www.cbs.dtu.dk/services/LipoP/) [21].

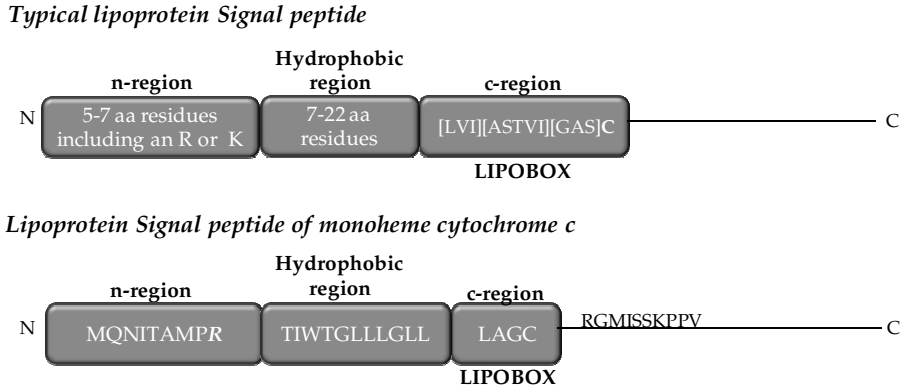

Figure 5.6

Lipoproteins signal peptide. Upper: Typical lipoprotein signal peptide with the three different regions. The n-region is composed by five to seven amino acid residues including two positively charged residues; the hydrophobic region has seven to twenty two amino acid residues mainly hydrophobic and uncharged; the c-region contains the consensus sequence [LVI][ASTVI][GAS] and the conserved lipid modified cysteine (lipobox). Lower: Lipoprotein signal peptide present in the monoheme cytochrome *c* subunit.

Usually, the covalent binding of the lipid to the protein occurs in three steps catalyzed each one by a different enzyme [22]. In the first step, a diacylglycerol molecule is bound to the conserved cysteine residue by a thioether linkage in a reaction catalyzed by the

phosphatidylglycerol:pre-lipoprotein diacylglycerol transferase (Lgt). In the second step, the prolipoprotein signal peptidase/ signal peptidase II (LspA) catalyzes the cleavage of the N-terminus signal peptide at the level of the cysteine residue. The last step was only observed in Gram negative bacteria and consists in the amino acylation of the conserved cysteine and is catalyzed by the phospholipid: apolipoprotein N-acyltransferase (Lnt). In order to analyze if the presence of lipoproteins is viable in *Rhodothermus marinus*, searches were performed to identify genes coding for the three needed enzymes. Indeed, homologous enzymes were found in its genome. Therefore, it is possible that the mhc is lipid modified.

In order to investigate the presence of a lipid molecule bound to the mhc a peptide mass fingerprint approach was used with the subunit expressed in *E. coli* and the native cytochrome *c* (part of the ACIII). If a lipid was present the first 22 amino acid residues of the N-terminus would be absent and a difference in the molecular masses predicted for the peptides would be expected. Thus, the mhc expressed in *E. coli* and the ACIII were treated with a lipase which catalyzes the hydrolysis of an ester bond. The incubated and non-incubated mhc expressed in *E. coli* and the ACIII were subjected to SDS-PAGE and the protein band with apparent molecular mass of 22 kDa of the ACIII lanes and the 18 and 20 kDa protein bands of the mhc were excised from the gel and analyzed. However, the obtained results were not conclusive since the observed molecular masses for the peptides of the N-terminal of the protein only matched the predicted values if several modifications were considered. Namely, the peptide composed by the first nine amino acid residues (MQNITAMPR) would be considered if two or three modifications have occurred (the oxidation of one

methionine residue and one deamidation[1] reaction or the oxidation of the two methionine residue plus deamidation). This makes the identification of the N-terminus uncertain.

5.4.3 - Within ACIII the mhc subunit is the electron donor of *caa*$_3$ oxygen reductase

The moneheme cytochrome *c* subunit was proposed to be the last electron acceptor within the ACIII (as cytochrome c_1 in the bc_1 complex) and also to mediate the electron transfer between ACIII and the *caa*$_3$ oxygen reductase (equivalent role to the periplasmic electron carrier, such as cytochrome *c* and/or HiPIP) (see chapters 1 and 4). In order to test this hypothesis, dioxygen consumption measurements were performed using the mhc as substrate. The assay was started by

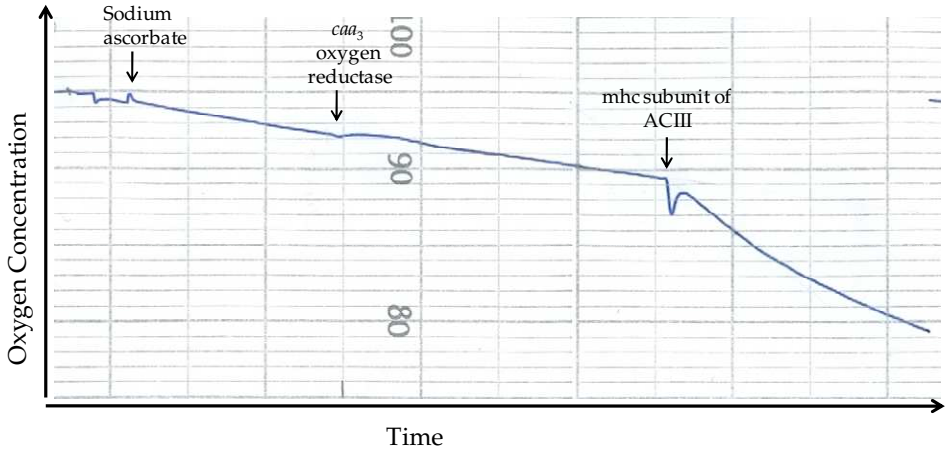

Figure 5.7

Example of the assay done to measure the oxygen consumption by *caa*$_3$ oxygen reductase using the monoheme: cytochrome c subunit of the alternative complex III as electron donor. Sodium ascorbate was used to reduce the electron donor.

the addition of the mhc and a average value of 459 μM O_2. min^{-1}. mg^{-1} was obtained (figure 5.7). This O_2 consumption ceased completely

[1] Deamidation- glutamine (Q) modified to glutamate (E)

upon addition of KCN to the assay which demonstrated the specificity of the reaction. The activity corresponded to a turnover value of 99 min^{-1}. It is important to mention that the obtained value is most probably underestimated since it was determined at 30 ºC (due to technical constrains of the oxygen electrode) and the optimal temperature for the activity of the enzyme was determined to be 70 ºC [23]. HiPIP and the soluble monoheme cytochrome *c* of *Rhodothermus marinus* were also proposed to be electron donors of the caa_3 oxygen reductase and turnovers of 208 and 26 min^{-1}, respectively, have been obtained [24]. Although the activity determined with mhc was lower than that with HiPIP it should be noticed that physiologically the mhc is not isolated. In fact, it is integrated into the ACIII and the affinity and the interaction between the subunits and even between the complexes should have a strong influence.

5.5- Conclusions

The expression of the cytochromes *c* subunits of ACIII in *E. coli* allowed the spectroscopic, biochemical and functional characterization of the monoheme subunit and the spectroscopic characterization of the pentaheme cytochrome *c*. The two subunits showed UV-visible spectra with the typical features of low-spin hemes. For the mhc subunit, a reduction potential of +160 mV was determined by UV-visible absorption spectroscopy at pH 7.5.

In this work, the functional role of the monoheme cytochrome *c* was addressed and it was showed that, indeed, this subunit is an electron donor of the oxygen reductase in the structural and functional association established between the ACIII and the caa_3 oxygen

reductase. Therefore, the monoheme cytochrome *c* is the last electron acceptor within the ACIII. In conclusion, the monoheme cytochrome *c* of ACIII is able to perform an equivalent functional role of the cytochrome c_1 in the bc_1 complexes and of a periplasmic electron carrier. The attachment of the mhc to the membrane, due to the eventual presence of covalently bound lipids in its N-terminus, could provide some mobility to the subunit facilitating its function as an electron carrier between the complexes.

5.5 - References

1. Stevens, J.M., et al., *C-type cytochrome formation: chemical and biological enigmas.* Acc Chem Res, 2004. **37**(12): p. 999-1007.
2. Aragao, D., et al., *Structure of dimeric cytochrome c3 from Desulfovibrio gigas at 1.2 A resolution.* Acta Crystallogr D Biol Crystallogr, 2003. **59**(Pt 4): p. 644-53.
3. Jungst, A., et al., *The nirSTBM region coding for cytochrome cd_1-dependent nitrite respiration of Pseudomonas stutzeri consists of a cluster of mono-, di-, and tetraheme proteins.* FEBS Lett, 1991. **279**(2): p. 205-9.
4. Hartshorne, R.S., et al., *A dedicated haem lyase is required for the maturation of a novel bacterial cytochrome c with unconventional covalent haem binding.* Mol Microbiol, 2007. **64**(4): p. 1049-60.
5. Einsle, O., et al., *Structure of cytochrome c nitrite reductase.* Nature, 1999. **400**(6743): p. 476-80.
6. Ikegami, I., S. Katoh, and A. Takamiya, *Nature of heme moiety and oxidation-reduction potential of cytochrome 558 in Euglena chloroplasts.* Biochim Biophys Acta, 1968. **162**(4): p. 604-6.

7. Pettigrew, G.W., et al., *Purification, properties and amino acid sequence of atypical cytochrome c from two protozoa, Euglena gracilis and Crithidia oncopelti.* Biochem J, 1975. **147**(2): p. 291-302.
8. Bowman, S.E. and K.L. Bren, *The chemistry and biochemistry of heme c: functional bases for covalent attachment.* Nat Prod Rep, 2008. **25**(6): p. 1118-30.
9. Kranz, R.G., et al., *Cytochrome c biogenesis: mechanisms for covalent modifications and trafficking of heme and for heme-iron redox control.* Microbiol Mol Biol Rev, 2009. **73**(3): p. 510-28, Table of Contents.
10. Sharma, S., G. Cavallaro, and A. Rosato, *A systematic investigation of multiheme c-type cytochromes in prokaryotes.* J Biol Inorg Chem, 2010. **15**(4): p. 559-71.
11. Mowat, C.G. and S.K. Chapman, *Multi-heme cytochromes--new structures, new chemistry.* Dalton Trans, 2005(21): p. 3381-9.
12. Arslan, E., et al., *Overproduction of the Bradyrhizobium japonicum c-type cytochrome subunits of the cbb_3 oxidase in Escherichia coli.* Biochem Biophys Res Commun, 1998. **251**(3): p. 744-7.
13. Smith, P.K., et al., *Measurement of protein using bicinchoninic acid.* Anal Biochem, 1985. **150**(1): p. 76-85.
14. Berry, E.A. and B.L. Trumpower, *Simultaneous determination of hemes a, b, and c from pyridine hemochrome spectra.* Anal Biochem, 1987. **161**(1): p. 1-15.
15. Laemmli, U.K., *Cleavage of Structural Proteins during the Assembly of the Head of Bacteriophage T4.* Nature, 1970. **227**: p. 680-685.
16. Schagger, H. and G. von Jagow, *Tricine-sodium dodecyl sulfate-polyacrylamide gel electrophoresis for the separation of proteins in the range from 1 to 100 kDa.* Anal Biochem, 1987. **166**(2): p. 368-79.
17. Goodhew, C.F., K.R. Brown, and G.W. Pettigrew, *Haem staining in gels, a useful tool in the study of bacterial c-type cytochromes.* . Biochem. Biophys. Acta, 1986. **852**: p. 288-294.

18. Wilkins, M.R., et al., *Detailed peptide characterization using PEPTIDEMASS--a World-Wide-Web-accessible tool.* Electrophoresis, 1997. **18**(3-4): p. 403-8.

19. Pereira, M.M., J.N. Carita, and M. Teixeira, *Membrane-bound electron transfer chain of the thermohalophilic bacterium Rhodothermus marinus: a novel multihemic cytochrome bc, a new complex III.* Biochemistry, 1999. **38**(4): p. 1268-75.

20. Babu, M.M., et al., *A database of bacterial lipoproteins (DOLOP) with functional assignments to predicted lipoproteins.* J Bacteriol, 2006. **188**(8): p. 2761-73.

21. Juncker, A.S., et al., *Prediction of lipoprotein signal peptides in Gram-negative bacteria.* Protein Sci, 2003. **12**(8): p. 1652-62.

22. Hayashi, S. and H.C. Wu, *Lipoproteins in bacteria.* J Bioenerg Biomembr, 1990. **22**(3): p. 451-71.

23. Pereira, M.M., et al., *The caa_3 terminal oxidase of the thermohalophilic bacterium Rhodothermus marinus: a HiPIP:oxygen oxidoreductase lacking the key glutamate of the D-channel.* Biochim Biophys Acta, 1999. **1413**(1): p. 1-13.

24. Pereira, M.M., J.N. Carita, and M. Teixeira, *Membrane-bound electron transfer chain of the thermohalophilic bacterium Rhodothermus marinus: characterization of the iron-sulfur centers from the dehydrogenases and investigation of the high-potential iron-sulfur protein function by in vitro reconstitution of the respiratory chain.* Biochemistry, 1999. **38**(4): p. 1276-83.

Chapter 6

The alternative complex III: a different architecture using known building modules

The results presented in this chapter were published in:

Patrícia N. Refojo, Filipa L. Sousa, Miguel Teixeira, Manuela M. Pereira (2010) *The alternative complex III: A different architecture using known building modules* Biochim Biophys Acta *IN PRESS*

Acknowledgments:

Dr. Inês Cardoso Pereira is acknowledged for the critical reading. Filipa L. Sousa contributed to the bioinformatics analysis.

6.1 – Summary

Until recently cytochrome bc_1 complexes were the only known enzymes able to transfer electrons from reduced quinones to cytochrome *c*. However, a complex with the same activity and with a unique subunit composition was purified from *Rhodothermus marinus* membranes and biochemical, spectroscopic and genetically characterized. This complex was named alternative complex III (ACIII). Its presence is not exclusive of *R. marinus* being the genes coding for this novel complex widespread in the Bacteria domain. In this work, a comprehensive description of the current knowledge on ACIII is presented. The relation of ACIII with members of the complex iron-sulfur molybdoenzyme family is investigated by analyzing all the available completely sequenced genomes. It is concluded that ACIII is a new complex composed by a novel combination of modules already identified in other respiratory complexes.

6.2 – Introduction

Cytochrome bc_1 complexes are part of the respiratory chains and have quinol: cytochrome *c* oxidoreductase activity (see chapter 1). Besides this family, several other enzymes are able to oxidize quinols, namely quinol oxidases from the heme-copper oxygen reductases superfamily [1], and DMSO reductase, nitrite and nitrate reductases from the complex iron-sulfur molybdoenzyme (CISM) family [2]. However, and until recently, the cytochrome bc_1 complex family was the only one described to receive electrons from quinols and transfer them to cytochrome *c*. The alternative complex III (ACIII), purified for the first

time from *Rhodothermus (R.) marinus* membranes and structural and functionally characterized [3-5], was the first example of a complex performing the same function as the bc_1 complex but not belonging to its family.

6.3- The alternative complex III is a widespread quinol: electron acceptor oxidoreductase

The *R. marinus* respiratory chain has been extensively studied [1, 3-13] and the presence of three different oxygen reductases, a caa_3 [11, 12], a ba_3 [13] and a cbb_3 [10] was observed. These enzymes are unable to receive electrons from reduced quinones and therefore a complex which transfers electrons from quinols to periplasmatic electron carriers is required. A cytochrome bc_1 complex was never observed at the protein level and its absence has now been corroborated by the analysis of the recently sequenced *R. marinus* genome [14], in which genes coding for such a complex are not present. Instead, a seven subunits complex (chapter 3 and [15]) with quinol: HiPIP oxidoreductase activity was isolated from the membranes of *R.marinus* [3-5]. This complex is structurally different from the cytochrome bc_1 complexes, even though it performs the same function. By this reason the complex was named alternative complex III (ACIII) [5, 16].

The presence of ACIII is not exclusive of *R.marinus*. A homologous complex was also isolated from the membranes of the green non-sulfur proteobacterium *Choroflexus (C.) aurantiacus* [16-18] and was recently shown to have menaquinone: aurocyanin oxidoreductase activity [16]. As in the case of the *R. marinus* enzyme [5], it was not inhibited by the typical inhibitors of the cytochrome bc_1 complex, such as antimycin A.

The genes coding for ACIII were also identified in the δ-Proteobacterium *Myxococcus xanthus* and the same function for the complex was proposed [19]. Furthermore, Yanyushin and coworkers observed that the new complex was widespread and related to the complex iron-sulfur molybdoenzyme (CISM) family [18]. Due to the similarity with the members of that family, the name MFIcc (molybdopterin, FeS, integral membrane subunits, with two *c*-type heme subunits) has been proposed. This designation may be misleading since the complex does not contain molybdenum [5, 18], and thus the name alternative complex III was adopted [5, 16].

In this work, we performed an exhaustive search for ACIII coding genes in organisms with a completely sequenced genome, by September 2009. We confirmed that ACIII is a widespread enzyme in the Bacteria domain (figure 6.1). The genes coding for the complex may be present in genomes that do not contain coding genes for bc_1 complex subunits and in which genes coding for a quinol: cytochrome c oxidoreductase should exist, but there are also examples of genomes where ACIII genes coexist with those coding for the classical complexes III (figure 6.1).

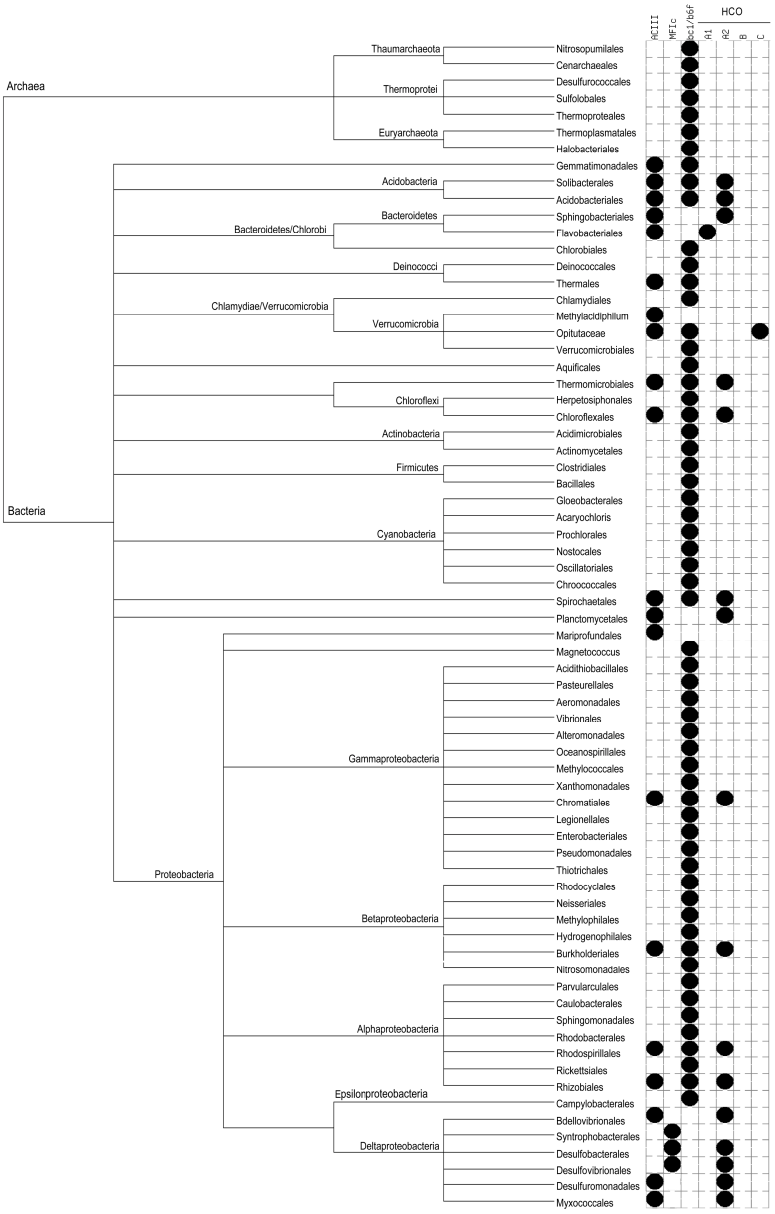

Figure 6.1

Phylogenetic profile of the presence of alternative complex III (ACIII), MFIc complex and cytochrome bc_1 complex family (bc_1/b_6f). The type of heme-copper oxygen reductases (HCO) coded by the gene cluster following the ACIII gene cluster is also indicated. The black dots represent the presence of the corresponding gene clusters. For the construction of this phylogenetic profile only aerobic organisms were considered.

The genes encoding ACIII form a cluster composed by six to eight genes (*ActABCDEFG*); in some cases *ActG* is absent, while in others *ActB* is splitted into two different genes $ActB_1$ and $ActB_2$, which correspond to the two domains of the gene *ActB* product (see below). A gene cluster with a similar organization but in which the *ActD*, *ActE* and *ActF* are absent was also earlier identified and its product named MFIc complex [18]; in this gene cluster the gene *ActB* is also splitted in two. The presence of MFIc complexes is only predicted for δ-Proteobacteria (figure 6.1), and their function has not been established yet[1].

The analysis of the gene clusters coding for ACIII in the sequenced genomes, in relation to their neighboring genes revealed that they may be isolated, ie, without any obvious functional relationship with preceding and following genes or gene clusters; or they may be followed by a gene cluster coding for a heme-copper oxygen reductase. This latter situation presents four possibilities; illustrative examples of each one are represented in figure 6.2. *R. marinus* is one example of the most observed organization in which the following gene cluster codes for subunits of the caa_3 oxygen reductase. *Salinibacter ruber* represents a similar example but in this case the SCOI gene (whose product is involved in copper incorporation [20]) is absent. The presence of a following gene cluster coding for subunits of cbb_3 oxygen reductases can also be observed in *Opitutu terreae*), as well

[1] After the publication of this work and during the writing of this thesis the work of Venceslau *et al* (2010, *in press*) showed that the MFIc of *Desulfovibrio vulgaris* Hildenborough have cytochrome c_3: quinone oxidoreductase activity and therefore, it was renamed Qrc (quinone reductase complex).

as genes coding only for subunits I and II of other oxygen reductases (*Flavobacterium psychrophilum*). *Thermus thermophilus* exemplifies a situation in which the gene cluster coding for ACIII is isolated. In

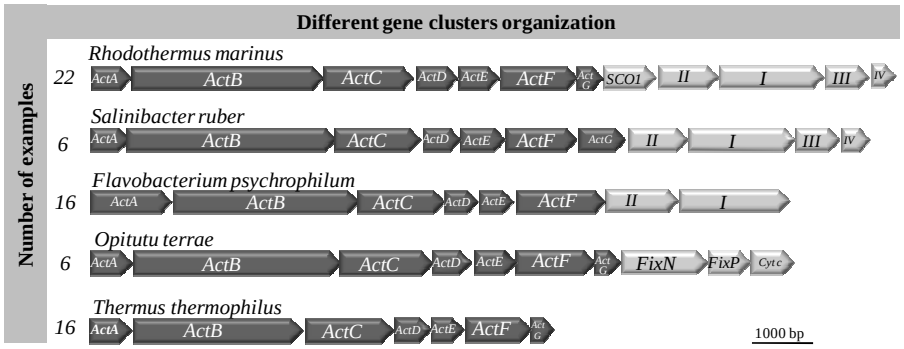

Figure 6.2

Organization of the gene clusters coding for alternative complex III subunits (dark grey) and those coding for the different heme-copper oxygen reductases (light grey). *SCOI* gene product is involved in the incorporation of copper. I, II, III and IV represent the different subunits of oxygen reductases while *FixN*, *FixP* and cyt *c* are the genes coding for subunits of cbb_3 oxygen reductase. An example of an organism for each organization is indicated. In eight of the sixteen cases exemplified by *Thermus thermophilus*, *ActG* is absent.

figure 6.1, the type of oxygen reductase (A1, A2, B and C-type, [21]) encoded by the gene cluster that follows the genes coding for ACIII is indicated.

6.4- Structural characterization of the alternative complex III

The first gene of the cluster (*ActA*) codes for a 27 kDa protein with five *c*-type heme binding motifs (CXXCH); the fifth motif is one amino acid residue apart from the C-terminus. Three methionine and seven other histidine residues are present in the sequence and are thus candidates for the sixth ligand of the hemes. However, the alignment

of the amino acid sequence of the subunits A of all ACIII showed that four histidine (H54, H57, H129, H132, *R. marinus* enzyme numbering) and one methionine (M160) residues are strictly conserved and are thus the most probable sixth heme ligands. A possible signal peptide in the N-terminal region is present, but its putative cleavage site is inside a predicted transmembrane helix, which suggests a membrane attachment mode for subunit A.

ActB codes for a 115 kDa protein with two distinct domains: domain B1, located in the N-terminus, is similar to molybdopterin containing proteins, while domain B2, located towards the C-terminus, has three binding motifs for $[4Fe\text{-}4S]^{2+/1+}$ clusters and one for a $[3Fe\text{-}4S]^{1+/0}$ cluster [5]. As mentioned before, the isolated complex does not have molybdenum [5, 18]. The A*ctC* gene encodes a 55 kDa protein predicted to have ten transmembrane helices, where two conserved possible quinone binding sites as those proposed by Fisher and Rich [22] can be detected [5]. However, this prediction should be considered with caution due to the variability of the quinone binding sites. *ActD* codes for a 25 kDa protein with two predicted transmembrane helices. The 22 kDa protein encoded by A*ctE* has a single *c*-type heme binding motif (CXXCH). Several methionine residues present in its sequence may act as the sixth ligand of the heme; however, the most probable is the methionine residue in the conserved motif MPA, as observed in many other cytochromes [23]. Subunit E is predicted to be a lipoprotein since in the N-terminal region a probable lipoprotein signal sequence (lipobox) [24] is present. A*ctF* codes for another integral membrane protein (48kDa), also predicted to have ten

transmembrane helices. Finally, the product of *ActG* is a small 15 kDa protein predicted to be membrane bound by a single transmembrane helix.

The subunits of ACIII can be divided in two groups according to the proposed function: i) membrane attachment and quinone interaction modules, subunits C, D, G and F, and ii) electron transfer modules composed by subunits A, B and E (figure 6.3).

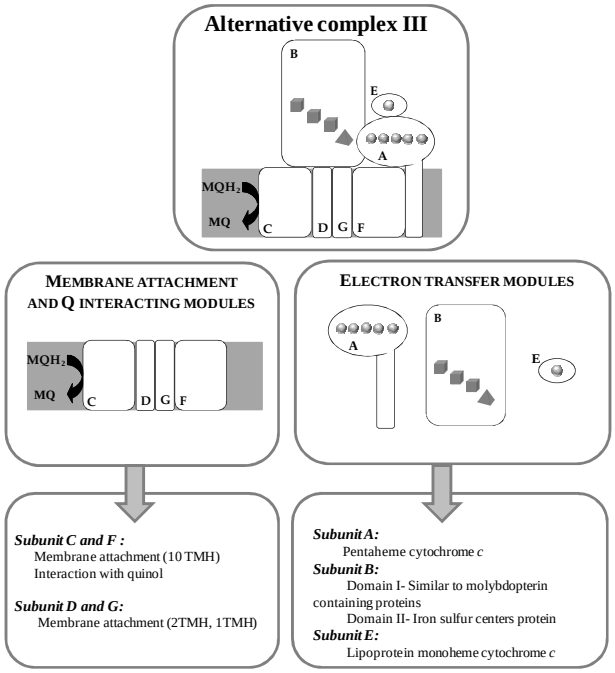

Figure 6.3

Schematic representation of the alternative complex III. The subunits (modules) of the complex may be separated according to their proposed function. The membrane attachment and quinone interacting modules correspond to subunits C, D, F and G, while subunits A, B and E are electron transfer modules. The spheres represent *c*-type hemes, cubes and pyramids represent $[4Fe\text{-}4S]^{2+/1+}$ and $[3Fe\text{-}4S]^{1+/0}$ clusters, respectively.

Despite the presence of the gene cluster coding for ACIII in many genomes, so far *R. marinus* and *C. aurantiacus* enzymes are the only complexes that were isolated. The presence of *c*-type hemes is the only

structural information available for ACIII from *C. aurantiacus* [17, 18]. On the other hand, the ACIII from *R. marinus* has been extensively investigated [4, 5, 15]. All the subunits coded by the respective genes were identified in the isolated complex and the redox centers were analyzed [4, 5, 15]. Besides the presence of low-spin *c*-type hemes detected by EPR and UV/visible absorption spectroscopies, a [3Fe-4S]$^{1+/0}$ center was also observed by EPR spectroscopy. Three redox transitions at -45, +80 and +235 mV were determined for the *c*-type hemes and a reduction potential of +140 mV was obtained for that iron-sulfur center [4].

6.5 - Comparison of ACIII with other complexes

In order to obtain the amino acid sequences of the subunits of the ACIII from other organisms a blast search using the sequences from *R. marinus* subunits as queries was performed. The amino acid sequences of each subunit of ACIII were aligned and the respective dendograms were constructed. It was observed that the sequences of each subunit showed high similarities among themselves (see below). The highest divergence was observed for subunit A, in which some members of the flavobacteriaceae family have an extra *c*-type heme binding motif (CXXCH) at the N-terminal region.

Despite the unique gene organization and subunit composition of the ACIII, the different subunits have homology with subunits of enzymatic complexes already characterized. In order to determine the most related proteins, the output number of sequences obtained by blast searches was enlarged. The sequences with the lower E-values

obtained, excluding those of ACIII, were the subunits of the MFIc complex, followed by the sequences of subunits of complexes belonging to the complex iron-sulfur molybdoenzyme family (CISM family) [2].

A relation between subunits B and C of ACIII and three subunits of those complexes had already been observed [5, 18]. The CISM family is characterized by the presence of three subunits [2]. A catalytic subunit which has a molybdo-bis(pyranopterin guanine dinucleotide) (Mo-*bis*PGD) cofactor and in some cases an iron-sulfur center (named FS0), a protein with four iron-sulfur clusters (FS1-FS4) named four cluster protein (FCP), and a membrane anchor protein (MAP). This family includes complexes such as DMSO reductase (DmsABC), polysulfide reductase (PsrABC), formate dehydrogenase (FdnGHI), and nitrate reductase (NarGHI). Also related to this family are the complexes nitrite reductase (NrfABCD), arsenite oxidase (AoxAB), TMAO reductase (TorCA), formate dehydrogenase (FdhAB), nitrate reductase

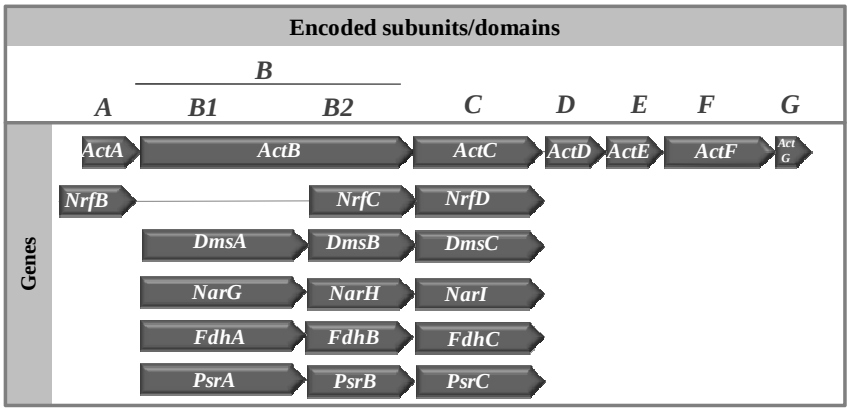

Figure 6.4

Comparison of the gene cluster of the alternative complex III with the gene clusters of the complexes iron-sulfur molybdoenzyme (CISM) family. The correspondence between genes and respective encoded domains or subunits is indicated

(NapAB), ethylbenzene dehydrogenase (EbdABC), and selenate reductase (YnfEFG). Schematic representations of some of these enzymes are presented further ahead in figure 6.5 and the respective gene cluster organization is shown in figure 6.4.

To obtain the amino acid sequence of each subunit of the complexes of this family, a new blast search against all genomes deposited at Kegg server (http://www.genome.jp/kegg/) [25-27] was performed using as initial query a sequence from a model organism, generally *Escherichia coli*. Also, when orthology information was available, all genes annotated as coding for proteins of the CISM family or for related proteins were retrieved. The gene organization of each complex within an organism was automatically inspected, and dubious gene organizations were manually inspected. All retrieved sequences were then mapped on NCBI Taxonomy using the BioSQL package available to download at ftp://ftp.ncbi.nih.gov/ from April 2009.

6.5.1- The iron-sulfur protein - Subunit B

Domain I of subunit B showed similarity with the catalytic subunit of the members of the CISM family, while domain II presented similarity with the four cluster protein. Since the two domains observed in subunit B are homologous to different proteins, the sequence was divided (800 amino acid residues from the N-terminal- Domain I and 240 amino acid residues from the C-terminal-Domain II) and the two parts analyzed separately. For the analysis of subunit B, the subunit NuoG (or Nqo3) of the complex I (NADH: quinone oxidoreductase)

was included, since this subunit is also related to the CISM family. Furthermore, this subunit is another example of a protein that has a molybdopterin-like domain, but lacks any molybdenum cofactor, and has an iron-sulfur domain [28]. As in the case of subunit B of ACIII, the NuoG amino acid sequence was also separated in two parts (NuoG_1, N-terminal and NuoG_2, C-terminal). Interestingly, subunit NuoG has the domains in a reverse order: the molybdopterin domain is located in the C-terminus while the iron-sulfur centers binding motifs are at the N-terminus, thus suggesting independent fusion processes. NuoG_1 and NuoG_2 were analyzed with B2 and B1 domains of subunit B, respectively.

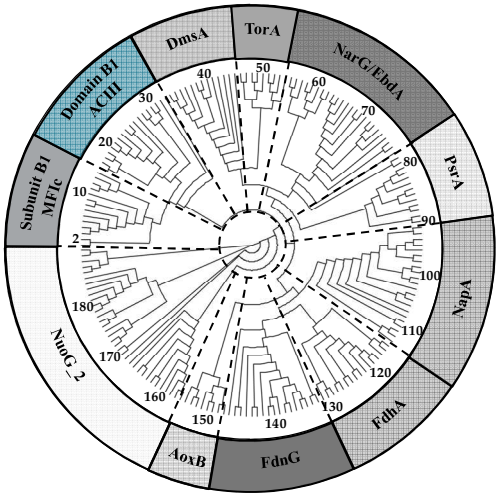

Figure 6.5

Dendogram obtained from the analysis of the domain B1 of the subunit B (15-32) of alternative complex III, subunit B of MFIc (1-14), NuoG (C-terminal sequence) (155-188), and related subunits of the members of the CISM family: DmsA and YnfEF (33-45), TorA (46-54), NarG and Ebda (55-80), PsrA (81-91), NapA (92-113), FdhA (114-129), FdnG (130-145), AoxB (146-154). Each branch is indicated by a number, which corresponds to subunits whose information can be consulted in the table 8.1 of chapter 8. For clarity only some of the numbers are indicated; however, the branches are numbered consecutively.

The amino acid sequence of domain I of subunit B was compared with sequences of catalytic subunits of complexes of the CISM family. From the dendogram obtained (figure 6.5) eleven different clades are observed, each clade being composed by subunits of the same enzymatic complex. The

similarity between the subunits of the members of the CISM family is in agreement with previous analyses [2, 29]. Domain I of subunit B of ACIII, subunit B1 of MFIc and NuoG are clearly related to those members. The subunits of ACIII and of MFIc are clustered together and seem to have a common origin. Besides the absence of molybdenum, the domain B1 of ACIII does not have the FS0 cluster, present in some catalytic subunits of the CISM family members.

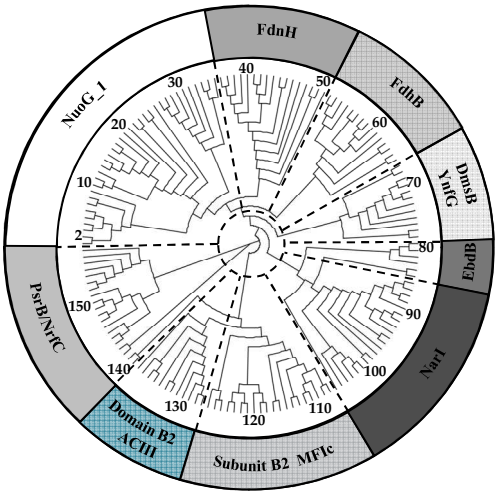

Figure 6.6

Dendogram obtained from the analysis of the domain B2 of subunit B of alternative complex III (127-138), subunit B2 of MFIc (107-126), NuoG (N-terminal sequence, 1-35), and subunits of the members of the CISM family:, FdnH (36-52), FdhB (53-67), DmsB and YnfG (68-79), EbdB (80-85), NarI (86-106) and PsrC and NrfD (139-158). Each branch is indicated by a number, which corresponds to subunits whose information can be consulted in the tables 8.2 of chapter 8. For clarity only some of the numbers are indicated; however, the branches are numbered consecutively.

The amino acid sequences of domain II of subunit B of ACIII were aligned with those of the FCP subunits of the CISM family and related members and the respective dendogram was constructed (figure 6.6). In contrast to what is observed for the domain I, NuoG is the less similar protein. The ACIII and MFIc subunits are closely related, being NrfC and PsrB their closest member of the CISM family and related complexes.

6.5.2- The membrane quinol interacting proteins- Subunits C and F

Subunits C and F are homologous to each other and to the subunits NrfD, DmsC and PsrC, although having a higher number of predicted transmembrane helices. NrfD, DmsC and PsrC have eight transmembrane segments. Subunits NarI and FdnI are also membrane anchor proteins of members of the CISM family. These subunits contain 5 and 6 transmembrane helices, respectively and 2 *b*-type hemes. NarI, FdnI and NrfD, DmsC and PsrC seem to constitute different subfamilies of membrane anchor proteins of the members of the CISM family [2]. Thus, only the amino acid sequences of subunits NrfD, DmsC and PsrC were included in the sequence alignment with subunits C and F of ACIII. As expected, this alignment revealed a low similarity between all the proteins. Nevertheless, it was possible to conclude that the subunits C and F are also related to the subunits NrfD, DmsC and PsrC of the CISM family. In contrast to what was observed for the domains of subunit B, the membrane subunits of the

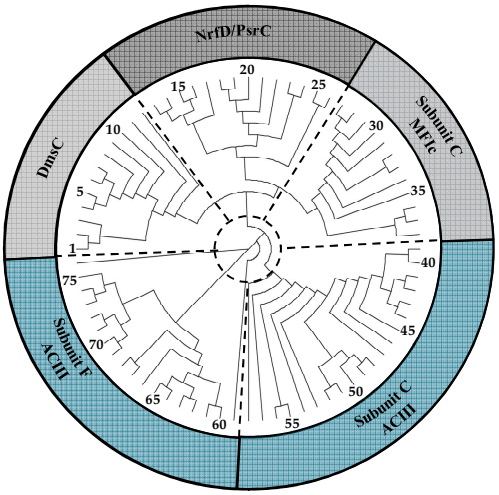

Figure 6.7

Dendogram obtained from the analysis of the subunit C (39-58) and F (59-76) of ACIII, subunit C of MFIc (27-38), NrfD and PsrC (13-26) and DmsC (1-12). Each branch is indicated by a number, which corresponds to subunits whose information can be consulted in the table 8.3 of chapter 8. For clarity only some of the numbers are indicated; however, the branches are numbered consecutively.

ACIII and MFIc complex seem to have had different origins (Figure 6.7).

6.5.3- *c*-type heme containing subunits- A and E

6.5.3.1- Subunit A

Although the typical CISM family members do not have *c*-type heme cytochrome subunits, variations of the subunit composition of complexes related to the family have been identified and subunits containing *c*-type hemes have been observed [2, 30, 31]. Therefore, the sequence of the pentahemic cytochrome *c* of the alternative complex was compared with that of other multi-hemes subunits of the CISM family and related complexes such as NrfA, NrfB, NrfH, NapC and TorC. All these proteins belong to the Napc/NrfH family of cytochromes [32] with the exception of NrfA and NrfB. That family plays an important role in the electron transfer between the quinone/quinol pool and

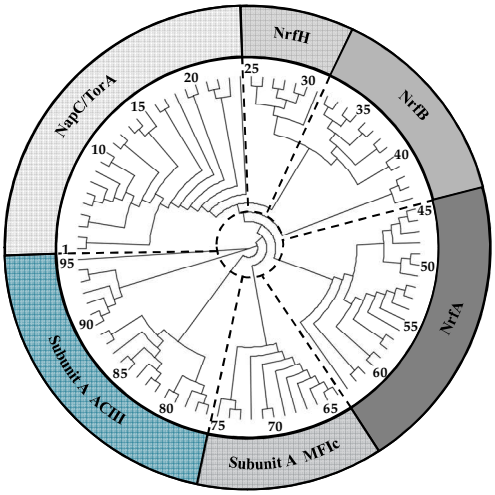

Figure 6.8

Dendogram obtained from the analysis of the subunit A of alternative complex III (76-95), subunit A of MFIc (64-75) and related subunits of the members of the CISM family: NapC and TorA (1-24), NrfH (25-31, 42-44), NrfB (32-41) and NrfA (45-63). Each branch is indicated by a number, which corresponds to subunits whose information can be consulted in the table 8.4 of chapter 8. For clarity only some of the numbers are indicated; however, the branches are numbered consecutively.

oxidoreductases located outside the cytoplasmatic membrane [32, 33]. NapC and NrfH are typical examples of the family, which have four *c*-type hemes and a membrane helix at the N-terminus; both are involved in the transfer of electrons to other cytochrome domains. NapA transfers electrons to the di-heme protein NapB from the NapAB complex [32], while NrfH transfers electrons to NrfA [34]. NrfA and NrfB are also pentaheme *c*-type cytochromes but the transmembrane anchor is absent [30, 35]. TorC belongs also to the NapC/NrfH family [36, 37]; it contains at the C-terminus an additional domain with a *c*-type heme described to be responsible for the interaction with the molybdenum-containing TMAO reductase [36]. Three different clades can be considered in the dendogram represented in figure 6.9: one formed by NapC, TorC, NrfH and NrfB, a second one formed only by NrfA and a last one formed by subunits A of the alternative complexes III and of the MFIc complexes. Within their clade, NapC and TorC are clustered together as expected, since both proteins belong to the same family; NrfH formed a sub-group inside of this clade, as previously observed [38]. NrfA is the only one of the analyzed proteins with an intrinsic catalytic activity; its catalytic heme is bound through an unconventional binding motif where a lysine replaces the typical histidine residue (CXXCK) [39, 40]. The specific properties of NrfA are in agreement with its place as an individual clade. The subunits A of the ACIII and of the MFIc complex were found to be part of the same clade, being closely related, and appear to have had the same evolutionary origin.

6.5.3.2- Subunit E

There are multiple examples of monoheme *c*-type cytochromes. The amino acid sequence of subunit E of ACIII was aligned with sequences from diverse *c*-type cytochromes, cytochrome c_1 from cytochrome bc_1 complex and also with monohemic domains of the oxygen reductases (*c*-domain of subunit II of caa_3 oxygen reductase and *c* domain of FixP subunit of cbb_3 oxygen reductase). A dendogram was constructed (data not shown); however, it was not possible to determine any closer protein since the bootstrap values obtained for the different branches of the dendogram were extremely low. Yet, it was possible to conclude that the subunit E of ACIII formed an independent clade. These observations suggest that the monoheme *c*-type subunit of ACIII is another example of a subfamily of *c*-type cytochromes.

6.5.4- The other membrane proteins- Subunits D and G

We were unable to identify any protein homologous of these two proteins; their presence seems to be restricted to the ACIII.

6.6 - The alternative complex III is a different complex composed by "old" modules

The ACIII has a unique subunit composition. However, the different constituting subunits show similarities with subunits of complexes already known, namely those of the CISM family. The subunits of the different complexes can be divided in several modules according to their function: 1-electron transfer, 2- catalytic and 3- membrane attachment and quinone interacting modules (Figure 6.9). These

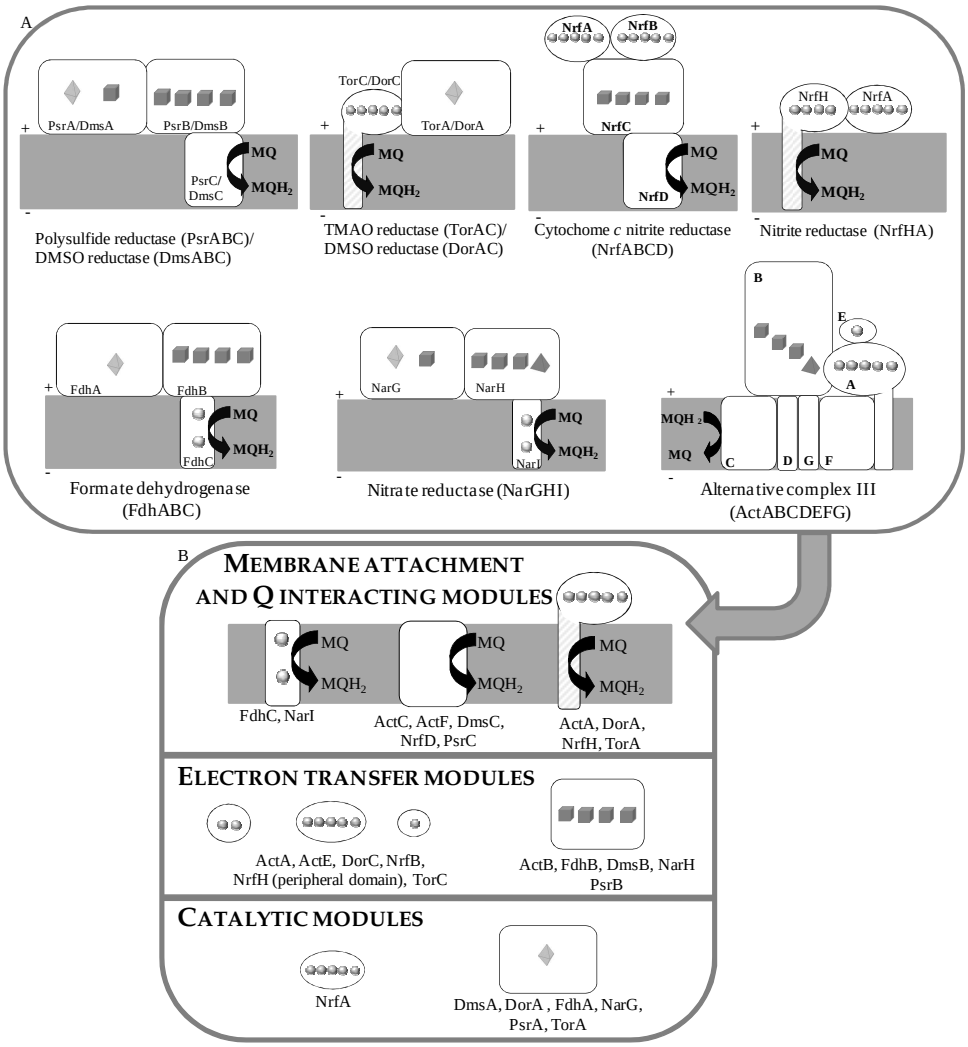

Figure 6.9

Schematic representation of complexes of the complex iron sulfur molybdenum (CISM) family and related complexes, including ACIII (A), and separation of the complexes in the three different types of modules: membrane attachment and quinone interaction, electron transfer and catalytic modules (B). The spheres represent *c*-type heme, and bipyramids corresponds to the molybdopterin cofactor. Cubes and pyramids represent $[4Fe\text{-}4S]^{2+/1+}$ and $[3Fe\text{-}4S]^{1+/0}$ clusters, respectively.

modules can be observed in complexes combined in multiple ways. The type of function performed could have influenced the different

combinations of those subunits. This idea of modularity in the construction of respiratory complexes has been proposed before, and respiratory complex I and hydrogenases are examples of such type of construction [41-43]. Furthermore, the existence of a redox protein construction kit has been even proposed, with enzymes being constructed from the limited set of modules present in that kit [44].

In conclusion, ACIII is a different complex composed by already known modules, and another example of how nature uses the same structural modules in different contexts according to the metabolic needs.

6.7- References

1. Pereira, M.M., et al., *Looking for the minimum common denominator in haem-copper oxygen reductases: towards a unified catalytic mechanism.* Biochim Biophys Acta, 2008. **1777**(7-8): p. 929-34.
2. Rothery, R.A., G.J. Workun, and J.H. Weiner, *The prokaryotic complex iron-sulfur molybdoenzyme family.* Biochim Biophys Acta, 2008. **1778**(9): p. 1897-929.
3. Pereira, M.M., J.N. Carita, and M. Teixeira, *Membrane-bound electron transfer chain of the thermohalophilic bacterium Rhodothermus marinus: characterization of the iron-sulfur centers from the dehydrogenases and investigation of the high-potential iron-sulfur protein function by in vitro reconstitution of the respiratory chain.* Biochemistry, 1999. **38**(4): p. 1276-83.

4. Pereira, M.M., J.N. Carita, and M. Teixeira, *Membrane-bound electron transfer chain of the thermohalophilic bacterium Rhodothermus marinus: a novel multihemic cytochrome bc, a new complex III.* Biochemistry, 1999. **38**(4): p. 1268-75.

5. Pereira, M.M., et al., *The alternative complex III from Rhodothermus marinus - a prototype of a new family of quinol:electron acceptor oxidoreductases.* FEBS Lett, 2007. **581**(25): p. 4831-5.

6. Fernandes, A.S., et al., *Quinone reduction by Rhodothermus marinus succinate:menaquinone oxidoreductase is not stimulated by the membrane potential.* Biochem Biophys Res Commun, 2005. **330**(2): p. 565-70.

7. Fernandes, A.S., M.M. Pereira, and M. Teixeira, *The succinate dehydrogenase from the thermohalophilic bacterium Rhodothermus marinus: redox-Bohr effect on heme b_L.* J Bioenerg Biomembr, 2001. **33**(4): p. 343-52.

8. Fernandes, A.S., M.M. Pereira, and M. Teixeira, *Purification and characterization of the complex I from the respiratory chain of Rhodothermus marinus.* J Bioenerg Biomembr, 2002. **34**(6): p. 413-21.

9. Fernandes, A.S., et al., *Electron paramagnetic resonance studies of the iron-sulfur centers from complex I of Rhodothermus marinus.* Biochemistry, 2006. **45**(3): p. 1002-8.

10. Pereira, M.M., et al., *Heme centers of Rhodothermus marinus respiratory chain. Characterization of its cbb_3 oxidase.* J Bioenerg Biomembr, 2000. **32**(2): p. 143-52.

11. Pereira, M.M., et al., *The caa_3 terminal oxidase of the thermohalophilic bacterium Rhodothermus marinus: a HiPIP:oxygen oxidoreductase lacking the key glutamate of the D-channel.* Biochim Biophys Acta, 1999. **1413**(1): p. 1-13.

12. Pereira, M.M., et al., *A tyrosine residue deprotonates during oxygen reduction by the caa_3 reductase from Rhodothermus marinus.* FEBS Lett, 2006. **580**(5): p. 1350-4.

13. Verissimo, A.F., et al., *A ba_3 oxygen reductase from the thermohalophilic bacterium Rhodothermus marinus.* FEMS Microbiol Lett, 2007. **269**(1): p. 41-7.
14. Lucas, S., et al., *The draft genome of Rhodothermus marinus DSM 4252.* 2009.
15. Refojo, P.N., M. Teixeira, and M.M. Pereira, *The alternative complex III from Rhodothermus marinus and its structural and functional association with caa_3 oxygen reductase.* BBA-Bioenergetics, 2010. ***In press***.
16. Gao, X., Y. Xin, and R.E. Blankenship, *Enzymatic activity of the alternative complex III as a menaquinol:auracyanin oxidoreductase in the electron transfer chain of Chloroflexus aurantiacus.* FEBS Lett, 2009. **583**(19): p. 3275-9.
17. Yanyushin, M.F., *Fractionation of cytochromes of phototrophically grown Chloroflexus aurantiacus. Is there a cytochrome bc complex among them?* FEBS Lett, 2002. **512**(1-3): p. 125-8.
18. Yanyushin, M.F., et al., *New class of bacterial membrane oxidoreductases.* Biochemistry, 2005. **44**(30): p. 10037-45.
19. Goldman, B., S. Bhat, and L.J. Shimkets, *Genome evolution and the emergence of fruiting body development in Myxococcus xanthus.* PLoS One, 2007. **2**(12): p. e1329.
20. Santana, M., et al., *Gene cluster of Rhodothermus marinus high-potential iron-sulfur Protein: oxygen oxidoreductase, a caa(3)-type oxidase belonging to the superfamily of heme-copper oxidases.* J Bacteriol, 2001. **183**(2): p. 687-99.
21. Pereira, M.M., M. Santana, and M. Teixeira, *A novel scenario for the evolution of haem-copper oxygen reductases.* Biochim Biophys Acta, 2001. **1505**(2-3): p. 185-208.
22. Rich, P.R., *The quinone chemistry of bc complexes.* Biochim Biophys Acta, 2004. **1658**(1-2): p. 165-71.

23. Stelter, M., et al., *A novel type of monoheme cytochrome c: biochemical and structural characterization at 1.23 A resolution of rhodothermus marinus cytochrome c.* Biochemistry, 2008. **47**(46): p. 11953-63.

24. Babu, M.M., et al., *A database of bacterial lipoproteins (DOLOP) with functional assignments to predicted lipoproteins.* J Bacteriol, 2006. **188**(8): p. 2761-73.

25. Kanehisa, M. and S. Goto, *KEGG: kyoto encyclopedia of genes and genomes.* Nucleic Acids Res, 2000. **28**(1): p. 27-30.

26. Kanehisa, M., et al., *From genomics to chemical genomics: new developments in KEGG.* Nucleic Acids Res, 2006. **34**(Database issue): p. D354-7.

27. Kanehisa, M., et al., *KEGG for linking genomes to life and the environment.* Nucleic Acids Res, 2008. **36**(Database issue): p. D480-4.

28. Sazanov, L.A. and P. Hinchliffe, *Structure of the hydrophilic domain of respiratory complex I from Thermus thermophilus.* Science, 2006. **311**(5766): p. 1430-6.

29. McDevitt, C.A., et al., *Molecular analysis of dimethyl sulphide dehydrogenase from Rhodovulum sulfidophilum: its place in the dimethyl sulphoxide reductase family of microbial molybdopterin-containing enzymes.* Mol Microbiol, 2002. **44**(6): p. 1575-87.

30. Clarke, T.A., et al., *The role of multihaem cytochromes in the respiration of nitrite in Escherichia coli and Fe(III) in Shewanella oneidensis.* Biochem Soc Trans, 2008. **36**(Pt 5): p. 1005-10.

31. Simon, J. and M. Kern, *Quinone-reactive proteins devoid of haem b form widespread membrane-bound electron transport modules in bacterial respiration.* Biochem Soc Trans, 2008. **36**(Pt 5): p. 1011-6.

32. Gross, R., R. Eichler, and J. Simon, *Site-directed modifications indicate differences in axial haem c iron ligation between the related NrfH and NapC families of multihaem c-type cytochromes.* Biochem J, 2005. **390**(Pt 3): p. 689-93.

33. Rodrigues, M.L., et al., *X-ray structure of the membrane-bound cytochrome c quinol dehydrogenase NrfH reveals novel haem coordination.* EMBO J, 2006. **25**(24): p. 5951-60.
34. Simon, J., et al., *A NapC/NirT-type cytochrome c (NrfH) is the mediator between the quinone pool and the cytochrome c nitrite reductase of Wolinella succinogenes.* Mol Microbiol, 2000. **35**(3): p. 686-96.
35. Einsle, O., et al., *Cytochrome c nitrite reductase from Wolinella succinogenes. Structure at 1.6 A resolution, inhibitor binding, and heme-packing motifs.* J Biol Chem, 2000. **275**(50): p. 39608-16.
36. Gon, S., et al., *Electron transfer and binding of the c-type cytochrome TorC to the trimethylamine N-oxide reductase in Escherichia coli.* J Biol Chem, 2001. **276**(15): p. 11545-51.
37. Ansaldi, M., et al., *TorC apocytochrome negatively autoregulates the trimethylamine N-oxide (TMAO) reductase operon in Escherichia coli.* Mol Microbiol, 1999. **33**(2): p. 284-95.
38. Simon, J., *Enzymology and bioenergetics of respiratory nitrite ammonification.* FEMS Microbiol Rev, 2002. **26**(3): p. 285-309.
39. Darwin, A., et al., *Regulation and sequence of the structural gene for cytochrome c_{552} from Escherichia coli: not a hexahaem but a 50 kDa tetrahaem nitrite reductase.* Mol Microbiol, 1993. **9**(6): p. 1255-65.
40. Eaves, D.J., et al., *Involvement of products of the nrfEFG genes in the covalent attachment of haem c to a novel cysteine-lysine motif in the cytochrome c_{552} nitrite reductase from Escherichia coli.* Mol Microbiol, 1998. **28**(1): p. 205-16.
41. Mathiesen, C. and C. Hagerhall, *The 'antiporter module' of respiratory chain complex I includes the MrpC/NuoK subunit -- a revision of the modular evolution scheme.* FEBS Lett, 2003. **549**(1-3): p. 7-13.
42. Friedrich, T., *Complex I: a chimaera of a redox and conformation-driven proton pump?* J Bioenerg Biomembr, 2001. **33**(3): p. 169-77.

43. Vignais, P.M., B. Billoud, and J. Meyer, *Classification and phylogeny of hydrogenases.* FEMS Microbiol Rev, 2001. **25**(4): p. 455-501.

44. Baymann, F., et al., *The redox protein construction kit: pre-last universal common ancestor evolution of energy-conserving enzymes.* Philos Trans R Soc Lond B Biol Sci, 2003. **358**(1429): p. 267-74.

Chapter 7

Concluding Remarks

Despite the large diversity and flexibility observed in the enzymatic complexes composition of electron transfer respiratory chains, the cytochrome bc_1 complex family was thought to be the only one able to perform the quinol: electron acceptor oxidoreductase activity. However, another family of complexes, named alternative complexes III (ACIII), able to catalyze the same reaction was identified. The enzyme from *Rhodothermus marinus* was the first member to be purified and characterized. *Chloroflexus aurantiacus* was also described to have this complex; however, the characterization of the heme proteins is the only structural information available for this enzyme.

In this work, it was observed that ACIII is widespread in the Bacteria domain being mostly present in genomes where the genes coding for the subunits of a typical complex III are absent and for which the presence of a quinol: electron carrier oxidoreductase complex is predicted. *R. marinus* ACIII is composed by three peripheral and four transmembrane proteins (figure 7.1). One of the latter is predicted to have quinone binding sites, while the largest peripheral subunit has one binding motif for a $[3Fe\text{-}4S]^{1+/0}$ cluster and three binding motifs for $[4Fe\text{-}4S]^{2+/1+}$ clusters. Two other subunits, one with five and another with one *c*-type heme binding motifs are also part of the complex.

The interaction of ACIII with its electron donor, menadiol (menaquinol-7 analogue), was demonstrated and the presence of, at least, one quinone binding site was established.

In several genomes, the gene cluster coding for ACIII is followed by genes coding for subunits of oxygen reductases. In *R. marinus*, the following genes were identified as those coding for the caa_3 oxygen

reductase. Furthermore, it was showed that ACIII and the caa_3 oxygen reductase are structural and functionally associated (figure 7.1) and that the monoheme cytochrome *c* is the electron donor of the oxygen reductase within ACIII.

Although functionally related to the bc_1 complexes, alternative complexes III have a different structural composition. However, the architecture of the ACIII family members is not completely new; these complexes are composed by structural modules already identified in members of the CISM family and related enzymes, also described as quinone/quinol interacting enzymes.

The electron transfer and energy conservation mechanisms of ACIII are not known. However, the absence of redox cofactors in the membrane bound subunits makes the presence of a Q-cycle mechanism unlikely. The possible existence of proton channels like in the heme-copper oxygen reductases or the formation of redox loops are possibilities to be considered.

According to what is known regarding the electron transfer mechanism operating in the structural modules which compose ACIII and, also that the monoheme cytochrome *c* subunit is, in *Rhodothermus marinus* enzyme, the last electron acceptor within the complex, the following order of electron transfer event is proposed: the quinol is oxidized in the quinone binding site at subunit C, the two electrons are then transferred to: 1) the iron sulfur centers at subunit B, 2) pentaheme cytochrome *c* (subunit A), 3) monoheme cytochrome *c* (subunit E). Since subunit F showed similarity to subunit C, the existence of a second quinone binding site cannot be excluded. The

apparent absence of redox cofactors in subunit D and G may indicate a structural and stabilizing role for those subunits.

For *Rhodothermus marinus* in particular, a further step in the identification and characterization of the complexes involved in its respiratory chain was achieved. This bacterium represents another example of the prokaryotic electron transfer chain diversity and flexibility. The three different oxygen reductases, the unusual presence of the HiPIP as an electron carrier protein, the complex I which is able to translocate sodium in opposite direction of protons and the existence of the alternative complex III confers the respiratory chain distinctive features. In figure 7.1 is presented a schematic representation of the *R. marinus* electron transfer respiratory chain.

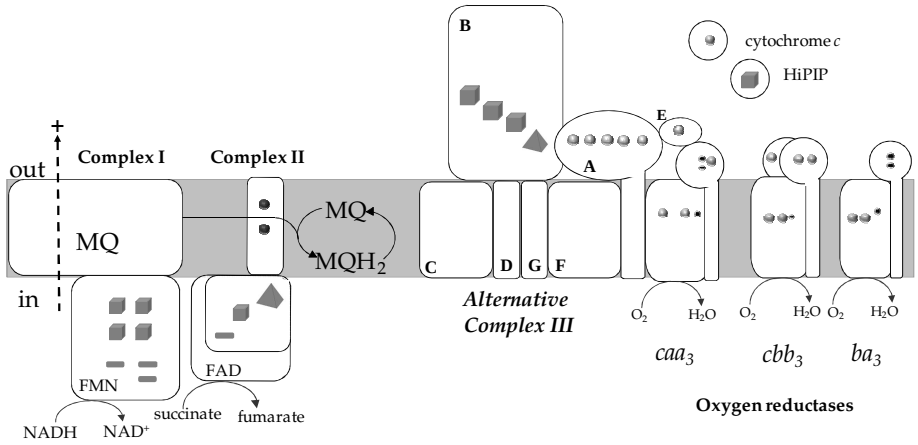

Figure 7.1

Schematic representation of the electron transfer respiratory chain of *Rhodothermus marinus*. The gray and black spheres represent *c*- and *b*-type hemes, respectively, while the smallest spheres represent copper,. Cubes, pyramids and rectangles represents $[4Fe\text{-}4S]^{2+/1+}$, $[3Fe\text{-}4S]^{1+/0}$ and $[2Fe\text{-}2S]^{2+/1+}$ centers, respectively.

In general, a family of enzymes with quinol: electron acceptor oxidoreductase activity, which is structurally unrelated to the cytochrome bc_1 complex, was identified for the first time and members of this family were observed to be widespread in the Bacteria domain. The identification of these enzymes was an important step for the recognition of the diversity and flexibility observed in the prokaryotic electron transfer respiratory chains.

Chapter 8

Supplementary information

Supplemental table 8.1: Proteins whose amino acid sequence was used to construct the dendogram from figure 6.6.

Number	keeg_ID	Type of protein	Accession	species	order
1	Gmet_1810	Subunit B1_MFIc	YP_384764.1	*Geobacter metallireducens*	Desulfuromonadales
2	ZP_01451016.1	Subunit B1_MFIc	ZP_01451016.1	*Maripro fundus ferrooxydans*	Maripro fundales
3	Dvul_2269	Subunit B1_MFIc	YP_967712.1	*Desulfovibrio vulgaris*	Desulfovibrionales
4	DVU0694	Subunit B1_MFIc	YP_009916.1	*Desulfovibrio vulgaris*	Desulfovibrionales
5	DvMF_MFIc	Subunit B1_MFIc	YP_002437096.1	*Desulfovibrio vulgaris*	Desulfovibrionales
6	Dde_2933	Subunit B1_MFIc	YP_389422.1	*Desulfovibrio desulfuricans*	Desulfovibrionales
7	DMR_18020	Subunit B1_MFIc	YP_002953179.1	*Desulfovibrio magneticus*	Desulfovibrionales
8	Dbac_3391	Subunit B1_MFIc	YP_003159879.1	*Desulfomicrobium baculatum*	Desulfovibrionales
9	Desal_1043	Subunit B1_MFIc	YP_002990647.1	*Desulfovibrio salexigens*	Desulfovibrionales
10	Dret_0271	Subunit B1_MFIc	YP_003197151.1	*Desulfohalobium retbaense*	Desulfovibrionales
11	HRM2_18940	Subunit B1_MFIc	YP_002603159.1	*Desulfobacterium autotrophicum*	Desulfobacterales
12	Dole_2547	Subunit B1_MFIc	YP_001530428.1	*Desulfococcus oleovorans*	Desulfobacterales
13	Dalk_1268	Subunit B1_MFIc	YP_002430439.1	*Desulfatibacillum alkenivorans*	Desulfobacterales
14	Sfum_0610	Subunit B1_MFIc	YP_844744.1	*Syntrophobacter fumaroxidans*	Syntrophobacterales
15	*ActB*	Domain B1_ACIII	ABV55245	*Rhodothermus marinus*	Sphingobacteriales
16	SRU_2106	Domain B1_ACIII	YP_446212.1	*Salinibacter ruber*	Sphingobacteriales
17	Oter_3934	Domain B1_ACIII	YP_001820808.1	*Opitutus terrae*	
18	A2cp1_0848	Domain B1_ACIII	YP_002491266.1	*Anaeromyxobacter dehalogenans*	Myxococcales
19	Acid345_3003	Domain B1_ACIII	YP_592078.1	*Acidobacteria bacterium Ellin345*	Acidobacteriales
20	Acid_0490	Domain B1_ACIII	YP_821785.1	*Solibacter usitatus*	Solibacterales
21	Noc_1238	Domain B1_ACIII	YP_343269.1	*Nitrosococcus oceani*	Chromatiales
22	Cagg_3386	Domain B1_ACIII	YP_002464666.1	*Chloroflexus aggregans*	Chloroflexales
23	Reut_B4428	Domain B1_ACIII	YP_298623.1	*Cupriavidus pinatubonensis*	Burkholderiales
24	M446_5824	Domain B1_ACIII	YP_001772545.1	*Methylobacterium sp. 4-46*	Rhizobiales

25	GDI2620	Domain B1_ACIII	YP_001602862.1	*Gluconacetobacter diazotrophicus*	Rhodospirillales
26	Minf_1961	Domain B1_ACIII	YP_001940612.1	*Methylacidiphilum infernorum*	
27	Bd1608	Domain B1_ACIII	NP_968492.1	*Bdellovibrio bacteriovorus*	Bdellovibrionales
28	LA3267	Domain B1_ACIII	NP_713447.1	*Leptospira interrogans*	Spirochaetales
29	FP0373	Domain B1_ACIII	YP_001295304.1	*Flavobacterium psychrophilum*	Flavobacteriales
30	CHU_2212	Domain B1_ACIII	YP_678817.1	*Cytophaga hutchinsonii*	Sphingobacteriales
31	GAU_2036	Domain B1_ACIII	YP_002761548.1	*Gemmatimonas aurantiaca*	Gemmatimonadales
32	TTC1404	Domain B1_ACIII	YP_005373.1	*Thermus thermophilus*	Thermales
33	APJL_1705	DmsA	YP_001652701.1	*Actinobacillus pleuropneumoniae*	Pasteurellales
34	Asuc_1523	ynfEF	YP_001344816.1	*Actinobacillus succinogenes*	Pasteurellales
35	APECO1_1195	DmsA	YP_851991.1	*Escherichia coli*	Enterobacteriales
36	LHK_02496	DmsA	YP_002796487.1	*Laribacter hongkongensis*	Neisseriales
37	VFMJ11_A0106	DmsA	YP_002157663.1	*Vibrio fischeri*	Vibrionales
38	APECO1_670	ynfEF	YP_852686.1	*Escherichia coli*	Enterobacteriales
39	Asuc_1524	ynfEF	YP_001344817.1	*Actinobacillus succinogenes*	Pasteurellales
40	APECO1_671	ynfEF	YP_852687.1	*Escherichia coli*	Enterobacteriales
41	DvMF_1612	DmsA	YP_002436028.1	*Desulfovibrio vulgaris*	Desulfovibrionales
42	Moth_1386	DmsA	YP_430242.1	*Moorella thermoacetica*	Thermoanaerobacterales
43	PPA0517	DmsA	YP_055228.1	*Propionibacterium acnes*	Actinomycetales
44	CJJ81176_1570	DmsA	YP_001001225.1	*Campylobacter jejuni*	Campylobacterales
45	Shal_0404	DmsA	YP_001672638.1	*Shewanella halifaxensis*	Alteromonadales
46	AHA_4049	torA	YP_858474.1	*Aeromonas hydrophila*	Aeromonadales
47	APJL_0686	torA	YP_001651699.1	*Actinobacillus pleuropneumoniae*	Pasteurellales
48	RSKD131_3219	torA	YP_002520152.1	*Rhodobacter sphaeroides*	Rhodobacterales
49	Rru_A1287	torA	YP_426375.1	*Rhodospirillum rubrum*	Rhodospirillales
50	RPC_0658	torA	YP_530549.1	*Rhodopseudomonas palustris*	Rhizobiales

51	CPS_1833	torA	YP_268563.1	*Colwellia psychrerythraea*	Alteromonadales
52	PBPRA1467	torA	YP_129680.1	*Photobacterium profundum*	Vibrionales
53	PsycPRwf_0214	torA	YP_001279123.1	*Psychrobacter sp. PRwf-1*	Pseudomonadales
54	APECO1_90	torA	YP_852108.1	*Escherichia coli*	Enterobacteriales
55	Pars_0499	FdhA	YP_001152746.1	*Pyrobaculum arsenaticum*	Thermoproteales
56	APE_1288.1	ebdA	NP_147849.2	*Aeropyrum pernix*	Desulfurococcales
57	M1425_0828	NarG	YP_002828931.1	*Sulfolobus islandicus*	Sulfolobales
58	ABC0715	NarG	YP_174215.1	*Bacillus clausii*	Bacillales
59	DSY0334	NarG	YP_516567.1	*Desulfitobacterium hafniense*	Clostridiales
60	LAF_1062	NarG	YP_001843878.1	*Lactobacillus fermentum*	Lactobacillales
61	CE1296	NarG	NP_737906.1	*Corynebacterium efficiens*	Actinomycetales
62	Rxyl_1205	NarG	YP_643983.1	*Rubrobacter xylanophilus*	Rubrobacterales
63	Maqu_3086	NarG	YP_960347.1	*Marinobacter hydrocarbonoclasticus*	Alteromonadales
64	ABO_0546	NarG	YP_692266.1	*Alcanivorax borkumensis*	Oceanospirillales
65	APECO1_341	NarG	YP_852355.1	*Escherichia coli*	Enterobacteriales
66	PA14_13780	NarG	YP_789246.1	*Pseudomonas aeruginosa*	Pseudomonadales
67	Smal_2236	NarG	YP_002028623.1	*Stenotrophomonas maltophila*	Xanthomonadales
68	Aave_0661	NarG	YP_969038.1	*Acidovorax avenae*	Burkholderiales
69	Mlg_1003	NarG	YP_741846.1	*Alkalilimnicola ehrlichei*	Chromatiales
70	CV_2543	NarG	NP_902213.1	*Chromobacterium violaceum*	Neisseriales
71	Caul_3864	NarG	YP_001685488.1	*Caulobacter sp. K31*	Caulobacterales
72	HNE_1560	NarG	YP_760271.1	*Hyphomonas neptunium*	Rhodobacterales
73	AZC_1425	NarG	YP_001524341.1	*Azorhizobium caulinodans*	Rhizobiales
74	Acry_1581	NarG	YP_001234706.1	*Acidiphilium cryptum*	Rhodospirillales
75	COSY_0649	NarG	YP_001219486.1	*Calyptogena okutanii thioautotrophic*	
76	Tbd_1403	NarG	YP_315161.1	*Thiobacillus denitrificans*	Hydrogenophilales

77	ebA6286	NarG	YP_160621.1	*Aromatoleum aromaticum*	Rhodocyclales
78	rrnAC1199	ebdA	YP_135852.1	*Haloarcula marismortui*	Halobacteriales
79	Dole_0194	ebdA	YP_001528081.1	*Desulfococcus oleovorans*	Desulfobacterales
80	c1A65	ebdA	YP_158333.1	*Aromatoleum aromaticum*	Rhodocyclales
81	Oter_1466	psrA	YP_001818350.1	*Opitutus terrae*	
82	Anae109_4110	FdhA	YP_001381272.1	*Anaeromyxobacter sp. Fw109-5*	Myxococcales
83	THEYE_A1157	psrA	YP_002248981.1	*Thermodesulfovibrio yellowstonii*	Nitrospirales
84	Clim_2400	psrA	YP_001944400.1	*Chlorobium limicola*	Chlorobiales
85	SO_4062	psrA	NP_719592.1	*Shewanella oneidensis*	Alteromonadales
86	CCC13826_0389	psrA	YP_001467234.1	*Campylobacter concisus*	Campylobacterales
87	CHY_2574	psrA	YP_361367.1	*Carboxydothermus hydrogenoformans*	Thermoanaerobacterales
88	CHY_0476	NapA	YP_359334.1	*Carboxydothermus hydrogenoformans*	Thermoanaerobacterales
89	AF2384	psrA	NP_071207.1	*Archaeoglobus fulgidus*	Archaeoglobales
90	Pcal_1500	psrA	YP_001056385.1	*Pyrobaculum calidifontis*	Thermoproteales
91	Tneu_0353	NarG	YP_001793749.1	*Thermoproteus neutrophilus*	Thermoproteales
92	Mmc1_1591	NapA	YP_865506.1	*Magnetococcus sp. MC-1*	
93	Dshi_3165	NapA	YP_001534499.1	*Dinoroseobacter shibae*	Rhodobacterales
94	AHA_1586	NapA	YP_856122.1	*Aeromonas hydrophila*	Aeromonadales
95	APECO1_4353	NapA	YP_853313.1	*Escherichia coli*	Enterobacteriales
96	Daro_3515	NapA	YP_286714.1	*Dechloromonas aromatica*	Rhodocyclales
97	CPS_1057	NapA	YP_267801.1	*Colwellia psychrerythraea*	Alteromonadales
98	PBPRA0853	NapA	YP_129068.1	*Photobacterium profundum*	Vibrionales
99	BB2800	NapA	NP_889336.1	*Bordetella bronchiseptica*	Burkholderiales
100	HCH_03364	NapA	YP_434542.1	*Hahella chejuensis*	Oceanospirillales
101	Atu4408	NapA	NP_356246.1	*Agrobacterium tumefaciens*	Rhizobiales
102	RC1_0457	NapA	YP_002296709.1	*Rhodospirillum centenum*	Rhodospirillales

103	APJL_1461	NapA	YP_001652457.1	*Actinobacillus pleuropneumoniae*	Pasteurellales
104	PERMA_0298	NapA	YP_002730091.1	*Persephonella marina*	Aquificales
105	NAMH_0556	NapA	YP_002606972.1	*Nautilia profundicola*	Nautiliales
106	Abu_0358	NapA	YP_001489302.1	*Arcobacter butzleri*	Campylobacterales
107	Glov_1056	NapA	YP_001951299.1	*Geobacter lovleyi*	Desulfuromonadales
108	sce4702	NapA	YP_001615345.1	*Sorangium cellulosum*	Myxococcales
109	DSY4078	NapA	YP_520311.1	*Desulfitobacterium hafniense*	Clostridiales
110	Ddes_0616	NapA	YP_002479203.1	*Desulfovibrio desulfuricans*	Desulfovibrionales
111	CV_2229	NapA	NP_901899.1	*Chromobacterium violaceum*	Neisseriales
112	XCV2095	NapA	YP_363826.1	*Xanthomonas euvesicatoria*	Xanthomonadales
113	PSPPH_2070	NapA	YP_274289.1	*Pseudomonas savastanoi*	Pseudomonadales
114	Mthe_1339	FdhA	YP_843754.1	*Methanosaeta thermophila*	Methanosarcinales
115	TGAM_0065	FdhA	YP_002958431.1	*Thermococcus gammatolerans*	Thermococcales
116	Mhun_1833	FdhA	YP_503272.1	*Methanospirillum hungatei*	Methanomicrobiales
117	AHA_3063	FdhA	YP_857565.1	*Aeromonas hydrophila*	Aeromonadales
118	PBPRA1862	FdhA	YP_130068.1	*Photobacterium profundum*	Vibrionales
119	Csal_1915	FdhA	YP_573966.1	*Chromohalobacter salexigens*	Oceanospirillales
120	SO_4509	FdhA	NP_720029.1	*Shewanella oneidensis*	Alteromonadales
121	Mlg_1286	FdhA	YP_742125.1	*Alkalilimnicola ehrlichei*	Chromatiales
122	amb2671	FdhA	YP_422034.1	*Magnetospirillum magneticum*	Rhodospirillales
123	Ajs_3464	FdhA	YP_987654.1	*Acidovorax sp. JS42*	Burkholderiales
124	azo3482	FdhA	YP_934984.1	*Azoarcus sp. BH72*	Rhodocyclales
125	M446_3087	FdhA	YP_001769931.1	*Methylobacterium sp. 4-46*	Rhizobiales
126	Dshi_0504	FdhA	YP_001531853.1	*Dinoroseobacter shibae*	Rhodobacterales
127	Abu_1498	FdhA	YP_001490422.1	*Arcobacter butzleri*	Campylobacterales
128	NAMH_1307	FdhA	YP_002607700.1	*Nautilia profundicola*	Nautiliales

129	DP1769	FdhA	YP_065505.1	*Desulfotalea psychrophila*	Desulfobacterales
130	DvMF_1217	FdnG	YP_002435636.1	*Desulfovibrio vulgaris*	Desulfovibrionales
131	GM21_2638	FdnG	YP_003022432.1	*Geobacter sp. M21*	Desulfuromonadales
132	BAV3142	FdnG	YP_787637.1	*Bordetella avium*	Burkholderiales
133	Daro_1818	FdnG	YP_285034.1	*Dechloromonas aromatica*	Rhodocyclales
134	Smal_3261	FdnG	YP_002029643.1	*Stenotrophomonas maltophilia*	Xanthomonadales
135	A2cp1_3894	FdnG	YP_002494283.1	*Anaeromyxobacter dehalogenans*	Myxococcales
136	MCA1210	FdnG	YP_113674.1	*Methylococcus capsulatus*	Methylococcales
137	APECO1_25712	FdnG	YP_859487.1	*Escherichia coli*	Enterobacteriales
138	Avin_03810	FdnG	YP_002797616.1	*Azotobacter vinelandii*	Pseudomonadales
139	CV_3839	FdnG	NP_903509.1	*Chromobacterium violaceum*	Neisseriales
140	APJL_0905	FdnG	YP_001651907.1	*Actinobacillus pleuropneumoniae*	Pasteurellales
141	AZC_1159	FdnG	YP_001524075.1	*Azorhizobium caulinodans*	Rhizobiales
142	Pden_2829	FdnG	YP_916609.1	*Paracoccus denitrificans*	Rhodobacterales
143	SO_0101	FdnG	NP_715743.1	*Shewanella oneidensis*	Alteromonadales
144	Acid_0837	FdnG	YP_822121.1	*Solibacter usitatus*	Solibacterales
145	aq_1039	FdnG	NP_213709.1	*Aquifex aeolicus*	Aquificales
146	trd_1974	FdnG	YP_002523172.1	*Thermomicrobium roseum*	Thermomicrobiales
147	BMULJ_05810	AoxB	YP_001941609.1	*Burkholderia multivorans*	Burkholderiales
148	Nham_4427	AoxB	YP_571843.1	*Nitrobacter hamburgensis*	Rhizobiales
149	Cagg_0377	AoxB	YP_002461759.1	*Chloroflexus aggregans*	Chloroflexales
150	TTHB127	AoxB	YP_145366.1	*Thermus thermophilus*	Thermales
151	Clim_0382	AoxB	YP_001942454.1	*Chlorobium limicola*	Chlorobiales
152	APE_2556.1	AoxB	NP_148692.2	*Aeropyrum pernix*	Desulfurococcales
153	Pcal_1369	AoxB	YP_001056256.1	*Pyrobaculum calidifontis*	Thermoproteales
154	ST2391	AoxB	NP_378391.1	*Sulfolobus tokodaii*	Sulfolobales

155	AHA_1777	NuoG_2	YP_856313.1	*Aeromonas hydrophila*	Aeromonadales
156	SO_1016	NuoG_2	NP_716644.1	*Shewanella oneidensis*	Alteromonadales
157	APECO1_4282	NuoG_2	YP_853385.1	*Escherichia coli*	Enterobacteriales
158	Csal_3127	NuoG_2	YP_575170.1	*Chromohalobacter salexigens*	Oceanospirillales
159	A1S_0757	NuoG_2	YP_001083799.1	*Acinetobacter baumannii*	Pseudomonadales
160	MCA1354	NuoG_2	YP_113815.1	*Methylococcus capsulatus*	Methylococcales
161	Acry_1115	NuoG_2	YP_001234246.1	*Acidiphilium cryptum*	Rhodospirillales
162	RSKD131_1421	NuoG_2	YP_002525782.1	*Rhodobacter sphaeroides*	Rhodobacterales
163	Sfum_1954	NuoG_2	YP_846074.1	*Syntrophobacter fumaroxidans*	Syntrophobacterales
164	DMR_13380	NuoG_2	YP_002952715.1	*Desulfovibrio magneticus*	Desulfovibrionales
165	GM21_0157	NuoG_2	YP_003020000.1	*Geobacter sp. M21*	Desulfuromonadales
166	GAU_1656	NuoG_2	YP_002761168.1	*Gemmatimonas aurantiaca*	Gemmatimonadales
167	Acel_0273	NuoG_2	YP_872033.1	*Acidothermus cellulolyticus*	Actinomycetales
168	DR_1499	NuoG_2	NP_295222.1	*Deinococcus radiodurans*	Deinococcales
169	TTC1914	NuoG_2	YP_005883.1	*Thermus thermophilus*	Thermales
170	NQO3	NuoG_2	NQO3	*Rhodothermus marinus*	Sphingobacteriales
171	Ctha_2011	NuoG_2	YP_001996910.1	*Chloroherpeton thalassium*	Chlorobiales
172	Amuc_1611	NuoG_2	YP_001878212.1	*Akkermansia muciniphila*	Verrucomicrobiales
173	A1C_06150	NuoG_2	YP_001493971.1	*Rickettsia akari*	Rickettsiales
174	PXO_01293	NuoG_2	YP_001914619.1	*Xanthomonas oryzae*	Xanthomonadales
175	Hhal_1759	NuoG_2	YP_001003325.1	*Halorhodospira halophila*	Chromatiales
176	AFE_2624	NuoG_2	YP_002427002.1	*Acidithiobacillus ferrooxidans*	Acidithiobacillales
177	NE1771	NuoG_2	NP_841801.1	*Nitrosomonas europaea*	Nitrosomonadales
178	Tbd_1148	NuoG_2	YP_314906.1	*Thiobacillus denitrificans*	Hydrogenophilales
179	Tmzlt_1748	NuoG_2	YP_002355396.1	*Thauera sp. MZ1T*	Rhodocyclales
180	Ajs_0963	NuoG_2	YP_985279.1	*Acidovorax sp. JS42*	Burkholderiales

181	Mfla_2055	NuoG_2	YP_546163.1	*Methylobacillus flagellatus*	Methylophilales
182	NGK_2147	NuoG_2	YP_002002772.1	*Neisseria gonorrhoeae*	Neisseriales
183	LPC_3069	NuoG_2	YP_001252303.1	*Legionella pneumophila*	Legionellales
184	Cagg_1043	NuoG_2	YP_002462393.1	*Chloroflexus aggregans*	Chloroflexales
185	Haur_3087	NuoG_2	YP_001545853.1	*Herpetosiphon auranticus*	Herpetosiphonales
186	pc0565	NuoG_2	YP_007564.1	*Candidatus Protochlamydia amoebophila*	Chlamydiales
187	Acid_0114	NuoG_2	YP_821414.1	*Solibacter usitatus*	Solibacterales
188	ACP_0290	NuoG_2	YP_002753433.1	*Acidobacterium capsulatum*	Acidobacteriales

Supplemental table 8.2: Proteins whose amino acid sequence was used to construct the dendogram 6.7.

Number	keeg_ID	Type of protein	Accession	Species	Order
1	Acid_0114	NuoG_1	YP_821414.1	*Solibacter usitatus*	Solibacterales
2	ACP_0290	NuoG_1	YP_002753433.1	*Acidobacterium capsulatum*	Acidobacteriales
3	Cagg_1043	NuoG_1	YP_002462393.1	*Chloroflexus aggregans*	Chloroflexales
4	Haur_3087	NuoG_1	YP_001545853.1	*Herpetosiphon aurantiacus*	Herpetosiphonales
5	pc0565	NuoG_1	YP_007564.1	*Candidatus Protochlamydia amoebophila*	Chlamydiales
6	Acel_0273	NuoG_1	YP_872033.1	*Acidothermus cellulolyticus*	Actinomycetales
7	DR_1499	NuoG_1	NP_295222.1	*Deinococcus radiodurans*	Deinococcales
8	TTC1914	NuoG_1	YP_005883.1	*Thermus thermophilus*	Thermales
9	RHE_CH03742	NuoG_1	YP_471224.1	*Rhizobium etli*	Rhizobiales
10	PXO_01293	NuoG_1	YP_001914619.1	*Xanthomonas oryzae*	Xanthomonadales
11	Hhal_1759	NuoG_1	YP_001003325.1	*Halorhodospira halophila*	Chromatiales
12	LPC_3069	NuoG_1	YP_001252303.1	*Legionella pneumophila*	Legionellales
13	NE1771	NuoG_1	NP_841801.1	*Nitrosomonas europaea*	Nitrosomonadales
14	Tbd_1148	NuoG_1	YP_314906.1	*Thiobacillus denitrificans*	Hydrogenophilales
15	Tmz1t_1748	NuoG_1	YP_002355396.1	*Thauera sp. MZ1T*	Rhodocyclales
16	Ajs_0963	NuoG_1	YP_985279.1	*Acidovorax sp. JS42*	Burkholderiales
17	NGK_2147	NuoG_1	YP_002002772.1	*Neisseria gonorrhoeae*	Neisseriales
18	Mfla_2055	NuoG_1	YP_546163.1	*Methylobacillus flagellatus*	Methylophilales
19	AFE_2624	NuoG_1	YP_002427002.1	*Acidithiobacillus ferrooxidans*	Acidithiobacillales
20	A1C_06150	NuoG_1	YP_001493971.1	*Rickettsia akari*	Rickettsiales
21	Amuc_1611	NuoG_1	YP_001878212.1	*Akkermansia muciniphila*	Verrucomicrobiales
22	GAU_1656	NuoG_1	YP_002761168.1	*Gemmatimonas aurantiaca*	Gemmatimonadales
23	NQO3	NuoG_1	NQO3	*Rhodothermus marinus*	Sphingobacteriales
24	Ctha_2011	NuoG_1	YP_001996910.1	*Chloroherpeton thalassium*	Chlorobiales

25	FIC_01666	NuoG_1	YP_003096172.1	*Flavobacteriaceae bacterium 3519-10*	Flavobacteriales
26	AHA_1777	NuoG_1	YP_856313.1	*Aeromonas hydrophila*	Aeromonadales
27	SO_1016	NuoG_1	NP_716644.1	*Shewanella oneidensis*	Alteromonadales
28	APECO1_4282	NuoG_1	YP_853385.1	*Escherichia coli*	Enterobacteriales
29	Csal_3127	NuoG_1	YP_575170.1	*Chromohalobacter salexigens*	Oceanospirillales
30	Acry_1115	NuoG_1	YP_001234246.1	*Acidiphilium cryptum*	Rhodospirillales
31	MCA1354	NuoG_1	YP_113815.1	*Methylococcus capsulatus*	Methylococcales
32	RSKD131_1421	NuoG_1	YP_002525782.1	*Rhodobacter sphaeroides*	Rhodobacterales
33	Sfum_1954	NuoG_1	YP_846074.1	*Syntrophobacter fumaroxidans*	Syntrophobacterales
34	DMR_13380	NuoG_1	YP_002952715.1	*Desulfovibrio magneticus*	Desulfovibrionales
35	GM21_0157	NuoG_1	YP_003020000.1	*Geobacter sp. M21*	Desulfuromonadales
36	BAV3144	FdnH	YP_787638.1	*Bordetella avium*	Burkholderiales
37	Smal_3262	FdnH	YP_002029644.1	*Stenotrophomonas maltophilia*	Xanthomonadales
38	Daro_1817	FdnH	YP_285033.1	*Dechloromonas aromatica*	Rhodocyclales
39	MCA1209	FdnH	YP_113673.1	*Methylococcus capsulatus*	Methylococcales
40	A2cp1_3895	FdnH	YP_002494284.1	*Anaeromyxobacter dehalogenans*	Myxococcales
41	CV_3840	FdnH	NP_903510.1	*Chromobacterium violaceum*	Neisseriales
42	Avin_03820	FdnH	YP_002797617.1	*Azotobacter vinelandii*	Pseudomonadales
43	APECO1_2572	FdnH	YP_859486.1	*Escherichia coli*	Enterobacteriales
44	APJL_0906	FdnH	YP_001651908.1	*Actinobacillus pleuropneumoniae*	Pasteurellales
45	AZC_1158	FdnH	YP_001524074.1	*Azorhizobium caulinodans*	Rhizobiales
46	Pden_2828	FdnH	YP_916608.1	*Paracoccus denitrificans*	Rhodobacterales
47	Acid_0836	FdnH	YP_822120.1	*Solibacter usitatus*	Solibacterales
48	SO_0102	FdnH	NP_715744.1	*Shewanella oneidensis*	Alteromonadales
49	aq_1046	FdnH	NP_213710.1	*Aquifex aeolicus*	Aquificales
50	GM21_2639	FdnH	YP_003022433.1	*Geobacter sp. M21*	Desulfuromonadales

51	trd_1973	FdnH	YP_002523171.1	*Thermomicrobium roseum*	Thermomicrobiales
52	DvMF_1216	FdhH	YP_002435635.1	*Desulfovibrio vulgaris*	Desulfovibrionales
53	AHA_3062	FdhB	YP_857564.1	*Aeromonas hydrophila*	Aeromonadales
54	PBPRA1861	FdhB	YP_130067.1	*Photobacterium profundum*	Vibrionales
55	SO_4510	FdhB	NP_720030.1	*Shewanella oneidensis*	Alteromonadales
56	Csal_1916	FdhB	YP_573967.1	*Chromohalobacter salexigens*	Oceanospirillales
57	Ajs_3463	FdhB	YP_987653.1	*Acidovorax sp. JS42*	Burkholderiales
58	azo3481	FdhB	YP_934983.1	*Azoarcus sp. BH72*	Rhodocyclales
59	M446_3088	FdhB	YP_001769932.1	*Methylobacterium sp. 4-46*	Rhizobiales
60	Dshi_0505	FdhB	YP_001531854.1	*Dinoroseobacter shibae*	Rhodobacterales
61	amb2672	FdhB	YP_422035.1	*Magnetospirillum magneticum*	Rhodospirillales
62	Mlg_1287	FdhB	YP_742126.1	*Alkalilimnicola ehrlichei*	Chromatiales
63	DP1768	FdhB	YP_065504.1	*Desulfotalea psychrophila*	Desulfobacterales
64	Abu_1497	FdhB	YP_001490421.1	*Arcobacter butzleri*	Campylobacterales
65	NAMH_1308	FdhB	YP_002607701.1	*Nautilia profundicola*	Nautiliales
66	Mthe_1338	FdhB	YP_843753.1	*Methanosaeta thermophila*	Methanosarcinales
67	PAB1390	FdhB	NP_127152.1	*Pyrococcus abyssi*	Thermococcales
68	PPA0516	DMSB	YP_055227.1	*Propionibacterium acnes*	Actinomycetales
69	DvMF_1611	DMSB	YP_002436027.1	*Desulfovibrio vulgaris*	Desulfovibrionales
70	APECO1_1194	DMSB	YP_851992.1	*Escherichia coli*	Enterobacteriales
71	APECO1_672	ynfG	YP_852688.1	*Escherichia coli*	Enterobacteriales
72	APJL_1706	DMSB	YP_001652702.1	*Actinobacillus pleuropneumoniae*	Pasteurellales
73	Asuc_1522	ynfG	YP_001344815.1	*Actinobacillus succinogenes*	Pasteurellales
74	VFMJ11_A0105	DMSB	YP_002157662.1	*Vibrio fischeri*	Vibrionales
75	Shal_0406	DMSB	YP_001672640.1	*Shewanella halifaxensis*	Alteromonadales
76	LHK_02497	DMSB	YP_002796488.1	*Laribacter hongkongensis*	Neisseriales

77	CJJ81176_1571	DMSB	YP_001001226.1	*Campylobacter jejuni*	Campylobacterales
78	Moth_1385	DMSB	YP_430241.1	*Moorella thermoacetica*	Thermoanaerobacterales
79	Amet_1331	DMSB	YP_001319192.1	*Alkaliphilus metalliredigens*	Clostridiales
80	rrnAC1200	ebdB	YP_135853.1	*Haloarcula marismortui*	Halobacteriales
81	PERMA_0658	ebdB	YP_002730447.1	*Persephonella marina*	Aquificales
82	c1A63	ebdB	YP_158332.1	*Aromatoleum aromaticum*	Rhodocyclales
83	Dole_0196	ebdB	YP_001528083.1	*Desulfococcus oleovorans*	Desulfobacterales
84	Pars_0498	FdhB	YP_001152745.1	*Pyrobaculum arsenaticum*	Thermoproteales
85	APE_1294.1	ebdB	NP_147850.2	*Aeropyrum pernix*	Desulfurococcales
86	Caul_3865	NarH	YP_001685489.1	*Caulobacter sp. K31*	Caulobacterales
87	HNE_1561	NarH	YP_760272.1	*Hyphomonas neptunium*	Rhodobacterales
88	AZC_1426	NarH	YP_001524342.1	*Azorhizobium caulinodans*	Rhizobiales
89	Acry_1582	NarH	YP_001234707.1	*Acidiphilium cryptum*	Rhodospirillales
90	COSY_0648	NarH	YP_001219485.1	*Calyptogena okutanii thioautotrophic*	
91	Maqu_3085	NarH	YP_960346.1	*Marinobacter hydrocarbonoclasticus*	Alteromonadales
92	PA14_13800	NarH	YP_789247.1	*Pseudomonas aeruginosa*	Pseudomonadales
93	ABO_0545	NarH	YP_692265.1	*Alcanivorax borkumensis*	Oceanospirillales
94	Smal_2235	NarH	YP_002028622.1	*Stenotrophomonas maltophilia*	Xanthomonadales
95	Aave_0662	NarH	YP_969039.1	*Acidovorax avenae*	Burkholderiales
96	CV_2542	NarH	NP_902212.1	*Chromobacterium violaceum*	Neisseriales
97	Mlg_1002	NarH	YP_741845.1	*Alkalilimnicola ehrlichei*	Chromatiales
98	APECO1_342	NarH	YP_852356.1	*Escherichia coli*	Enterobacteriales
99	Tbd_1404	NarH	YP_315162.1	*Thiobacillus denitrificans*	Hydrogenophilales
100	ebA6285	NarH	YP_160620.1	*Aromatoleum aromaticum*	Rhodocyclales
101	ABC0716	NarH	YP_174216.1	*Bacillus clausii*	Bacillales
102	LAF_1061	NarH	YP_001843877.1	*Lactobacillus fermentum*	Lactobacillales
103	Rxyl_1206	NarH	YP_643984.1	*Rubrobacter xylanophilus*	Rubrobacterales

104	DSY0335	NarH	YP_516568.1	*Desulfitobacterium hafniense*	Clostridiales
105	CE1295	NarH	NP_737905.1	*Corynebacterium efficiens*	Actinomycetales
106	M1425_0829	NarH	YP_002828932.1	*Sulfolobus islandicus*	Sulfolobales
107	Reut_B4428	Domain B2_ACIII	YP_298623.1	*Cupriavidus pinatubonensis*	Burkholderiales
108	A2cp1_0848	Domain B2_ACIII	YP_002491266.1	*Anaeromyxobacter dehalogenans*	Myxococcales
109	Acid345_3003	Domain B2_ACIII	YP_592078.1	*Acidobacteria bacterium Ellin345*	Acidobacteriales
110	Acid_0490	Domain B2_ACIII	YP_821785.1	*Solibacter usitatus*	Solibacterales
111	Cagg_3386	Domain B2_ACIII	YP_002464666.1	*Chloroflexus aggregans*	Chloroflexales
112	Noc_1238	Domain B2_ACIII	YP_343269.1	*Nitrosococcus oceani*	Chromatiales
113	M446_5824	Domain B2_ACIII	YP_001772545.1	*Methylobacterium sp.4-46*	Rhizobiales
114	GDI2620	Domain B2_ACIII	YP_001602862.1	*Gluconacetobacter diazotrophicus*	Rhodospirillales
115	Oter_3934	Domain B2_ACIII	YP_001820808.1	*Opitutus terrae*	
116	Minf_1961	Domain B2_ACIII	YP_001940612.1	*Methylacidiphilum infernorum*	
117	*ActB*	Domain B2_ACIII	ABV55245	*Rhodothermus marinus*	Sphingobacteriales
118	SRU_2106	Domain B2_ACIII	YP_446212.1	*Salinibacter ruber*	Sphingobacteriales
119	TTC1404	Domain B2_ACIII	YP_005373.1	*Thermus thermophilus*	Thermales
120	Bd1608	Domain B2_ACIII	NP_968492.1	*Bdellovibrio bacteriovorus*	Bdellovibrionales
121	LA3267	Domain B2_ACIII	NP_713447.1	*Leptospira interrogans*	Spirochaetales
122	FP0373	Domain B2_ACIII	YP_001295304.1	*Flavobacterium psychrophilum*	Flavobacteriales
123	CHU_2212	Domain B2_ACIII	YP_678817.1	*Cytophaga hutchinsonii*	Sphingobacteriales
124	Gmet_1811	Subunit B2_MFIc	YP_384765.1	*Geobacter metallireducens*	Desulfuromonadales
125	GAU_2036	Subunit B2_MFIc	YP_002761548.1	*Gemmatimonas aurantiaca*	Gemmatimonadales
126	ZP_01451015.1	Subunit B2_MFIc	ZP_01451015.1	*Maripro fundus ferrooxydans*	Maripro fundales
127	Dvul_2270	Subunit B2_MFIc	YP_967713.1	*Desulfovibrio vulgaris*	Desulfovibrionales
128	DVU0693	Subunit B2_MFIc	YP_009915.1	*Desulfovibrio vulgaris*	Desulfovibrionales
130	Dde_2934	Subunit B2_MFIc	YP_389423.1	*Desulfovibrio desulfuricans*	Desulfovibrionales
131	DMR_18030	Subunit B2_MFIc	YP_002953180.1	*Desulfovibrio magneticus*	Desulfovibrionales

132	Dret_0272	Subunit B2_MFIc	YP_003197152.1	*Desulfohalobium retbaense*	Desulfovibrionales
133	Dbac_3392	Subunit B2_MFIc	YP_003159880 1.1	*Desulfomicrobium baculatum*	Desulfovibrionales
134	Desal_1044	Subunit B2_MFIc	YP_002990648.1	*Desulfovibrio salexigens*	Desulfovibrionales
135	HRM2_18950	Subunit B2_MFIc	YP_002603160.1	*Desulfobacterium autotrophicum*	Desulfobacterales
136	Dole_2548	Subunit B2_MFIc	YP_001530429.1	*Desulfococcus oleovorans*	Desulfobacterales
137	Dalk_1269	Subunit B2_MFIc	YP_002430440.1	*Desulfatibacillum alkenivorans*	Desulfobacterales
138	Sfum_0609	Subunit B2_MFIc	YP_844743.1	*Syntrophobacter fumaroxidans*	Syntrophobacterales
139	Pars_0937	nrfC	YP_001153169.1	*Pyrobaculum arsenaticum*	Thermoproteales
140	Pcal_1499	psrB	YP_001056384.1	*Pyrobaculum calidifontis*	Thermoproteales
141	DehaBAV1_0265	nrfC	YP_001213731.1	*Dehalococcoides sp. BAV1*	
142	CHY_2573	psrB	YP_361366.1	*Carboxydothermus hydrogenoformans*	Thermoanaerobacterales
143	HY04AAS1_0308	nrfC	YP_002120976.1	*Hydrogenobaculum sp. Y04AAS1*	Aquificales
144	CHY_0477	nrfC	YP_359335.1	*Carboxydothermus hydrogenoformans*	Thermoanaerobacterales
145	Hbut_0372	nrfC	YP_001012588.1	*Hyperthermus butylicus*	Desulfurococcales
146	AF2385	psrB	NP_071208.1	*Archaeoglobus fulgidus*	Archaeoglobales
147	Oter_1465	psrB	YP_001818349.1	*Opitutus terrae*	
148	Anae109_4109	nrfC	YP_001381271.1	*Anaeromyxobacter sp. Fw109-5*	Myxococcales
149	Clim_2401	psrB	YP_001944401.1	*Chlorobium limicola*	Chlorobiales
150	Cag_0619	nrfC	YP_378935.1	*Chlorobium chlorochromatii*	Chlorobiales
151	THEYE_A1156	psrB	YP_002248980.1	*Thermodesulfovibrio yellowstonii*	Nitrospirales
152	AHA_2466	nrfC	YP_856980.1	*Aeromonas hydrophila*	Aeromonadales
153	APECO1_2383	nrfC	YP_859677.1	*Escherichia coli*	Enterobacteriales
154	PBPRA1260	nrfC	YP_129473.1	*Photobacterium profundum*	Vibrionales
155	APJL_0102	nrfC	YP_001651152.1	*Actinobacillus pleuropneumoniae*	Pasteurellales
156	Sama_2903	nrfC	YP_928775.1	*Shewanella amazonensis*	Alteromonadales
157	SO_4061	psrB	NP_719591.1	*Shewanella oneidensis*	Alteromonadales
158	CCC13826_0388	nrfC	YP_001467233.1	*Campylobacter concisus*	Campylobacterales

Supplemental table 8.3: Proteins whose amino acid sequence was used to the construct dendogram 6.8.

Number	keeg_ID	Type of protein	Accession	Species	Order
1	DSY0188	DMSC	YP_516421.1	*Desulfitobacterium hafniense*	Clostridiales
2	Moth_1384	DMSC	YP_430240.1	*Moorella thermoacetica*	Thermoanaerobacterales
3	DvMF_1610	DMSC	YP_002436026.1	*Desulfovibrio vulgaris*	Desulfovibrionales
4	APECO1_1193	DMSC	YP_851993.1	*Escherichia coli*	Enterobacteriales
5	APECO1_673	ynfH	YP_852689.1	*Escherichia coli*	Enterobacteriales
6	APJL_1707	DMSC	YP_001652703.1	*Actinobacillus pleuropneumoniae*	Pasteurellales
7	Asuc_1521	ynfH	YP_001344814.1	*Actinobacillus succinogenes*	Pasteurellales
8	VFMJ11_A0104	DMSC	YP_002157661.1	*Vibrio fischeri*	Vibrionales
9	LHK_02498	DMSC	YP_002796489.1	*Laribacter hongkongensis*	Neisseriales
10	Shal_0405	DMSC	YP_001672639.1	*Shewanella halifaxensis*	Alteromonadales
11	CJJ81176_1572	DMSC	YP_001001227.1	*Campylobacter jejuni*	Campylobacterales
12	PPA0515	DMSC	YP_055226.1	*Propionibacterium acnes*	Actinomycetales
13	Oter_1464	psrC	YP_001818348.1	*Opitutus terrae*	
14	Anae109_4106	nrfB	YP_001381268.1	*Anaeromyxobacter sp. Fw109-5*	Myxococcales
15	Clim_2402	psrC	YP_001944402.1	*Chlorobium limicola*	Chlorobiales
16	Cag_0618	nrfD	YP_378934.1	*Chlorobium chlorochromatii*	Chlorobiales
17	THEYE_A1155	psrC	YP_002248979.1	*Thermodesulfovibrio yellowstonii*	Nitrospirales
18	AHA_2467	nrfD	YP_856981.1	*Aeromonas hydrophila*	Aeromonadales
19	PBPRA1261	nrfD	YP_129474.1	*Photobacterium profundum*	Vibrionales
20	APECO1_2382	nrfD	YP_859678.1	*Escherichia coli*	Enterobacteriales
21	APJL_0103	nrfD	YP_001651153.1	*Actinobacillus pleuropneumoniae*	Pasteurellales
22	Sama_2904	nrfD	YP_928776.1	*Shewanella amazonensis*	Alteromonadales
23	SO_4060	psrC	NP_719590.1	*Shewanella oneidensis*	Alteromonadales
24	CCC13826_0387	psrC	YP_001467232.1	*Campylobacter concisus*	Campylobacterales

25	Pcal_1498	psrC	YP_001056383.1	*Pyrobaculum calidifontis*	Thermoproteales
26	Pars_0936	nrfD	YP_001153168.1	*Pyrobaculum arsenaticum*	Thermoproteales
27	Dvul_2271	Subunit C_MFIc	YP_967714.1	*Desulfovibrio vulgaris*	Desulfovibrionales
28	DVU0692	Subunit C_MFIc	YP_009914.1	*Desulfovibrio vulgaris*	Desulfovibrionales
30	Dde_2935	Subunit C_MFIc	YP_389424.1	*Desulfovibrio desulfuricans*	Desulfovibrionales
31	Desal_1045	Subunit C_MFIc	YP_002990649.1	*Desulfovibrio salexigens*	Desulfovibrionales
32	Dret_0273	Subunit C_MFIc	YP_003197153.1	*Desulfohalobium retbaense*	Desulfovibrionales
33	Dbac_3393	Subunit C_MFIc	YP_003159881.1	*Desulfomicrobium baculatum*	Desulfovibrionales
34	DMR_18040	Subunit C_MFIc	YP_002953181.1	*Desulfovibrio magneticus*	Desulfovibrionales
35	Sfum_0608	Subunit C_MFIc	YP_844742.1	*Syntrophobacter fumaroxidans*	Syntrophobacterales
36	HRM2_18960	Subunit C_MFIc	YP_002603161.1	*Desulfobacterium autotrophicum*	Desulfobacterales
37	Dole_2549	Subunit C_MFIc	YP_001530430.1	*Desulfococcus oleovorans*	Desulfobacterales
38	Dalk_1270	Subunit C_MFIc	YP_002430441.0	*Desulfatibacillum alkenivorans*	Desulfobacterales
39	Gene_C	Subunit C_ACIII	ABV55246	*Rhodothermus marinus*	Sphingobacteriales
40	SRU_2105	Subunit C_ACIII	YP_446211.1	*Salinibacter ruber*	Sphingobacteriales
41	Bd1609	Subunit C_ACIII	NP_968493.1	*Bdellovibrio bacteriovorus*	Bdellovibrionales
42	LA3266	Subunit C_ACIII	NP_713446.1	*Leptospira interrogans*	Spirochaetales
43	FP0374	Subunit C_ACIII	YP_001295305.1	*Flavobacterium psychrophilum*	Flavobacteriales
44	CHU_2211	Subunit C_ACIII	YP_678816.1	*Cytophaga hutchinsonii*	Sphingobacteriales
45	Oter_3933	Subunit C_ACIII	YP_001820807.1	*Opitutus terrae*	
46	Minf_1960	Subunit C_ACIII	YP_001940611.1	*Methylacidiphilum infernorum*	
47	A2cp1_0849	Subunit C_ACIII	YP_002491267.1	*Anaeromyxobacter dehalogenans*	Myxococcales
48	Acid345_3002	Subunit C_ACIII	YP_592077.1	*Acidobacteria bacterium Ellin345*	Acidobacteriales
49	Acid_0491	Subunit C_ACIII	YP_821786.1	*Solibacter usitatus*	Solibacterales
50	Cagg_3385	Subunit C_ACIII	YP_002464665.1	*Chloroflexus aggregans*	Chloroflexales
51	Reut_B4429	Subunit C_ACIII	YP_298624.1	*Cupriavidus pinatubonensis*	Burkholderiales

52	Noc_1239	Subunit C_ACIII	YP_343270.1	*Nitrosococcus oceani*	Chromatiales
53	TTC1403	Subunit C_ACIII	YP_005372.1	*Thermus thermophilus*	Thermales
54	GAU_2035	Subunit C_ACIII	YP_002761547.1	*Gemmatimonas aurantiaca*	Gemmatimonadales
55	M446_5823	Subunit C_ACIII	YP_001772544.1	*Methylobacterium sp. 4-46*	Rhizobiales
56	GDI2619	Subunit C_ACIII	YP_001602861.1	*Gluconacetobacter diazotrophicus*	Rhodospirillales
57	ZP_01451014.1	Subunit C_ACIII	ZP_01451014.1	*Mariprofundus ferrooxydans*	Mariprofundales
58	Gmet_1812	Subunit C_ACIII	YP_384766.1	*Geobacter metallireducens*	Desulfuromonadales
59	GAU_2032	Subunit F_ACIII	YP_002761544.1	*Gemmatimonas aurantiaca*	Gemmatimonadales
60	*Gene_F*	Subunit F_ACIII	ABV55249	*Rhodothermus marinus*	Sphingobacteriales
61	SRU_2102	Subunit F_ACIII	YP_446208.1	*Salinibacter ruber*	Sphingobacteriales
62	Bd1612	Subunit F_ACIII	NP_968496.1	*Bdellovibrio bacteriovorus*	Bdellovibrionales
63	LA3263	Subunit F_ACIII	NP_713443.1	*Leptospira interrogans*	Spirochaetales
64	FP0377	Subunit F_ACIII	YP_001295308.1	*Flavobacterium psychrophilum*	Flavobacteriales
65	CHU_2208	Subunit F_ACIII	YP_678813.1	*Cytophaga hutchinsonii*	Sphingobacteriales
66	Minf_1957	Subunit F_ACIII	YP_001940608.1	*Methylacidiphilum infernorum*	
67	Oter_3930	Subunit F_ACIII	YP_001820804.1	*Opitutus terrae*	
68	A2cp1_0852	Subunit F_ACIII	YP_002491270.1	*Anaeromyxobacter dehalogenans*	Myxococcales
69	Acid_0494	Subunit F_ACIII	YP_821789.1	*Solibacter usitatus*	Solibacterales
70	Noc_1242	Subunit F_ACIII	YP_343273.1	*Nitrosococcus oceani*	Chromatiales
71	Acid345_2999	Subunit F_ACIII	YP_592074.1	*Acidobacteria bacterium Ellin345*	Acidobacteriales
72	Cagg_3382	Subunit F_ACIII	YP_002464662.1	*Chloroflexus aggregans*	Chloroflexales
73	M446_5820	Subunit F_ACIII	YP_001772541.1	*Methylobacterium sp. 4-46*	Rhizobiales
74	GDI2616	Subunit F_ACIII	YP_001602858.1	*Gluconacetobacter diazotrophicus*	Rhodospirillales
75	Reut_B4432	Subunit F_ACIII	YP_298627.1	*Cupriavidus pinatubonensis*	Burkholderiales
76	TTC1400	Subunit F_ACIII	YP_005369.1	*Thermus thermophilus*	Thermales

Supplemental table 8.4: Proteins whose amino acid sequence was used to construct the dendogram 6.9.

Number	keeg_ID	Type of protein	Accession	species	order
1	Mmc1_1587	NapC	YP_865502.1	*Magnetococcus sp.MC-1*	
2	Dshi_3161	NapC	YP_001534495.1	*Dinoroseobacter shibae*	Rhodobacterales
3	AHA_1590	NapC	YP_856126.1	*Aeromonas hydrophila*	Aeromonadales
4	PBPRA0855	NapC	YP_129070.1	*Photobacterium profundum*	Vibrionales
5	CPS_1055	NapC	YP_267799.1	*Colwellia psychrerythraea*	Alteromonadales
6	PA1172	NapC	NP_249863.1	*Pseudomonas aeruginosa*	Pseudomonadales
7	HCH_03367	NapC	YP_434544.1	*Hahella chejuensis*	Oceanospirillales
8	BB2802	NapC	NP_889338.1	*Bordetella bronchiseptica*	Burkholderiales
9	RC1_0459	NapC	YP_002296711.1	*Rhodospirillum centenum*	Rhodospirillales
10	Atu4410	NapC	NP_356244.1	*Agrobacterium tumefaciens*	Rhizobiales
11	APECO1_4357	NapC	YP_853309.1	*Escherichia coli*	Enterobacteriales
12	APJL_1457	NapC	YP_001652453.1	*Actinobacillus pleuropneumoniae*	Pasteurellales
13	Daro_2579	NapC	YP_285780.1	*Dechloromonas aromatica*	Rhodocyclales
14	RPC_0656	torC	YP_530547.1	*Rhodopseudomonas palustris*	Rhizobiales
15	LHK_02085	NapC	YP_002796078.1	*Laribacter hongkongensis*	Neisseriales
16	RSKD131_3217	torC	YP_002520150.1	*Rhodobacter sphaeroides*	Rhodobacterales
17	Rru_A1283	torC	YP_426371.1	*Rhodospirillum rubrum*	Rhodospirillales
18	APECO1_89	torC	YP_852107.1	*Escherichia coli*	Enterobacteriales
19	AHA_4048	torC	YP_858473.1	*Aeromonas hydrophila*	Aeromonadales
20	APJL_0687	torC	YP_001651700.1	*Actinobacillus pleuropneumoniae*	Pasteurellales
21	CPS_1832	torC	YP_268562.1	*Colwellia psychrerythraea*	Alteromonadales
22	PBPRA1468	torC	YP_129681.1	*Photobacterium profundum*	Vibrionales
23	PsycPRwf_0213	torC	YP_001279122.1	*Psychrobacter sp.PRwf-1*	Pseudomonadales
24	Ddes_0082	NapC	YP_002478680.1	*Desulfovibrio desulfuricans*	Desulfovibrionales

25	THEYE_A0192	nrfH	YP_002248042.1	*Thermodesulfovibrio yellowstonii*	Nitrospirales
26	DMR_06510	nrfH	YP_002952028.1	*Corynebacterium diphtheriae*	Actinomycetales
27	BDI_0108	nrfH	YP_001301525.1	*Parabacteroides distasonis*	Bacteroidales
28	Coch_1100	nrfH	YP_003141216.1	*Capnocytophaga ochracea*	Flavobacteriales
29	DP0343	nrfH	YP_064079.1	*Desulfotalea psychrophila*	Desulfobacterales
30	Abu_0348	nrfH	YP_001489292.1	*Arcobacter butzleri*	Campylobacterales
31	CHY_0242	nrfH	YP_359114.1	*Carboxydothermus hydrogenoformans*	Thermoanaerobacterales
32	CKO_03812	nrfB	YP_001455324.1	*Citrobacter koseri*	Enterobacteriales
33	ECBD_3961	nrfB	YP_003038132.1	*Escherichia coli*	Enterobacteriales
34	AHA_2465	nrfB	YP_856979.1	*Aeromonas hydrophila*	Aeromonadales
35	AHA_2762	nrfB	YP_857270.1	*Aeromonas hydrophila*	Aeromonadales
36	APP7_0100	nrfB	YP_001967894.1	*Actinobacillus pleuropneumoniae*	Pasteurellales
37	NT05HA_0038	nrfB	YP_003006573.1	*Aggregatibacter aphrophilus*	Pasteurellales
38	PBPRA1259	nrfB	YP_129472.1	*Photobacterium profundum*	Vibrionales
39	VF_1553	nrfB	YP_204936.1	*Vibrio fischeri*	Vibrionales
40	Sama_2902	nrfB	YP_928774.1	*Shewanella amazonensis*	Alteromonadales
41	Sbal_0181	nrfB	YP_001048584.1	*Shewanella baltica*	Alteromonadales
42	Oter_4607	nrfB	YP_001821478.1	*Opitutus terrae*	
43	Bd2824	nrfB	NP_969613.1	*Bdellovibrio bacteriovorus*	Bdellovibrionales
44	A2cp1_0964	nrfB	YP_002491381.1	*Anaeromyxobacter dehalogenans*	Myxococcales
45	Bd2825	nrfA	NP_969614.1	*Bdellovibrio bacteriovorus*	Bdellovibrionales
46	A2cp1_0963	nrfA	YP_002491380.1	*Anaeromyxobacter dehalogenans*	Myxococcales
47	Oter_4608	nrfA	YP_001821479.1	*Opitutus terrae*	
48	RB11165	nrfA	NP_869819.1	*Rhodopirellula baltica*	Planctomycetales
49	SYN_02616	nrfA	YP_462876.1	*Syntrophus aciditrophicus*	Syntrophobacterales
50	CHY_0243	nrfA	YP_359115.1	*Carboxydothermus hydrogenoformans*	Thermoanaerobacterales

51	Hhal_1374	nrfA	YP_001002943.1	*Halorhodospira halophila*	Chromatiales
52	AHA_2464	nrfA	YP_856978.1	*Aeromonas hydrophila*	Aeromonadales
53	APECO1_2385	nrfA	YP_859675.1	*Escherichia coli*	Enterobacteriales
54	PBPRA1258	nrfA	YP_1294711	*Photobacterium profundum*	Vibrionales
55	SO_3980	nrfA	NP_719510.1	*Shewanella oneidensis*	Alteromonadales
56	APJL_0100	nrfA	YP_001651150.1	*Actinobacillus pleuropneumoniae*	Pasteurellales
57	Abu_0347	nrfA	YP_001489291.1	*Arcobacter butzleri*	Campylobacterales
58	DP0344	nrfA	YP_064080.1	*Desulfotalea psychrophila*	Desulfobacterales
59	BDI_0109	nrfA	YP_001301526.1	*Parabacteroides distasonis*	Bacteroidales
60	Coch_1101	nrfA	YP_003141217.1	*Capnocytophaga ochracea*	Flavobacteriales
61	DMR_06520	nrfA	YP_002952029.1	*Desulfovibrio magneticus*	Desulfovibrionales
62	THEYE_A0193	nrfA	YP_002248043.1	*Thermodesulfovibrio yellowstonii*	Nitrospirales
63	Ccur_13420	nrfA	YP_003151700.1	*Cryptobacterium curtum*	Coriobacteriales
64	Dvul_2268	SubunitA_MFIc	YP_967711.1	*Desulfovibrio vulgaris*	Desulfovibrionales
65	DVU0695	SubunitA_MFIc	*	*Desulfovibrio vulgaris*	Desulfovibrionales
66	DvMF_2690	SubunitA_MFIc	YP_002437097.1	*Desulfovibrio vulgaris*	Desulfovibrionales
67	Dde_2932	SubunitA_MFIc	YP_389421.1	*Desulfovibrio desulfuricans*	Desulfovibrionales
68	Dret_0270	SubunitA_MFIc	YP_003197150.1	*Desulfohalobium retbaense*	Desulfovibrionales
69	Dbac_3390	SubunitA_MFIc	YP_003159878.1	*Desulfomicrobium baculatum*	Desulfovibrionales
70	Desal_1042	SubunitA_MFIc	YP_002990646.1	*Desulfovibrio salexigens*	Desulfovibrionales
71	DMR_18010	SubunitA_MFIc	YP_002953178.1	*Desulfovibrio magneticus*	Desulfovibrionales
72	Sfum_0611	SubunitA_MFIc	YP_844745.1	*Syntrophobacter fumaroxidans*	Syntrophobacterales
73	HRM2_18930	SubunitA_MFIc	YP_002603158.1	*Desulfobacterium autotrophicum*	Desulfobacterales
74	Dole_2546	SubunitA_MFIc	YP_001530427.1	*Desulfococcus oleovorans*	Desulfobacterales
75	Dalk_1267	SubunitA_MFIc	YP_002430442.1	*Desulfatibacillum alkenivorans*	Desulfobacterales
76	*ActA*	Subunit A_ACIII	ABV55244	*Rhodothermus marinus*	Sphingobacteriales

77	SRU_2107	Subunit A_ACIII	YP_446213.1	*Salinibacter ruber*	Sphingobacteriales
78	Cagg_3387	Subunit A_ACIII	YP_002464667.1	*Chloroflexus aggregans*	Chloroflexales
79	Oter_3935	Subunit A_ACIII	YP_001820809.1	*Opitutus terrae*	
80	Minf_1962	Subunit A_ACIII	YP_001940613.1	*Methylacidiphilum infernorum*	
81	Acid345_3004	Subunit A_ACIII	YP_592079.1	*Acidobacteria bacterium Ellin345*	Acidobacteriales
82	Acid_0489	Subunit A_ACIII	YP_821784.1	*Solibacter usitatus*	Solibacterales
83	Noc_1237	Subunit A_ACIII	YP_343268.1	*Nitrosococcus oceani*	Chromatiales
84	M446_5825	Subunit A_ACIII	YP_001772546.1	*Methylobacterium sp. 4-46*	Rhizobiales
85	GDI2621	Subunit A_ACIII	YP_001602863.1	*Gluconacetobacter diazotrophicus*	Rhodospirillales
86	Reut_B4427	Subunit A_ACIII	YP_298622.1	*Cupriavidus pinatubonensis*	Burkholderiales
87	A2cp1_0847	Subunit A_ACIII	YP_002491265.1	*Anaeromyxobacter dehalogenans*	Myxococcales
88	TTC1406	Subunit A_ACIII	YP_005375.1	*Thermus thermophilus*	Thermales
89	CHU_2213	Subunit A_ACIII	YP_678818.1	*Cytophaga hutchinsonii*	Sphingobacteriales
90	Bd1607	Subunit A_ACIII	NP_968491.1	*Bdellovibrio bacteriovorus*	Bdellovibrionales
91	LA3268	Subunit A_ACIII	NP_713448.1	*Leptospira interrogans*	Spirochaetales
92	FP0372	Subunit A_ACIII	YP_001295303.1	*Flavobacterium psychrophilum*	Flavobacteriales
93	Gmet_1809	Subunit A_ACIII	YP_384763.1	*Geobacter metallireducens*	Desulfuromonadales
94	ZP_01451017.1	Subunit A_ACIII	ZP_01451017.1	*Maripro fundus ferrooxydans*	Maripro fundales
95	GAU_2037	Subunit A_ACIII	YP_002761549.1	*Gemmatimonas aurantiaca*	Gemmatimonadales